Conceptual Design of the RCMS

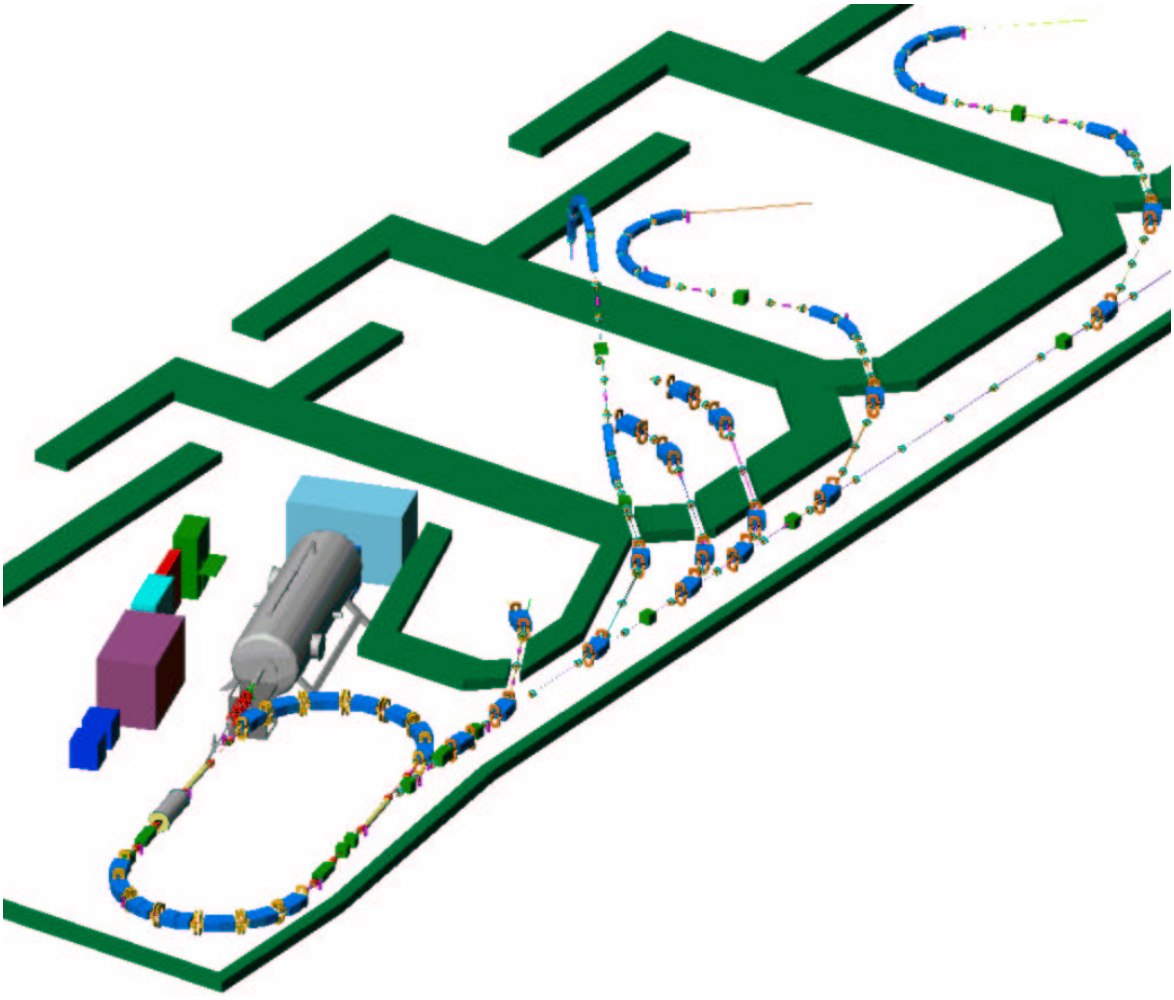

BNL	C.Gardner, S.Peggs (editors), D.Barton, J.Beebe-Wang, M.Brennan, J.Cardona, W.Fischer, D.Gassner, H.Hseuh, J.Kewisch, I.Marneris, G.McIntyre, J.Morris, B.Oerter, D.Phillips, L.Snydstrup, J.Tuozzolo, A.Zaltsman, J.van Zeijts, A.Zhang, S.Y.Zhang, Y.Zhao, N.Tsoupas,
ACCEL	U.Klein, D.Krischel, M.Schillo
AES	A.Favale, T.Myers, J.Sredniawski

March 27, 2003

Contents

1 Introduction

The Rapid Cycling Medical Synchrotron (RCMS) is a state-of-the-art second generation proton synchrotron design, with the primary parameters listed in **Table 1**. A clinical facility based on the RCMS would be the most advanced in the world, capable of treating 200–250 patients per day, operating 16 hours per day, 5 days a week, after a build up of patient numbers over a 1-2 year period. Safe, efficient, reliable patient care is of the utmost importance everywhere, and at all stages, in the RCMS design.

The primary distinguishing feature of the RCMS is the **rapid cycling** oscillation of its main magnets, at a frequency of 30 Hz [1, 2, 3, 4]. The electrical circuit of the RCMS main magnets is very similar to the circuitry of a transformer, leading to very **stable, simple, and reliable** performance. Since the RCMS cycle is about 100 times faster than other "slow cycling" synchrotrons, the number of protons accelerated per cycle can be as much as 100 times smaller, for a fixed treatment time. This leads to three main advantages:

- faster treatment times,
- less beam per cycle, and
- easy, flexible beam extraction.

With much less beam in the accelerator at any time, there is almost **no capacity for a worst case accident**, in which a lot of beam is suddenly and inadvertently dumped into the wrong location in the patient. Low beam intensities also **avoid the ravages of space charge effects,** which at best cause the beam size to increase with intensity, and at worst put a hard limit on the intensity of the beam. Low beam intensities (per cycle) also allow the beam to be extracted from the synchrotron in a single turn of the accelerator, at an energy that can be trivially modified from one cycle to the next. Rapid cycling enables the simplicity and robustness of fast extraction, while delivering the **ultimate energy flexibility. Figure 1** illustrates how the beam extraction energy is trivially adjusted from one synchrotron cycle to the next.

Another distinguishing feature of the RCMS is the **strong focusing** arrangement of its magnetic optics. Combined with the avoidance of space charge effects, with fast extraction, and with the intrinsically small size of the injected beam, this leads to very small beam sizes (of approximately 1 mm). **Small beams** enable **smaller, lighter, and less power-hungry magnets,** not only in the synchrotron, but also in the beam transport lines, and (most critically) in the gantries.

Maximum extraction energy	[MeV]	250
Minimum extraction energy	[MeV]	60
Injection kinetic energy	[MeV]	7
Repetition rate f_{rep}	[Hz]	30
Treatment protons per bunch N, min		1.0×10^7
Treatment protons per bunch N, max		1.7×10^9
Proton flux R, max	[1/min]	3.0×10^{12}
Circumference C	[m]	30.65
Normalized RMS emittance, ϵ	[μm]	0.15

Table 1: Primary parameters of the Rapid Cycling Medical Synchrotron.

1.1 The continuous upgrade path to 3-D stereo-tactic irradiation

First and foremost, the RCMS design is driven by clinical needs and specifications, not only in initial operation, but also in future evolution to sophisticated treatment modalities. The RCMS has been designed with a continuous upgrade path in mind, from the most conventional beam delivery with a passive scatterer, through active scanning, to the future possibility of full 3-D conformal irradiation from many field angles.

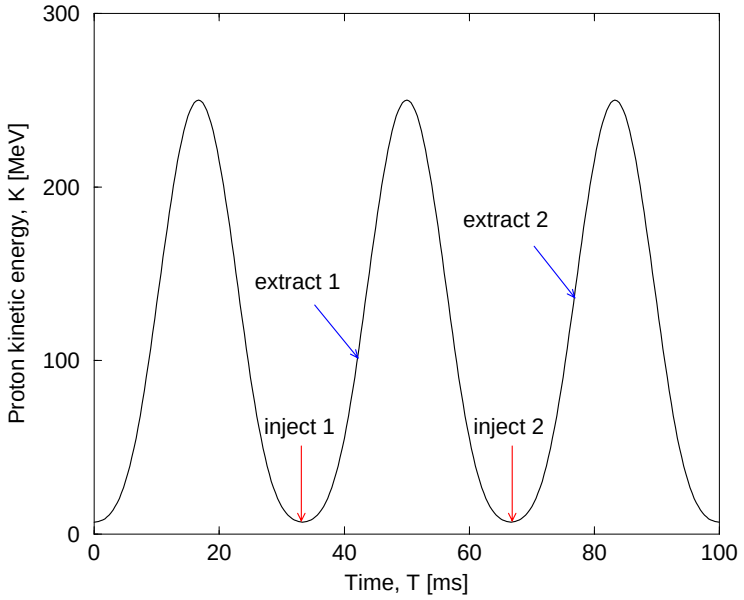

Figure 1: Three cycles of the synchrotron, illustrating the ultimate energy flexibility of the RCMS. Beam is injected at the minimum energy on cycles 1 and 2 ("inject 1" and "inject 2"). The relative timing of the extraction is trivially changed from cycle to cycle, to adjust the extraction energy ("extract 1" and "extract 2").

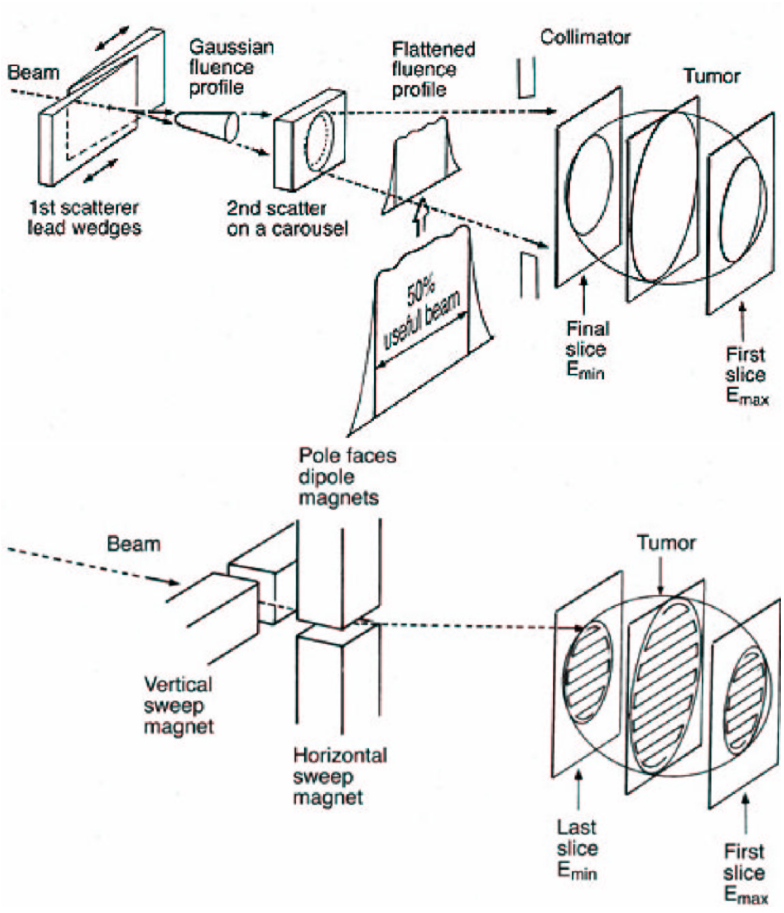

Figure 2: Schematic representation of conventional passive scattering (TOP) and active scanning (BOTTOM).

The incoming beam in many contemporary passive scattering nozzles, such as that shown schematically in **Figure 2**, first encounters an energy degrader that reduces the beam energy to its desired value. This is explicitly unnecessary in the RCMS, thanks to the energy flexibility inherent in its design. By avoiding the unnecessary introduction of material into the path of the beam, the beam size is kept small, even in the patient.

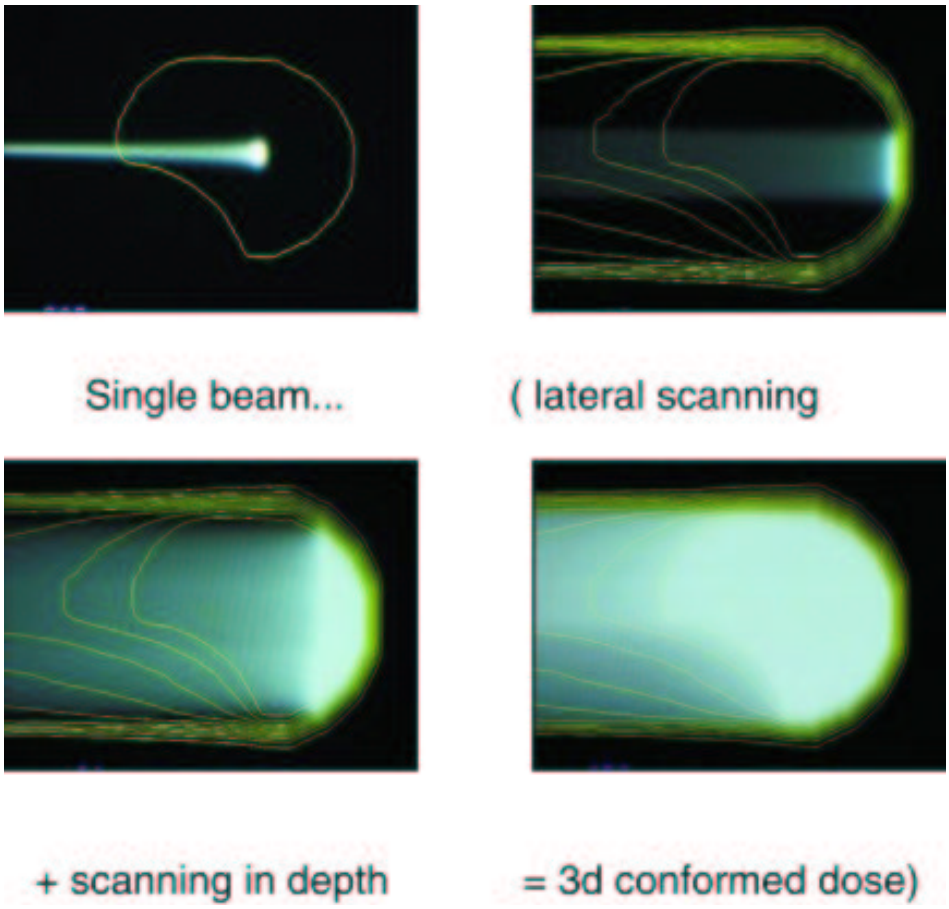

Figure 3: Building up a 3-D conformal dose from a single field in active scanning. (Pedroni et al [5].)

A realistic case of conformal treatment by active scanning from a single field (gantry angle) is shown in **Figure 3**. This shows how the energy is usually set at its maximum value first, while the first transverse scan is performed, and then the energy is gradually decreased. The dose distribution in the tumor contour is very uniform, and there is no dose delivered beyond or to either side of the tumor. Nonetheless, an inevitable result of treatment from a single field – even with active scanning – is that a significant collateral dose is delivered upstream of the tumor.

Figure 4 illustrates how the quality of the dose delivery improves as the treatment modality is upgraded. The yellow contour outlines a tumor that is wrapped around a critical structure, outlined in red. In passive scattering beam delivery from a single field (top left) the dose delivery to the tumor is quite uniform, but the critical structure is not spared, and there is a significant upstream dose. At the other extreme, when the patient is treated by active scanning from three different fields, illustrated by the white arrows (bottom right), the critical structure receives almost no dose, and the collateral dose is better distributed. This illustrates, graphically, why it is important to design a continuous upgrade path into a proton therapy facility right from the beginning. This is the design philosophy of the RCMS.

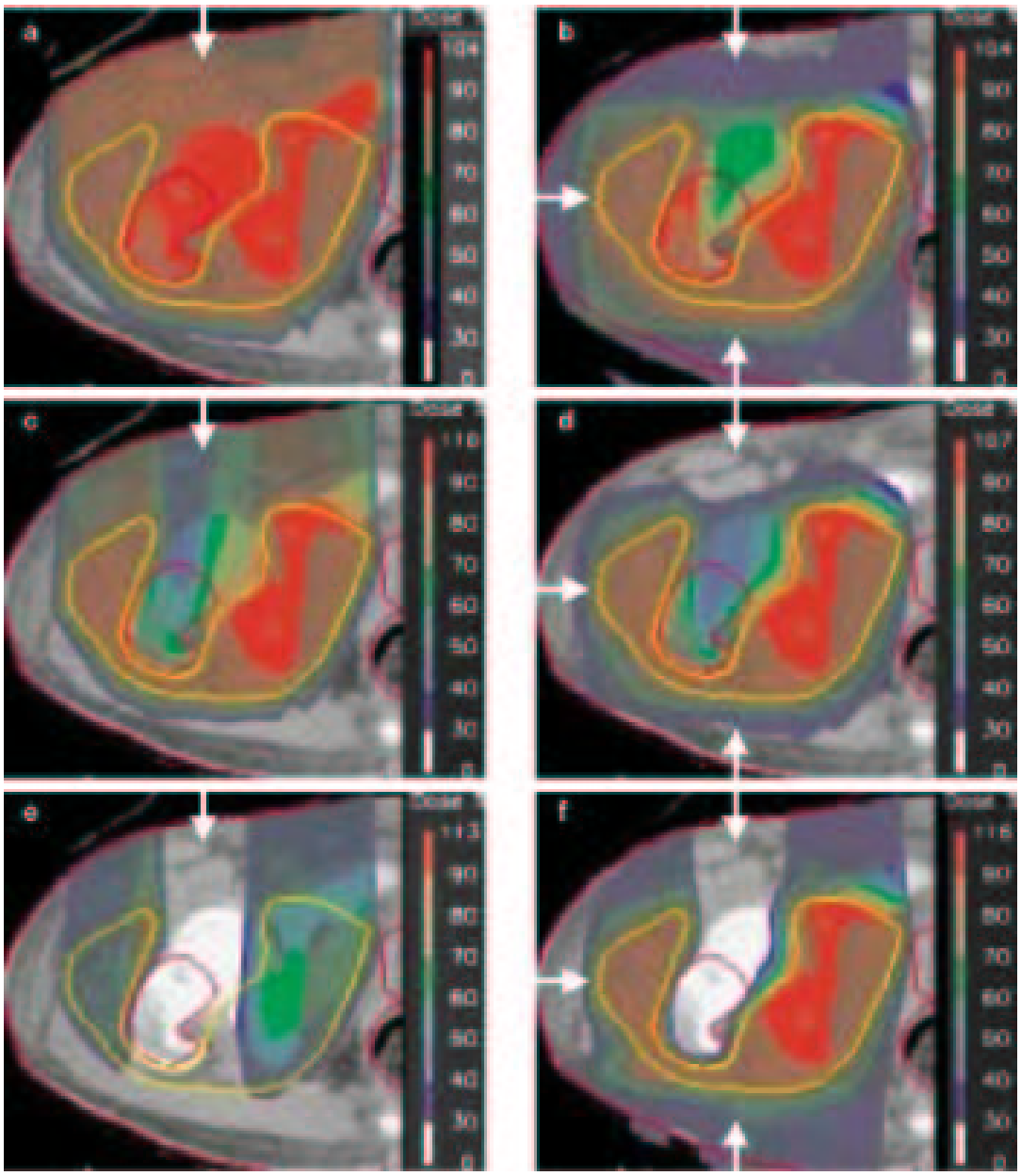

Figure 4: A treatment planning example, from the simplest beam delivery (a single field, passive scattering, in the top left) to the most sophisticated (three fields, active scanning, in the bottom right). The yellow contour outlines a tumor that is wrapped around a critical structure, outlined in red. White arrows indicate the direction of one, or three, treatment fields. The color wash represents the accumulated dose. (Goitein et al [6].)

1.2 Active scanning with pulsed beams

Protons or other ions that enter a patient deposit much of their energy at the end of their range, in a sharp "Bragg peak", as illustrated in **Figure 5** (LEFT). This behavior gives protons a unique advantage over conventional radiation therapy with X-rays, electrons, or neutrons. The Bragg peak for neon (or Carbon) ions is sharper than for protons, enhancing their clinical desirability. However, ions other than protons deliver a significant dose beyond the sharp distal edge of the proton Bragg peak (beyond 16 cm in **Figure 5**), due to the creation of "knock-on" nuclear fragments. Protons also have the advantage of requiring far less bending magnetic field (measured in Tesla-meters) to achieve the same penetration.

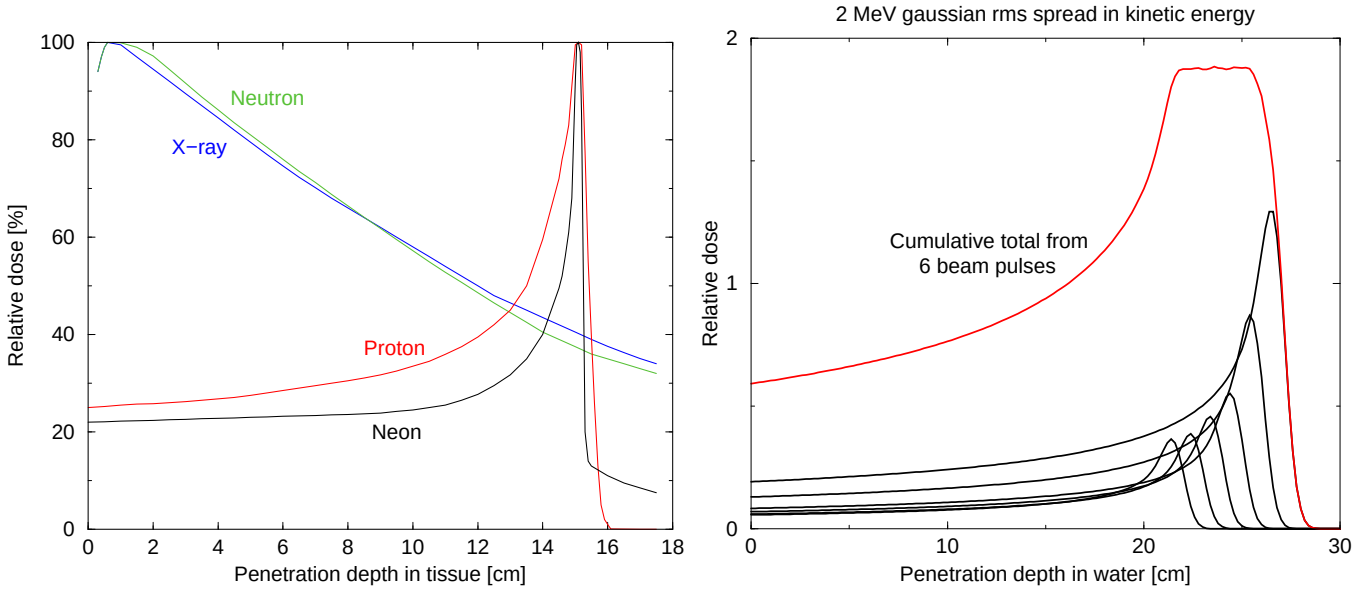

Figure 5: LEFT: Dose versus depth, showing sharp Bragg peaks for protons and neon ions, and poor penetration for X-rays and neutrons. RIGHT: A "Spread Out Bragg Peak", accumulated by scanning the beam energy in 2 MeV steps.

When active scanning is performed, a proton beam pulse extracted from the RCMS encounters almost no extraneous material before it enters the patient. In this case there is essentially no increase from the small energy spread and small transverse beam size that are intrinsic to the RCMS design, and the most precise stereo-tactic irradiation is possible – within fundamental physical limits. For example, the width of the Bragg peak shown in **Figure 5** (LEFT) is due purely to the "energy straggling" statistical fluctuations that accumulate as the protons traverse the patient, with no contribution from the energy spread of the incoming beam. **Figure 5** (RIGHT) shows how the dose from successive beam pulses accumulates during active scanning to treat a tumor, by scanning the beam energy in 2 MeV steps. This creates a spread out Bragg peak that is approximately 4 cm deep, since the depth of each voxel is about 0.7 cm. Similarly, "multiple Coulomb scattering" fluctuations cause the transverse beam size to grow and become significant, even for an idealized incoming beam with zero initial size. For example, **Figure 6** (LEFT) shows that a proton bunch with a kinetic energy of 175 MeV accumulates a width of 0.5 cm by the end of its 20 cm range. **Figure 6** (RIGHT) shows how a beam that is scanned horizontally (or vertically) in steps of one beam width yields a remarkably flat total dose profile.

In the particular example illustrated by **Figures 5** and **6**, with the sharpest possible 175 MeV voxels (0.7 cm $\times$ 0.5 cm $\times$ 0.5 cm) about 600 beam pulses are used for one scan over a tumor with a volume of 100 cc. This takes about 20 seconds per pass. In practice it is likely that such sharp beam pulses will only be used for small tumors, and near the surface of typical or large tumors. The scanning nozzle optics are readily tuned to deliver beam in larger voxel volumes, for most of the beam pulses. For example, using round numbers, a one liter tumor can be treated in 1,000 pulses delivered to voxels that have an average volume of 1 cc. This takes about 35 seconds per pass.

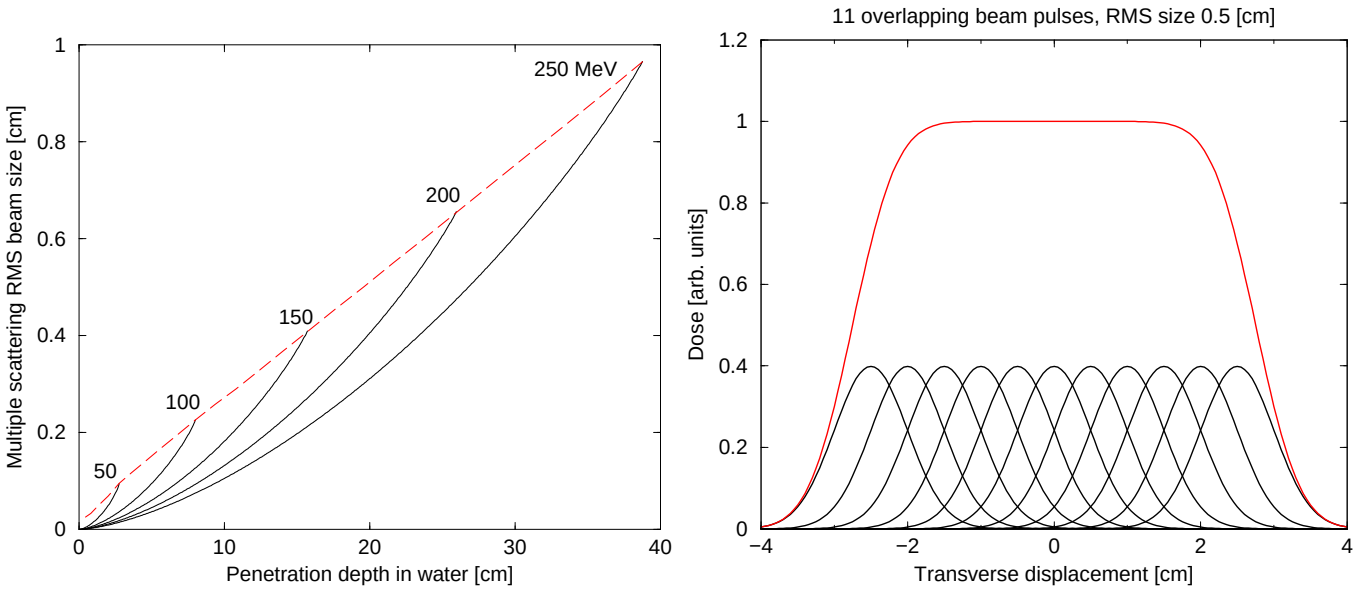

Figure 6: LEFT: Transverse proton beam size due to "multiple Coulomb scattering" versus depth in water. RIGHT: Discrete beam pulses overlapping transversely to irradiate the entire tumor.

1.3 Facility overview

The RCMS footprint shown in **Figure 7** contains an injector, a synchrotron accelerator, and a switchyard feeding independent beam lines in one research room and five treatment rooms. Perspective views of some of the major beam delivery systems are shown in **Figure 8**.

Four of the five treatment rooms have rotating gantries. The first two gantries to be installed will use passive scattering. These first two gantries can be upgraded to use beam scanning at a later date. The third gantry will be installed with a scattered or scanned beam depending on the availability of reliable and suitably proven scanning technology at the time of installation. It, too, can be upgraded to a scanned beam at a later date. The fourth gantry will be installed using a scanned beam. The fixed beam treatment room has three beam lines – a small field beam line directed to a chair for eye treatments and two orthogonal (horizontal and vertical) large field beam lines. A research room is available for research and calibration purposes, with a entrance separate from the patient areas. This research room includes a switching magnet capable of bending the incoming by 30 degrees, between two independent beam lines.

The treatment rooms, and in particular the gantry rooms, are laid out in a linear fashion, so that routine operation is possible even with a partial complement of finished rooms. It will be possible to run beam into the initial fixed beam and gantry rooms while the rest of the facility is being constructed. The facility is designed so each component treatment room operates independently of the others – it is possible to remove one beam line from service without affecting the rest of the facility.

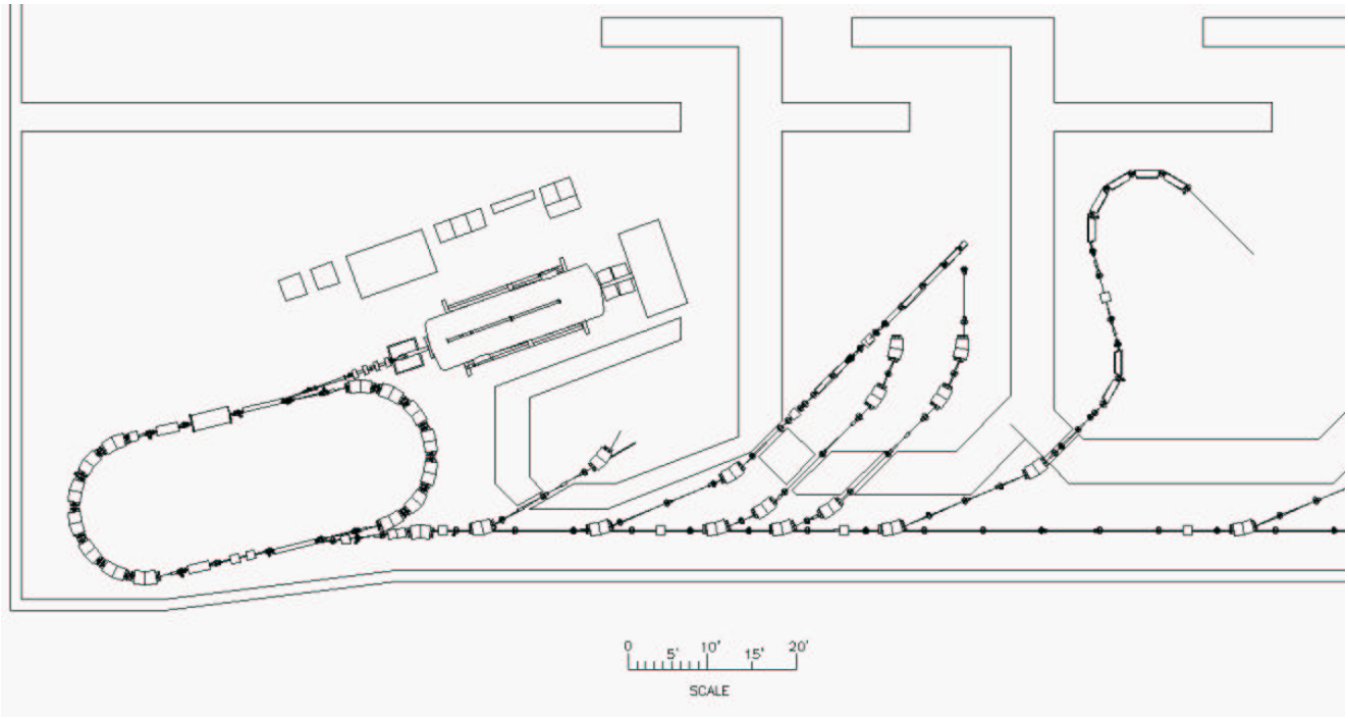

Figure 7: Plan view of the RCMS facility. The entire facility, with 4 gantry rooms, fits in a footprint of approximately 20 m by 80 m.

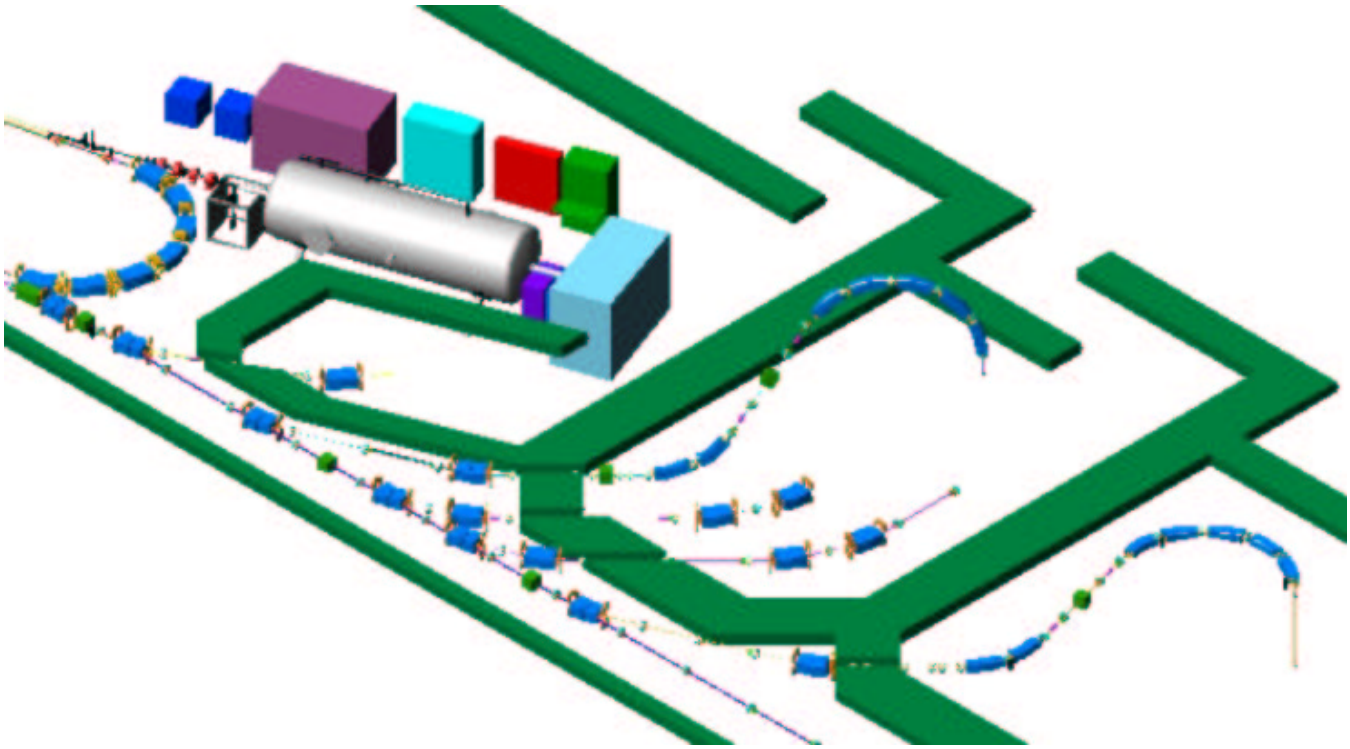

Figure 8: Perspective view of the RCMS, showing the injector, the research room, the fixed beam room, and the first gantry room.

2 Clinical specifications

2.1 Scope of the conceptual design

1. The *Conceptual Design of the RCMS* is a technical description of a proton therapy facility based on a 30 Hz strong focusing rapid cycling fast extraction synchrotron.

2. The technical description includes conceptual designs for an injector, RF system, magnets, power supplies, instrumentation, vacuum systems, injection and extraction, beam dumps, switchyard, fixed beam delivery lines, and gantries.

3. The gantries are capable of supporting either double scattering nozzles or scanning nozzles, and can be upgraded from the former to the latter. Feedback to gate beam delivery on patient breathing is available.

4. The integrated control system includes the *Treatment Control System*, *Dispatcher System*, *Accelerator Control System*, and the *Safety and Monitoring System*. It does not include a *Treatment Planning System* or a *Personnel Access Safety System* for public and employee safety, although interfaces are present for both. (See Section 2.2.3, and Chapter 10.)

5. This version of the report does not include detailed nozzle designs, nor does it include CT scan equipment, alignment equipment, or patient couches.

6. Cost and Schedule information available under separate cover includes:

   (a) Beam facility installation.

   (b) Utility installation, not including civil construction. For example, the cost of installing resonant power supplies is available, but not the cost of installing the transformer pads that deliver them power.

   (c) Beam component water cooling installation, but not air conditioning chillers.

   (d) Commissioning the entire facility through first patient treatment.

   (e) Contingencies in cost and schedule, and escalation costs, corresponding to a nominal funding profile.

2.2 Machine and beam lines

1. **Energy and energy width**

   (a) The kinetic energy of the beam entering the nozzle is variable between a minimum of 60 MeV and a maximum of 250 MeV. This maximum corresponds to a range in the patient greater than 30 cm after passive scattering for field sizes less than 20 cm $\times$ 20 cm. For a scanned beam the range in the patient is greater than 30 cm.

   (b) The facility could be made more capable of full depth proton radiography by raising the maximum energy to about 270 MeV.

   (c) Energy steps of much less than 1 MeV are possible. A 1 MeV energy step size defines the distal range to about 1 mm at 60 MeV and 2.5 mm at 220 MeV.

   (d) The time to change the treatment energy by 10 MeV in scanning mode is less than 1 s.

   (e) Between patients the time to change the energy over the entire range available is less than 30 s.

   (f) The beam transport lines act as independent magnet aperture systems that verify the beam energy and define the maximum energy spread of the beam delivered to the patient.

   (g) The beam energy spread is less than 0.1% Full Width at Half Maximum as it enters the treatment room.

2. **Dose rate and intensities**

   (a) When passive scattering is used, at least 3×10^{12} protons per minute (1.7×10^{9} protons per pulse at 30 Hz) are available to be delivered to the scattering foils. This intensity delivers 2 Gy/minute to a 1 liter treatment volume, after passive scattering losses are taken into account.

(b) The beam intensity is regulated and controlled at the level of 10^8 protons when scattering is used, controlling the dose to small fields at the 2 cGy level.

(c) In scanning mode, an intensity of more than 5×10^{11} protons per minute is delivered, corresponding to a dose rate of up to 20 Gy/minute to a 1 liter treatment volume with an *average* of 3×10^8 protons per pulse at 30 Hz.

(d) In spot scanning, the intensity is regulated so that the number of protons per pulse is controlled over a range from a minimum of 1×10^7 to a maximum of 1×10^9 protons per pulse.

3. **Personnel safety**

(a) The integrated design of the *Personnel Access Safety System* is the joint responsibility of the Medical Center and the RCMS consortium, since it must be customized for each specific implementation.

(b) ALARA principles are followed to minimize the exposure of workers and the general public.

(c) Both manual and automatic "emergency off" interfaces will be present in each treatment room, and at the console, to inhibit extraction of beam from the accelerator.

(d) The design of the facility minimizes the activation of materials so there is no unnecessary exposure to personnel or patients, and to ensure there are no delays when the equipment needs to be serviced.

(e) All applicable safety requirements, by the Medical Centers own radiation safety committee and by the State, will be met.

(f) Alarm dosimeters, warning lights, emergency-off buttons, interlocks, and control system monitoring of these items are required.

(g) A means to observe and communicate with the patient in the treatment room, and with the collision prevention system, is provided.

(h) The design of shielding to protect personnel and visitors is the responsibility of the Medical Center.

4. **Uptime and availability**

(a) The facility will operate 16 hours per day, 5 days a week, year round. Preventive maintenance is performed only during the 8 hours available at night, or on weekends.

(b) The accelerator will deliver beam to the treatment rooms within 30 minutes after being switched on from standby mode. There is no manual tuning of the beam after the morning warmup.

(c) Up-time availability will be greater than 98% during scheduled operation.

(d) High availability in general precludes the possibility of performing beam diagnostic studies in *maintenance mode* in between patient treatments, since a somewhat lengthy re-verification is likely to be required whenever moving from *maintenance mode* to *treatment mode*.

(e) The accelerator is designed so that no regular maintenance causes the machine to be down for more than 60 consecutive hours (Friday night to Monday morning).

(f) There is no scheduled interruption of patient treatment for maintenance, except for a small number of planned 3 day weekends throughout the year that coincide with holidays.

2.3 Nozzles

1. **Passive scattering**

(a) If desired, the gantries can be slightly enlarged to provide 4 meters of free space between the first scattering foil and the isocenter.

(b) There is a separate beam line in the fixed beam room for eye treatments, with a maximum diameter of less than 5 cm.

(c) The beam size at the first scattering foil is less than 7 mm FWHM with directional control to ensure that the centroid position at the second scattering foil is located with an accuracy of 0.5 mm.

(d) The beam position will be stable to satisfy dose field uniformity requirements, ensuring that the beam is correctly aligned with the scattering foils. Beam delivery will terminate if dose flatness and symmetry conditions are not met.

(e) At least three independent dosimetry systems will be present, to ensure beam uniformity and position, and to monitor the total integrated dose at the 0.1 cGy level.

2. **Spot scanning**

(a) The gantries permit field sizes of 40 cm × 30 cm.

(b) The beam uniformity is better than ±2% over the central 80% of the lateral beam profile, and ±2% along the whole length of the SOBP.

(c) The maximum allowed difference between symmetric points is <2% and the largest deviation compared to the central axis is <2%.

(d) The dose is nominally delivered in 3 complete volume scans.

(e) The energy variation over the field diameter is $\ll$0.5 MeV.

(f) The size of the scanned beam is <7 mm FWHM at the exit of the gantry, and <10 mm FWHM at isocenter, in the absence of scattering material.

(g) The beam is scanned with a transverse accuracy of ±0.5 mm on each of the orthogonal scanning axes, measured at the plane of the isocenter.

(h) At least four independent dosimetry systems will be present, with two independent monitoring channels, to ensure beam intensity uniformity, to monitor the total integrated dose delivered to the treatment volume within a precision of 0.1 cGy, and to monitoring beam position with an accuracy of ±0.5 mm on both orthogonal axes at the plane of the isocenter.

2.4 Treatment rooms

1. **Gantry rooms**

(a) There will be four gantry treatment rooms. The first two gantry rooms will be commissioned with passive scattering, but will be upgradable to scanning. If the third gantry room is commissioned with a passive scattering nozzle, it too will be upgradable. The fourth gantry will be commissioned with a scanning nozzle.

(b) The gantries are movable from both the treatment room and the console area. They move only when a dead-man switch is pressed, and stop within 1 degree when the dead-man switch is released.

(c) The gantries rotate ±200 degrees from the vertical.

(d) Full rotation is possible within 1 minute, with a setting accuracy of ±0.1 degree.

(e) The intersection of the central axis of the beam and axis-of-rotation of the gantry is contained within a 1 mm diameter sphere as the gantry rotates.

(f) Collision sensors will stop couch, nozzle, and gantry movement when activated.

2. **Fixed beam and research rooms**

(a) The sole fixed beam treatment room will have three beam lines. One is for low energy eye treatments with the patient in a chair, while the other two are for full energy horizontal or vertical delivery to a patient on a couch.

(b) The eye beam line generates a beam up to 5 cm diameter that is uniform to ±3% in the central 80% of the beam profile.

(c) The eye beam line can treat to a depth of 5 cm.

(d) A dual dosimeter system monitors the dose and terminates the beam if the uniformity is outside flatness and symmetry requirements.

(e) A machined aperture can be positioned on the eye beam line within 5 cm of the patient.

(f) The research room will have two independent horizontal beam lines, without nozzles, digital imagers, or multi-leaf collimators.

3. **Beam gating**

(a) It is possible to switch the beam on and off synchronously with the patient breathing, assuming that a device is available to generate a signal at precise points in the breathing cycle, via a standard logic signal into the *Treatment Control System*.

(b) When indicated, the beam is shut off or turned on within 33 ms, one cycle of the RCMS.

2.5 Control systems

1. The control systems monitor and adjust the operation of the entire proton delivery system to deliver beam in a fail-safe manner, allowing no beam to the patient when any of the monitors are out of specification or unable to be accessed.

2. In general the design of the control systems follows LBL Report #33749, *Performance Specifications for a Proton Medical Facility* [7].

3. An interface to a *Record and Verify* system ensures that all of the machine settings agree with the patient treatment plan, before treatment is enabled.

4. Information about each treatment is reported to the *Record and Verify* system.

2.6 Installation, commissioning, and maintenance

1. The RCMS consortium is responsible for the installation of the proton accelerator, beam lines, gantries, nozzles, and associated hardware, including spare parts for facility maintenance.

2. Acceptance testing will provide measured data showing the *clinical specifications* described above have been met.

3. Initial commissioning is a primary responsibility of the RCMS consortium, including coordination with the medical physicists who are commissioning the *treatment planning system.*

4. One gantry, one fixed beam room beam line, and the research room beam lines, will be completed and fully operational on the first day the facility opens for patient treatment.

5. The other rooms will be completed and commissioned sequentially, without interfering with the routine daily operation of the facility.

6. It is possible to remove a beam line from service to perform routine maintenance without affecting the rest of the facility.

7. Routine operations and maintenance, in a warranty and service contract, will be performed by a permanent local support group reporting directly to the Medical Center. This group is not necessarily any member of the RCMS consortium.

8. The RCMS consortium will remain available, after stable operations have been established, to support appropriate non-routine interventions and facility developments.

3 Synchrotron

Figure 9 shows the racetrack footprint of the synchrotron, consisting of two straight sections and two 180 degree arcs. Each straight section contains five half-cells without dipoles and each arc consists of seven half-cells with combined function dipoles. The straight sections accommodate the functions of injection, extraction, and acceleration. Primary physical and optical parameters for the synchrotron are listed in **Table 2**.

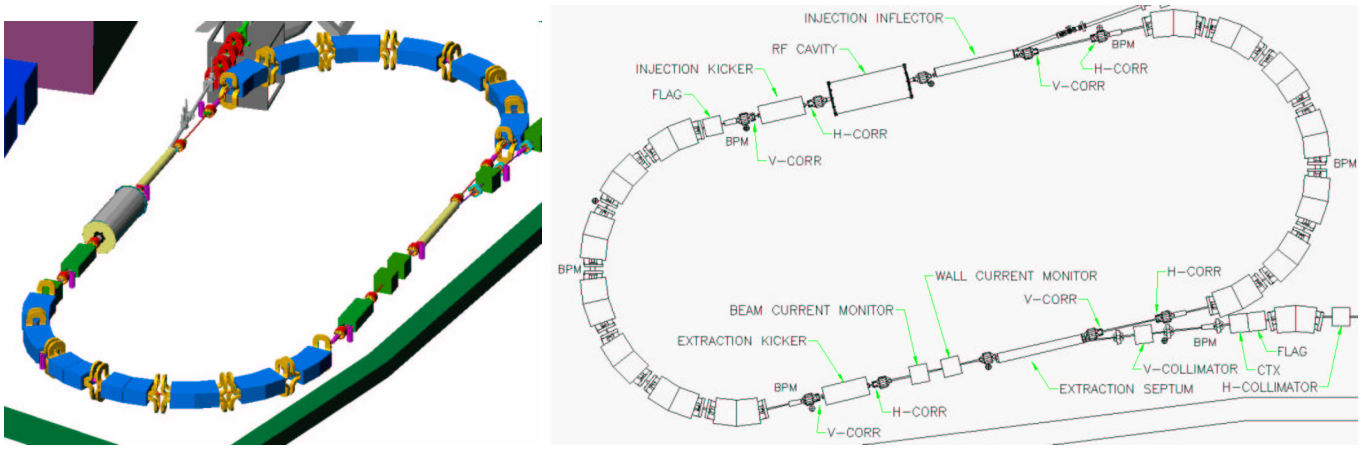

Figure 9: Perspective and plan views of the racetrack layout of the synchrotron.

Figure 10 displays the combined function main magnet that is the sole optical component of the arcs. It comes in focusing (F) and defocusing (D) styles that differ only slightly in the 2-D cross section of the magnet laminations. The quadrupole magnet shown in **Figure 11** is used in the straight sections. The optical lattice also includes a modest number of dipole correctors and Beam Position Monitors (BPMs). Each BPM is integrated into the vacuum pipe near the RCMS quadrupoles. Only one type of each of these magnets (and diagnostics) is used, simplifying the design and reducing the required number of spares.

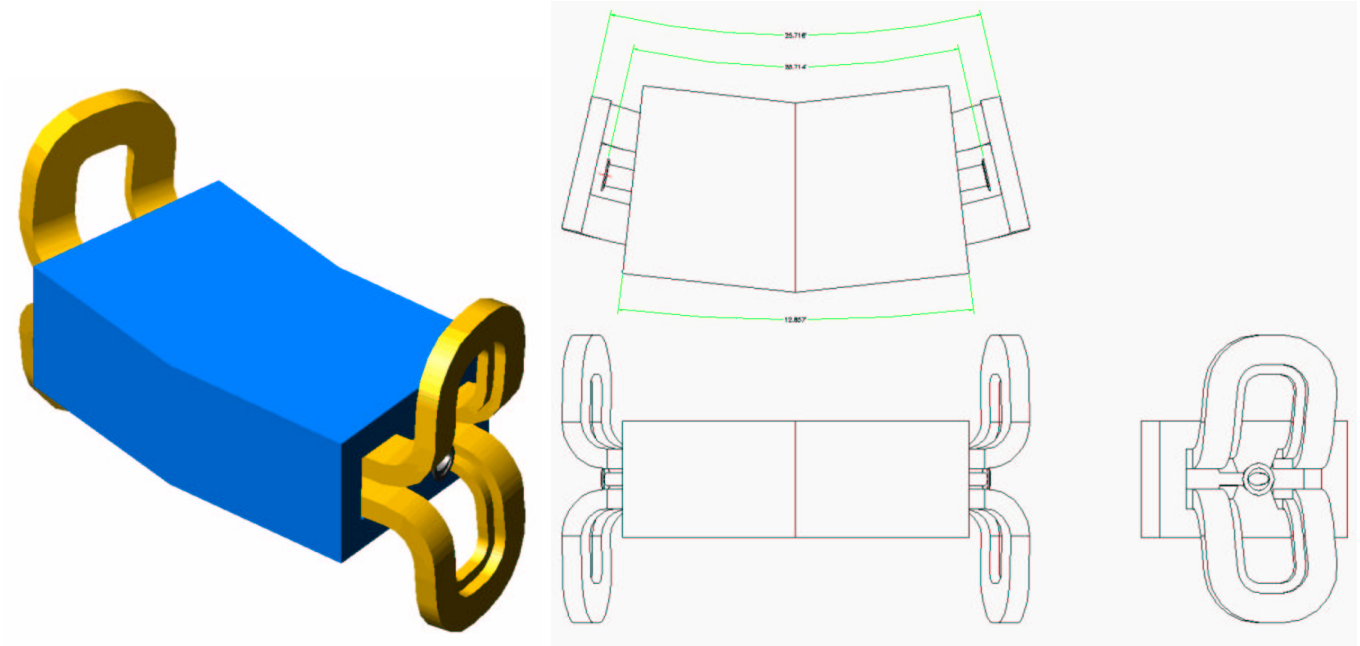

Figure 10: Perspective and plan views of the combined function magnet used in the synchrotron arcs.

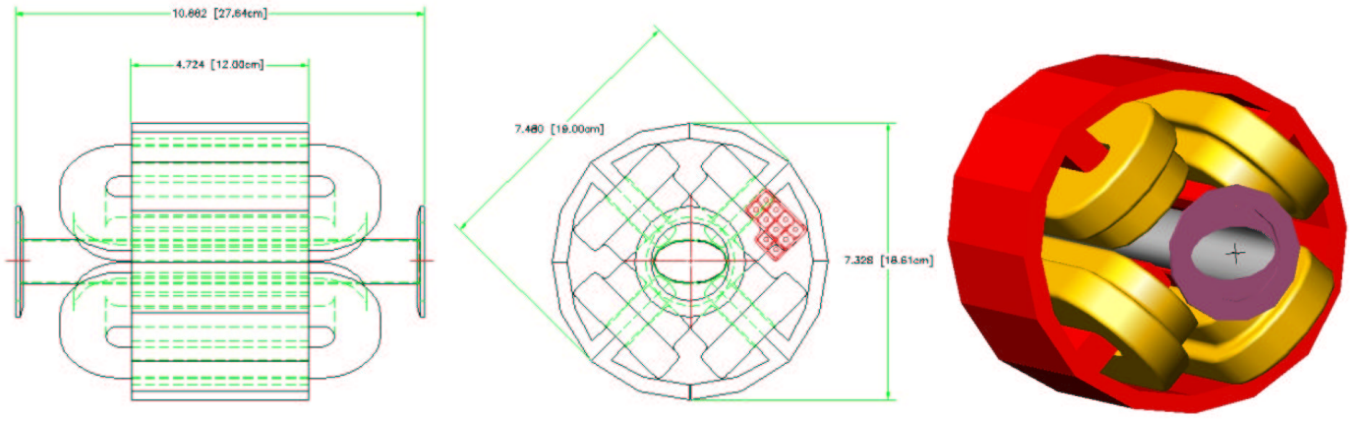

Figure 11: Plan and end views of the quadrupole used in the straights of the synchrotron.

Circumference, C	[m]	30.65
Number of FODO cells in the arcs		7
Half-cell length in the arc	[m]	1.1
Maximum distance between quadrupoles	[m]	1.8
Dipole magnetic length	[m]	0.760
Quadrupole magnetic length	[m]	0.14
Injection pulse length, Δt [ns]		25–100
Injection pulse current [mA]		0.06–2.72
Normalized rms emittance, ϵ [μm]		0.15
Momentum width at injection (rms), σ_p/p		0.001
Total momentum width at injection, $\Delta p/p$		$\pm$0.0023
Total kinetic energy width at injection, ΔK [keV]		$\pm$32
Horizontal tune, Q_x		3.38
Vertical tune, Q_y		3.36
Average phase advance per cell, Horizontal (Arcs)	[deg]	108
Average phase advance per cell, Vertical (Arcs)	[deg]	92.16
Max. horizontal beta function, β_{xmax}	[m]	5.79
Max. vertical beta function, β_{ymax}	[m]	6.23
Max. dispersion function, η_{max}	[m]	2.01
Natural horizontal chromaticity, ξ_x		-1.48
Natural vertical chromaticity, ξ_y		-4.14
Transition gamma, γ_T		2.72

Table 2: Primary physical and optical parameters of the RCMS synchrotron, lattice version 2.1.

Variation of the extraction energy is achieved by adjusting a trigger based on the RF frequency to control the extraction time. This avoids the necessity for energy degraders, delivering high quality beam with better resolution and few losses. Although the excitation of the transport line magnets needs to change in proportion to the extraction momentum, the transport lines are designed to be insensitive to momentum matching errors and magnet settling effects, since they are achromatic and (mostly) dispersionless.

3.1 Optics

The dispersion at the entrance and exit points of the arcs is zero, so the straight sections are dispersion free. The dispersion matching in the arcs is performed by choosing suitable values for the quadrupole components of the two different kinds of combined function dipole. The quadrupole components have also been chosen to make the beam size as small as possible. Since the half cells in the straight sections are longer than those in the arcs, it is necessary to match the beta functions between the arcs and the straight sections. Due to the symmetry of the lattice displayed in **Figure 12,** the matching is exactly the same on both sides of the ring. This minimizes the number of power supplies required in the ring [8]. One half-cell in one straight is occupied by a radio frequency cavity. Each straight has a fast kicker and a septum magnet separated by one half-cell.

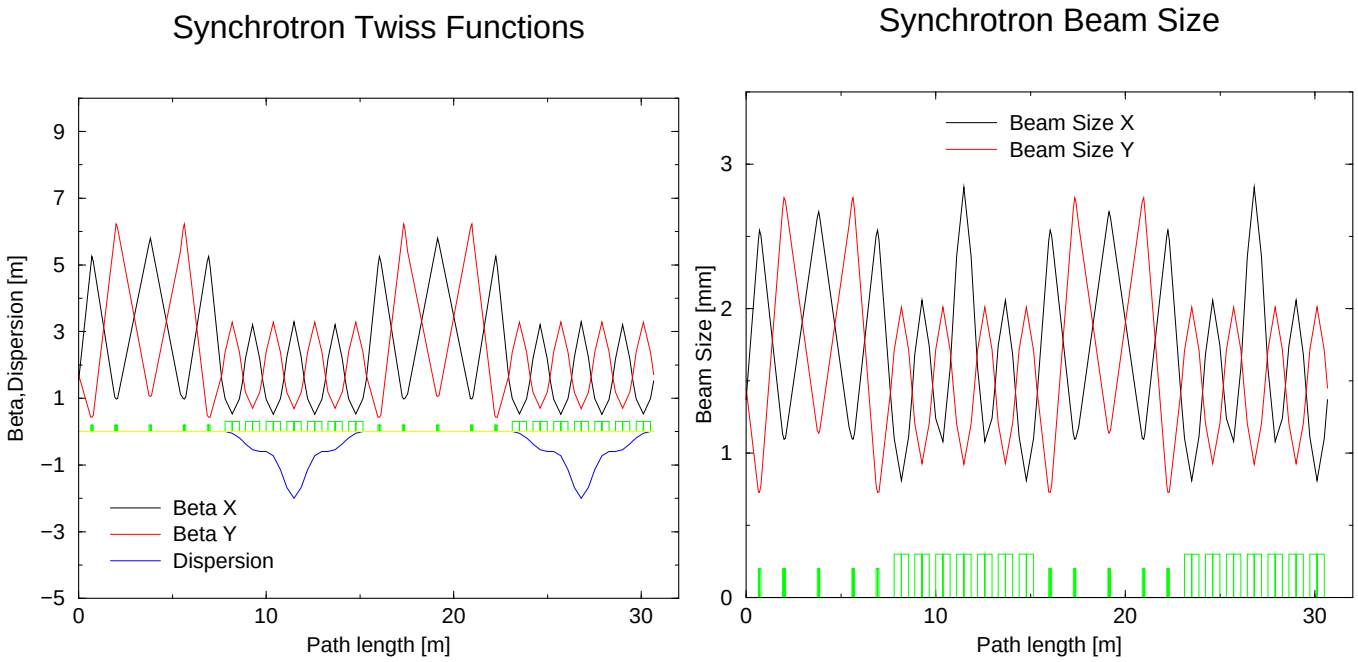

Figure 12: Synchrotron optical functions, and beam sizes at injection, in RCMS lattice version 2.1.

Table 2 lists a selection of parameters that summarize the optical functions of the synchrotron. **Figure 12** shows both optical functions – β_x and β_y, and the horizontal dispersion η – and also the beam sizes (at injection) around the synchrotron. The horizontal and vertical root mean square (rms) beam sizes σ_x and σ_y are related to the optical functions as follows:

$$\sigma_x = \left(\frac{\beta_x \epsilon}{(\beta\gamma)} + \left(\eta \frac{\sigma_p}{p} \right)^2 \right)^{1/2} \quad (1)$$

$$\sigma_y = \left(\frac{\beta_y \epsilon}{(\beta\gamma)} \right)^{1/2} \quad (2)$$

where the normalized emittance ϵ is taken to be the same in both planes, σ_p is the rms momentum spread, and $(\beta\gamma)$ is a relativistic Lorentz factor. The second term in the brackets is absent in the vertical case because the vertical

dispersion is zero. **Table 3** lists the expected beam sizes and other parameters at 3 times corresponding to injection, minimum extraction energy, and maximum extraction energy, using the beam parameters from **Table 2** and the optical parameters shown in **Figure 12.** Note that the "maximum dispersive size" is a full width value that depends on beam evolution in longitudinal phase space, discussed in Chapter 6.

		injection	**minimum**	**maximum**
Kinetic energy, K	[MeV]	7.0	60.0	250.0
Momentum, p	[MeV/c]	114.8	340.87	729.1
Lorentz γ		1.0075	1.0639	1.2664
Lorentz β		0.122	0.3415	0.614
Revolution frequency, F_{rev}	[MHz]	1.188	3.340	6.002
Revolution period, T_{rev}	[μs]	0.842	0.300	0.166
Rigidity, $B\rho$	[Tm]	0.383	1.137	2.432
Dipole field, B	[T]	0.226	0.671	1.436
Normalized rms emittance	[μm]	0.15	0.15	0.15
Unnormalized RMS emittance ϵ_u	[μm]	1.22	0.413	0.193
Max vertical rms beam size	[mm]	2.76	1.60	1.10
Max horizontal rms beam size	[mm]	2.66	1.55	1.06
Max dispersive (horz) size, HWFM	[mm]	6.50	2.67	0.97

Table 3: Kinematic and beam parameters at injection, at the minimum extraction energy, and at the maximum extraction energy at the top of the ramp.

3.2 Acceleration cycle

A single resonant power supply drives all the synchrotron bending magnets in series, combining a sinusoidal alternating current of amplitude I_{AC} with a constant direct current I_{DC}, so that the total bending magnet current is

$$I(t) \;=\; I_{DC} \;-\; I_{AC}\,\cos(2\pi f_{rep} t) \tag{3}$$

Injection occurs at $t = 0$ when the current $I = I_{DC} - I_{AC}$ is at its minimum. Extraction may occur at any time between $t \approx 7$ ms and $t = 16.7$ ms, when the kinetic energy K is in the range 60 to 250 MeV. This is illustrated in **Figures 1** and **13**. The magnetic field B in the bending magnets, and the beam momentum P are both proportional to the main magnet current (except for small saturation effects). **Figure 13** plots these quantities, the kinetic energy K, and other parameters of interest, as a function of time in the acceleration cycle. Many of these quantities are also listed quantitatively in **Table 4**. The energy for proton beam acceleration is supplied by a single Radio Frequency (RF) cavity, with a voltage that varies sinusoidally during the acceleration half of the magnetic cycle, as shown on the right of **Figure 13**. The RF system and beam performance in longitudinal phase space are discussed at greater length in Chapter 6.

Figure 14 (LEFT) shows the evolution during acceleration of the three contributions to beam size, at the different locations in the synchrotron where each one of them is a maximum. The maximum horizontal and vertical RMS betatron sizes occur in the straights, where the beta functions β_x and β_y take their maximum values, but where the dispersion is zero. The maximum dispersive (horizontal) size occurs in the arcs, where the dispersion has its maximum value but the beta functions are modest. Note that the dispersive size is a full size that contains 100% of the momentum spread of the beam.

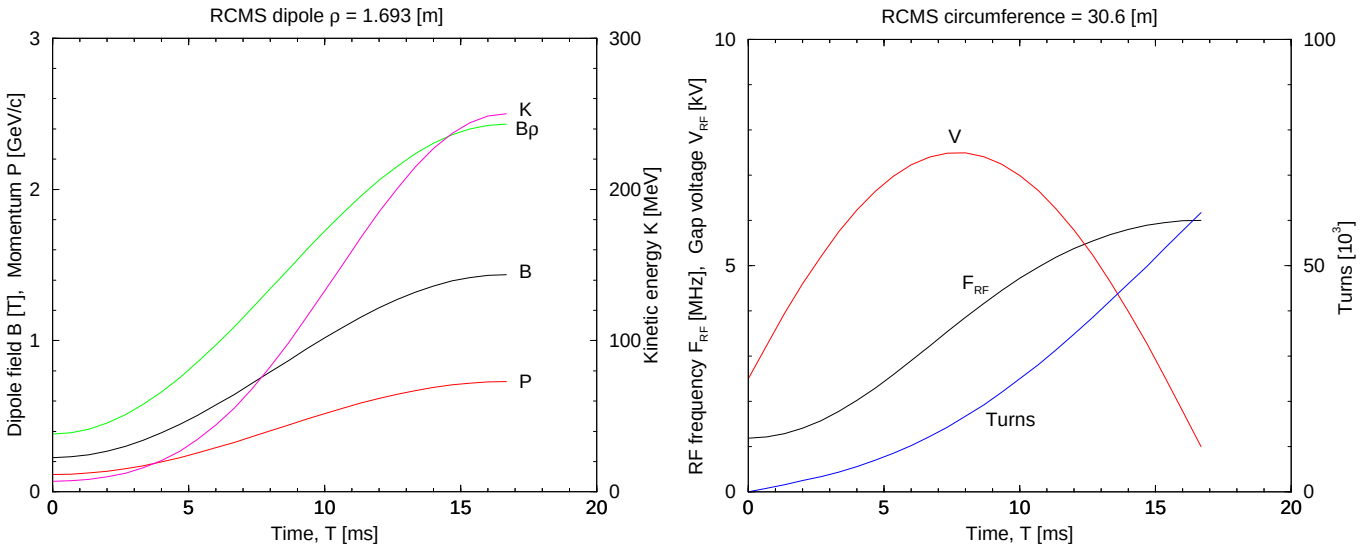

Figure 13: Key parameters in the acceleration cycle. LEFT: dipole field B, rigidity $B\rho$, kinetic energy K, and momentum P, in the acceleration (rising) phase of a synchrotron cycle. RIGHT: RF frequency F_{RF}, RF gap voltage V_{RF}, and total number of turns, for the nominal RCMS ramp.

T ms	B T	$\dot{B}$ T/s	$\dot{B}/B$ Hz	β	γ	K MeV	P MeV/c	F_{rev} MHz	Turns	V_{rf} kV	ϕ_s deg
0.000	0.226	0.0	0.0	0.121	1.007	7.00	114.82	1.188	0	2.500	0.0
1.000	0.237	21.4	90.2	0.127	1.008	7.68	120.27	1.244	1198	3.595	17.4
2.000	0.269	42.0	156.3	0.144	1.011	9.86	136.39	1.407	2489	4.598	26.8
3.000	0.320	61.1	190.7	0.171	1.015	13.99	162.64	1.671	3977	5.484	33.0
4.000	0.390	78.1	200.1	0.207	1.022	20.68	198.07	2.020	5758	6.229	37.7
5.000	0.476	92.3	194.0	0.249	1.033	30.57	241.44	2.438	7913	6.816	41.5
6.000	0.574	103.2	179.9	0.296	1.047	44.15	291.20	2.899	10503	7.227	44.6
7.000	0.681	110.5	162.3	0.346	1.066	61.62	345.59	3.381	13562	7.454	47.2
8.000	0.793	113.8	143.5	0.394	1.088	82.76	402.69	3.858	17103	7.491	49.3
9.000	0.907	113.1	124.7	0.441	1.114	106.90	460.48	4.309	21114	7.336	50.7
10.000	1.018	108.5	106.5	0.483	1.142	132.96	516.89	4.720	25563	6.993	51.6
11.000	1.123	99.9	89.0	0.519	1.170	159.54	569.95	5.078	30407	6.471	51.6
12.000	1.217	87.9	72.2	0.550	1.197	185.11	617.77	5.379	35589	5.784	50.8
13.000	1.297	72.7	56.0	0.575	1.222	208.10	658.65	5.620	41053	4.949	48.8
14.000	1.361	54.9	40.4	0.593	1.242	227.07	691.14	5.801	46738	3.988	45.1
15.000	1.407	35.2	25.1	0.606	1.257	240.84	714.10	5.924	52584	2.924	38.4
16.000	1.431	14.3	10.0	0.612	1.265	248.52	726.71	5.990	58534	1.786	24.5
16.667	1.436	-0.0	-0.0	0.614	1.266	250.00	729.13	6.002	62530	1.000	0.0

Table 4: The main accelerator and beam parameters during the acceleration phase of the synchrotron cycle.

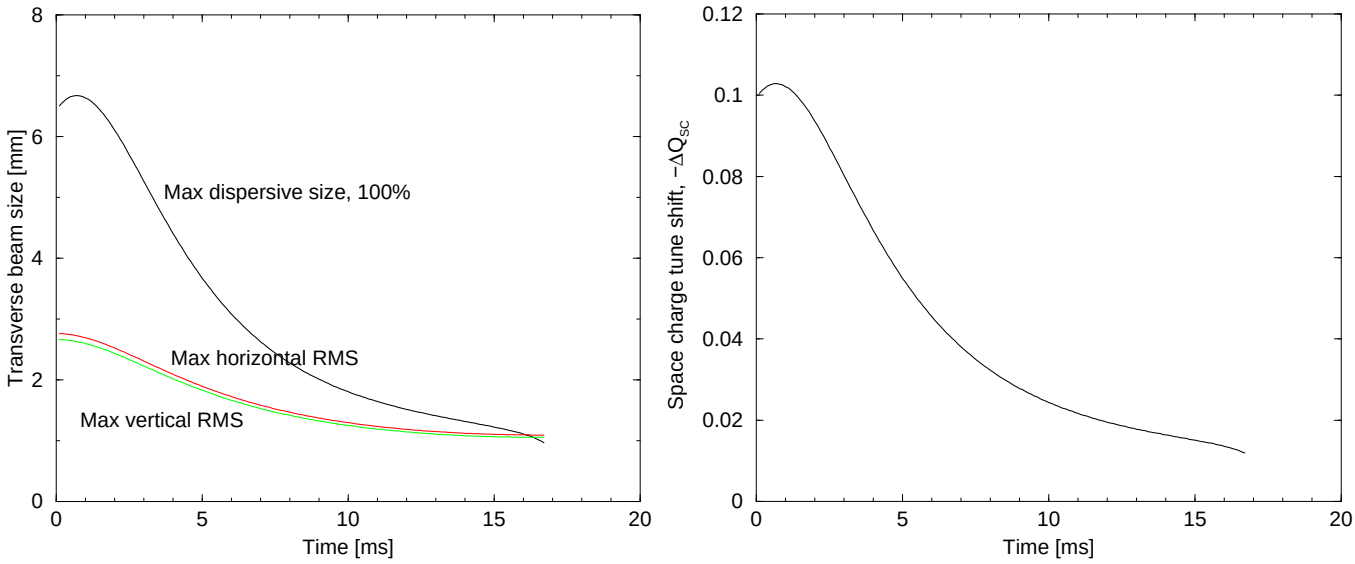

Figure 14: Transverse beam parameters in the synchrotron cycle. LEFT: The maximum rms horizontal and vertical betatron beam sizes, at locations in the straights, and the maximum full (horizontal) dispersive beam size, in the arcs. RIGHT: Transverse space charge tune shift for a maximum intensity bunch, with no transverse emittance blowup.

The transverse space charge tune shift ΔQ_{SC} for a round Gaussian beam of RMS transverse size σ has a value

$$\Delta Q_{SC} \;=\; -\frac{\lambda r_0 R^2}{2Q\beta^2\gamma^3\sigma^2} \tag{4}$$

where λ is the longitudinal line density of protons in the bunch, r_0 is classical proton radius, $2\pi R$ is the circumference of the circular accelerator, and Q is the tune without space charge. **Figure 14** (RIGHT) confirms that ΔQ_{SC} is largest at the initial stage of acceleration when $\beta\gamma$ is smallest. The space charge limit at which the beam will spontaneously enlarge itself, or suffer losses, is about $\Delta Q_{SC} \approx 0.5$, much larger than the calculated and simulated values of $\Delta Q_{SC} \leq 0.1$. Thus the RCMS synchrotron operates very comfortably with small beams in a regime far short of the space charge limit, thanks to rapid cycling and consequently low bunch intensities.

3.3 Injection

Figure 15 shows a general view of the injection and extraction interfaces from the tandem Van de Graaf injector, and into the switchyard that serves the treatment rooms. **Figure 16** shows some perspective detail of the injection interface with the incoming beam merging with the circulating beam. While the incoming beam is always in the same horizontal plane as the circulating beam, the horizontal angle and displacement between the two must be reduced to zero. This is the function of the electrostatic inflector and the injection kicker, shown schematically, and in plan detail, in **Figure 17**. Most of the work is done by the inflector, a simple device with a constant electrostatic field. At the end of the inflector both beams are in the same beampipe for the first time. The injection kicker – a pulsed magnet – finishes the job.

The key parameters of the electrostatic inflector and the injection kicker are summarized in **Table 5**, for the nominal injection trajectory sketched in **Figure 18**. Using the nomenclature defined there, the radius of curvature in the inflector must be

$$\rho \;=\; \frac{D+d}{(\sin\phi + \sin\psi)} \;=\; 11.463 \text{ m} \tag{5}$$

where $D + d = 1.381$ m is the active length of the electrostatic field. The scale drawing of the electrostatic inflector in **Figure 19**, and the sketch of the apertures at the downstream end of the inflector in **Figure 20**, show a gap of

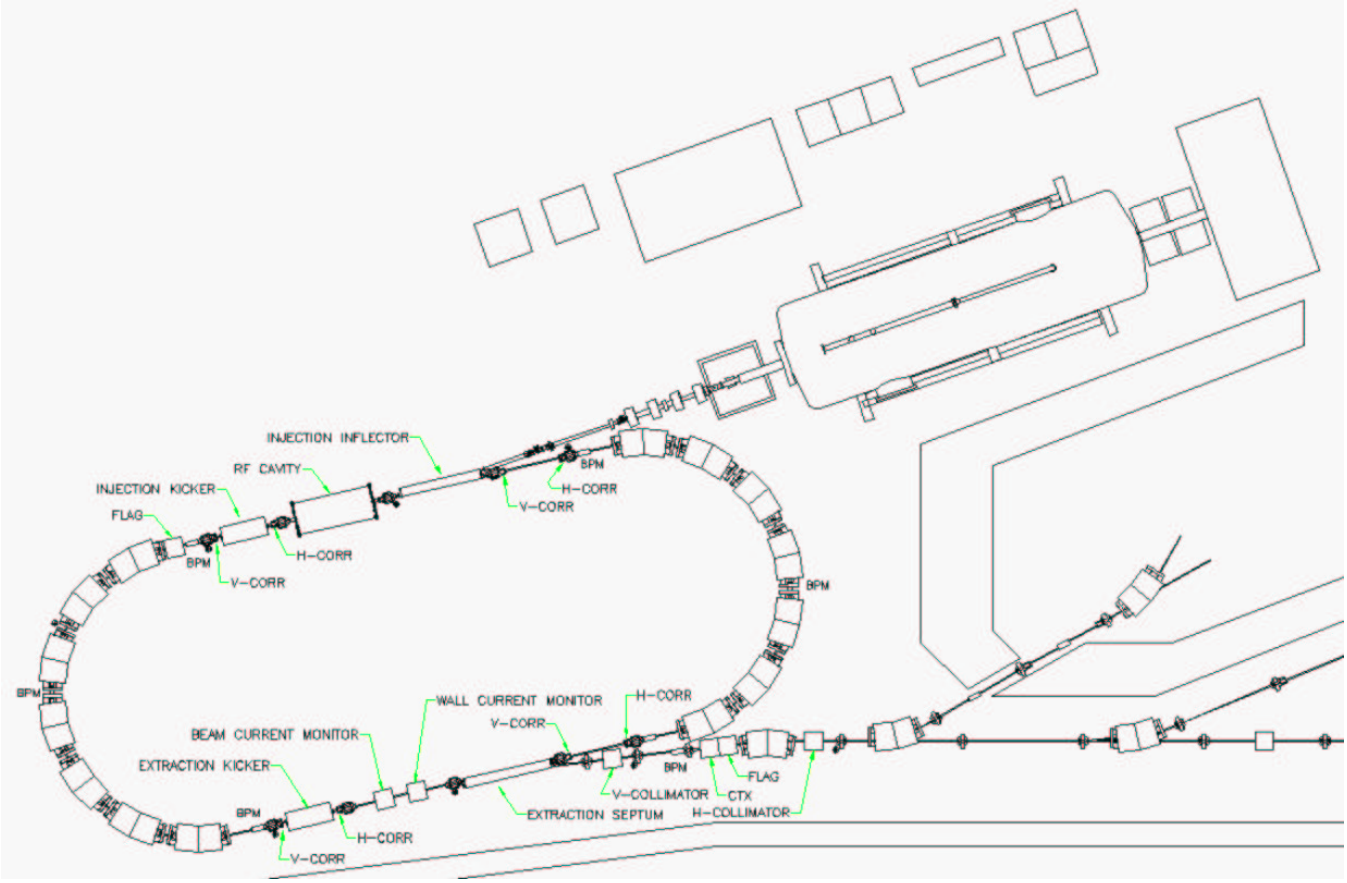

Figure 15: Plan drawing of the synchrotron, showing a broad view of the injection interface with the tandem Van de Graaf injector, and the extraction interface with the first few switchyard elements.

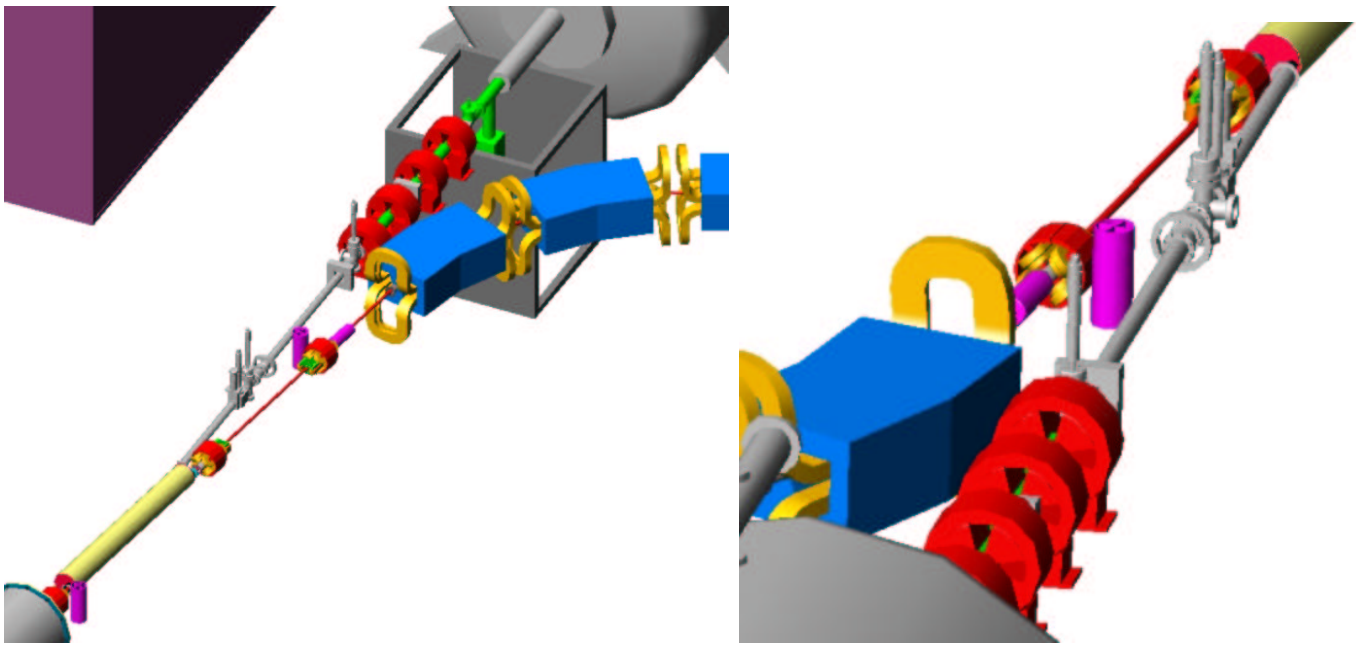

Figure 16: Perspective views of the injection interface. The injection inflector is visible at the top of the right view.

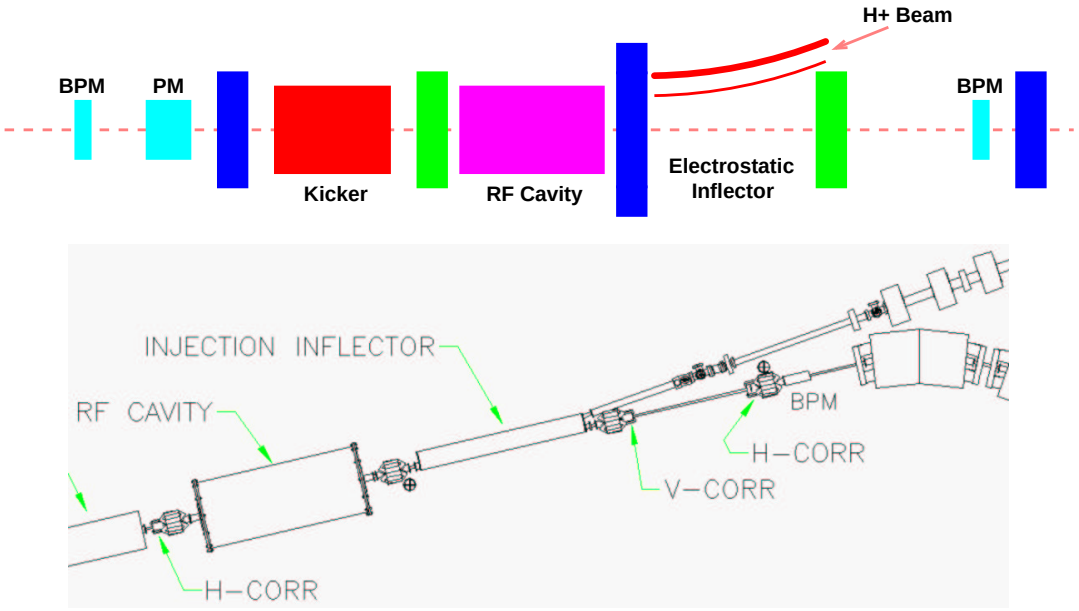

Figure 17: Schematic and plan views of the interface between the tandem Van de Graaf injector and the synchrotron.

Electrostatic Inflector		
Bend angle, ϕ		6.5°
Radius of curvature, ρ	[m]	11.5
Active length, $D + d$	[m]	1.4
Septum thickness	[mm]	1
Gap, g_I	[mm]	18
Voltage, V	[kV]	22
Electric field	[kV/cm]	12
Injection Kicker		
Kick angle, Φ_K	[mrad]	5.3
Magnetic length	[m]	0.2
Magnetic field, B	[G]	100
Gap, g_K	[mm]	30
Current, NI	[A]	240
Rise time	[ms]	< 16
Flat top	[ns]	> 100
Fall time	[ns]	< 600
(Revolution Period	[ns]	840)

Table 5: Injection Kicker and Inflector Parameters

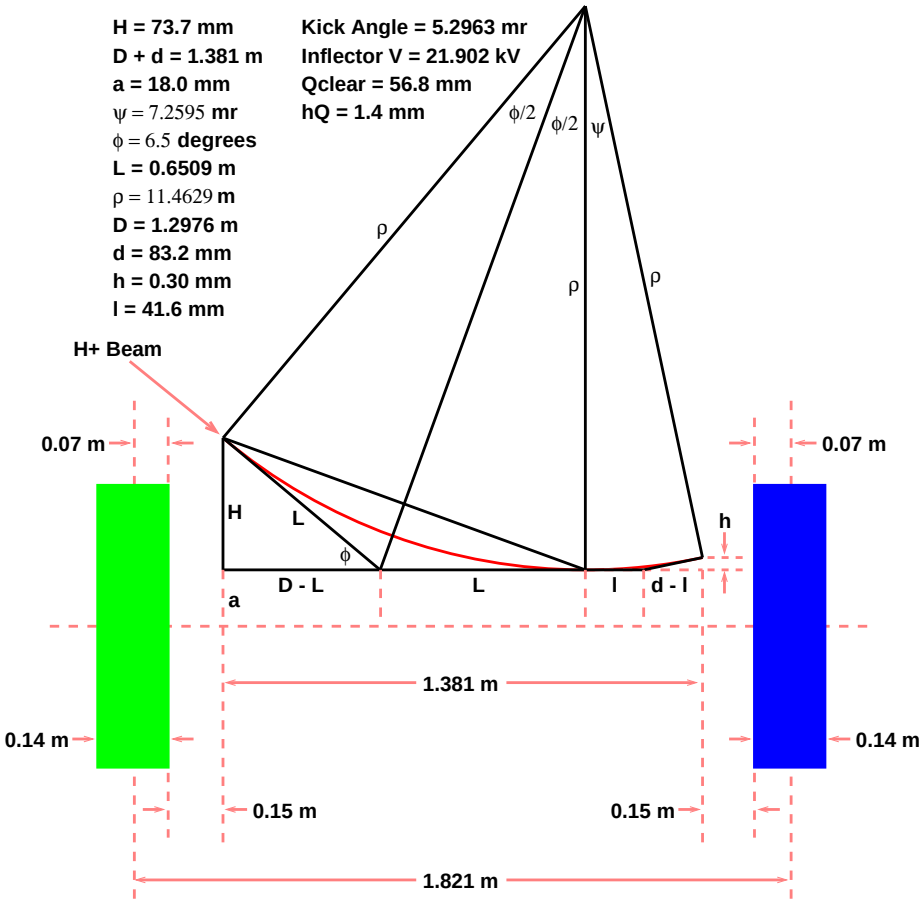

Figure 18: Nominal trajectory of beam passing through the injection inflector. (Note that beam enters from the left, in this sketch.)

g_I = 18 mm between the septum and the cathode in the inflector. Thus the required electrostatic voltage is

$$V = \frac{g_I}{\rho}\left(\frac{c^2p^2}{E}\right) = 21.9 \text{ kV} \tag{6}$$

Blue and green ellipses in **Figure 20** represent $\pm 2.5\sigma$ (rms) of the beam at focusing and defocusing locations in the straights during injection, according to the values recorded in **Table 3**. The comfortable physical aperture at injection becomes even more luxurious as the beam shrinks in transverse size during acceleration.

The injected beam leaving the inflector is on a trajectory that crosses the center line of the beam pipe at location K, in the middle of an injection kicker. This kicker is turned on to deliver a vertical magnetic field when the incoming beam passes for the first time, but is turned off on all subsequent beam passages. Thus it delivers a one-time horizontal kick to the beam, steering it to travel down the center of the beam pipe. The angle of the horizontal kick is

$$\Phi_K = \frac{X_I}{\sqrt{\beta_I\beta_K}\sin\mu} = 5.30 \text{ mr} \tag{7}$$

where $X_I = 18.3$ mm is the incoming beam displacement at location I, the downstream end of the inflector, μ is the betatron phase advance between I and K, and β_I and β_K are the horizontal beta functions at the two points. The magnetic field required to do this in a 0.2 m long kicker is $B = 101$ Gauss, which is delivered by a current I such that

$$NI = g_K B/\mu_0 = 242 \text{ A} \tag{8}$$

where N is the number of turns wound on the kicker, and $g_K = 30$ mm is the magnet gap.

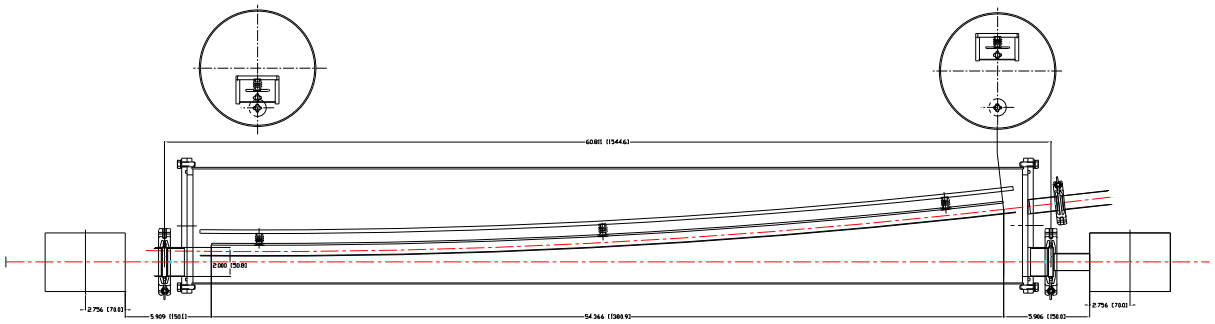

Figure 19: Plan view of the electrostatic injection inflector. Beam enters at the right from the tandem Van de Graaf injector.

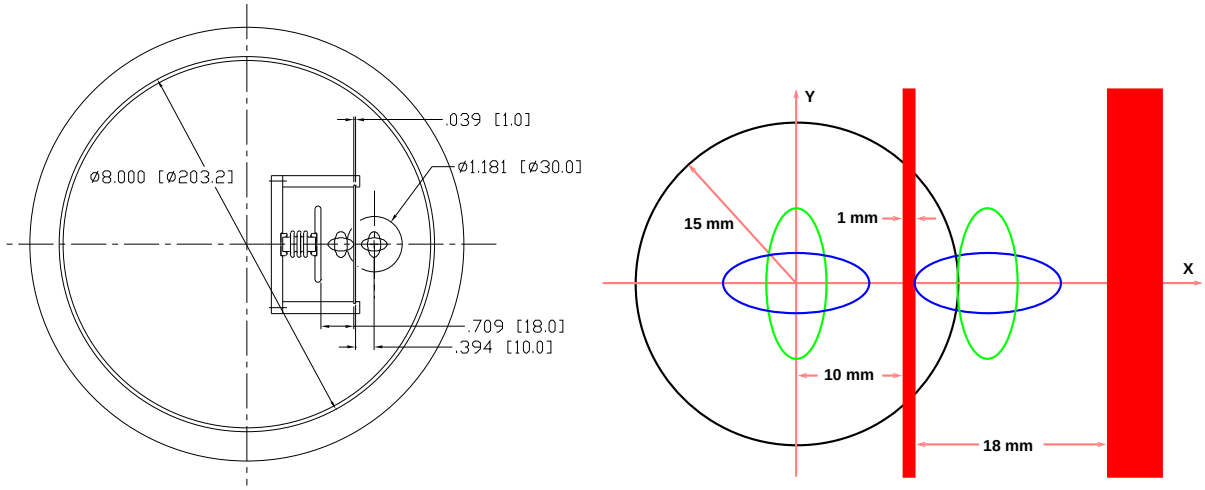

Figure 20: Apertures at downstream end of electrostatic inflector. The green and blue ellipses in the schematic on the right represent $\pm 2.5\sigma$ (rms) of the beam envelope at the upstream and downstream ends of the inflector.

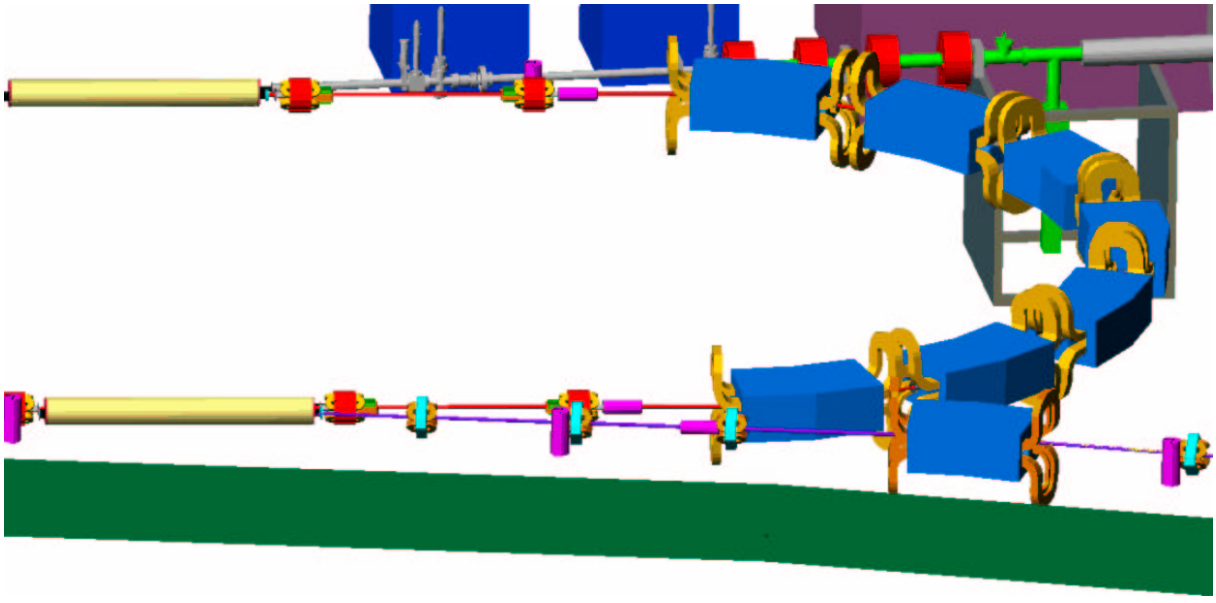

Figure 21: Perspective view of extraction (foreground) and injection (background) interfaces.

3.4 Extraction

Figure 21 shows a general perspective of both injection and extraction interfaces, which are similar in many ways. The extraction kicker begins the extraction process by quickly turning on a vertical magnetic field during a selected turn number, thereby selecting the energy of the extracted beam. The angle is sufficient to move the beam horizontally across a current sheet at the upstream end of the extraction septum magnet, which also bends the beam horizontally. The positions of the extraction kicker and the extraction septum are shown schematically and in plan view in **Figure 22**.

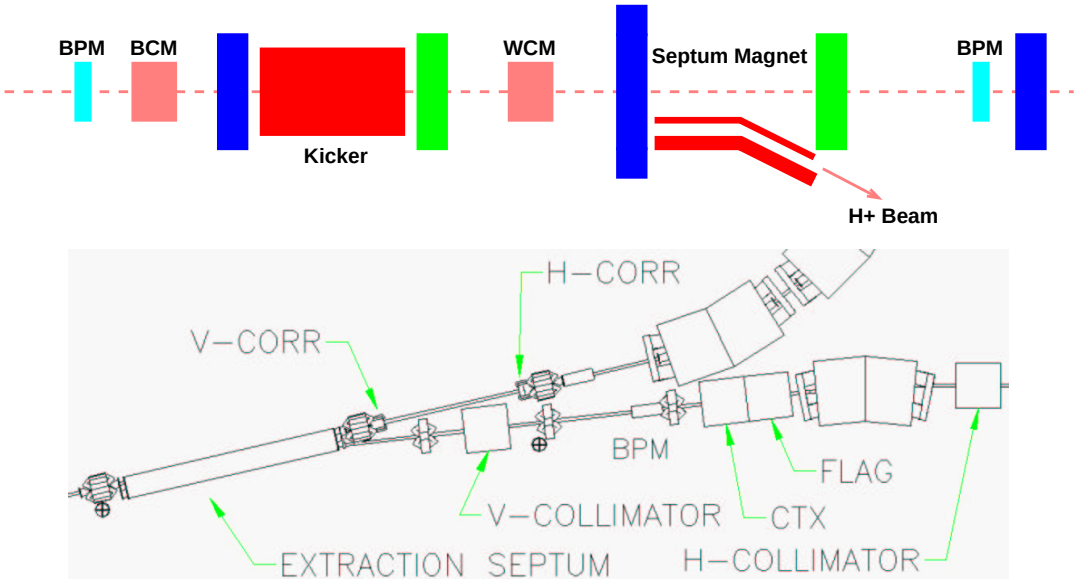

Figure 22: Schematic and plan views of the extraction interface layout.

Key parameters of the extraction kicker and the septum magnet are summarized in **Table 6**, for the nominal trajectory shown in **Figure 23**. The required displacement of the beam at S, the entrance to the septum, is

$$X_S \;=\; \Phi_K \sqrt{\beta_K \beta_S}\, \sin\mu \;=\; 19.3 \text{ mm} \tag{9}$$

where μ is the phase advance from the center of the kicker, and β_K and β_S are the horizontal beta functions. Solving this equation shows that the required extraction kick angle is $\Phi_K = 5.48$ mr, requiring an integrated kick field of 0.0133 Tm. For a 0.8 m long kicker the required field is $B = 167$ Gauss. This is delivered by a magnet with $NI = 398$ Ampere-turns, if the gap height is $g = 30$ mm, since

$$B \;=\; \mu_0 NI/g \tag{10}$$

The current required in the septum magnet shown in **Figure 24** is also given by Equation 10, only now $B = 0.1983$ T and the gap is taken to be $g = 0.012$ m, so that $NI = 1893$ Amps. The apertures at the upstream end of the septum magnet are shown in **Figure 25**, including ellipses representing $\pm$ 2.5 σ for the beam at its largest, for the minimum extraction energy of 60 MeV.

3.5 Delivery beam lines

The delivery beam lines connect the synchrotron to the treatment rooms. They are:

- the *extraction line,*
- the *switchyard,*
- the *transport lines,* and

Extraction Kicker		
Bend Angle	[mrad]	5.48
Magnetic strength	[Gm]	133
Magnetic length	[m]	0.8
Magnetic field	[G]	167
Gap	[mm]	30
Current	[A]	398
Rise time	[ns]	< 100
Flat top	[ns]	> 70
Fall time	[ms]	< 16
(Revolution Period	[ns]	167)
Septum Magnet		
Bend angle		6.5°
Radius of curvature	[m]	12.268
Length	[m]	1.481
Magnetic field	[G]	1983
Gap	[mm]	12
Septum (Cu) thickness	[mm]	4
Current	[A]	1893
Half-sine pulse length	[μs]	10
Ripple		$< 2\%$

Table 6: Extraction Kicker and Septum Magnet Parameters

- the *gantry optical interfaces.*

The *extraction line* comes just after the extraction septum magnet and before the *switchyard,* as shown in **Figure 26**. The *switchyard* is a periodic structure of FODO cells, providing identical lattice functions at the entrance to each beam line. This enables all the gantries to have the same optical design. The *transport lines* take the beam from the *switchyard* to the different rooms of the facility. The research room has two *transport lines* with bending angles that differ by 30 degrees. The fixed beam room has one 45 degree transport line that goes to the vertical fixed beam line, and two horizontal 90 degree *transport lines.* The *transport lines* that connect the *switchyard* to the *gantry optical interfaces* are identical, and the same as the 45 degree *transport lines* used in the the fixed beam room.

Since the beam energy in the delivery beam lines changes only relatively slowly, delivery line dipoles and quadrupoles have solid cores, instead of laminated cores. The same type of quadrupole is used in both the *transport lines* and in the gantries. The beam delivery dipoles are chevron magnets with a length of 0.68 m and a deflection angle of 22.5 degrees. These dipoles are big enough to allow the beam to exit in a straight line when the magnet is turned off, as required in some operational modes in the *switchyard* and in the research room. The 45 degree and 90 degree *transport lines* are built with 2 and 4 of these magnets, respectively. Research room *transport lines* are also built with 2 of these magnets, but they are powered to each produce a 30 degree bending angle.

The special optical structure called a *gantry optical interface* is designed to provide axially symmetric optics at the entrance point of rotation [9]. The horizontal and vertical beta functions are made equal, and the alpha functions are both made equal to zero, at the rotation point, as shown in **Figure 27.** This matching is performed by three quadrupoles placed between the *transport line* and the gantry. The distances between the quadrupoles, and the strengths of two of them, are varied until the matching conditions are satisfied [9].

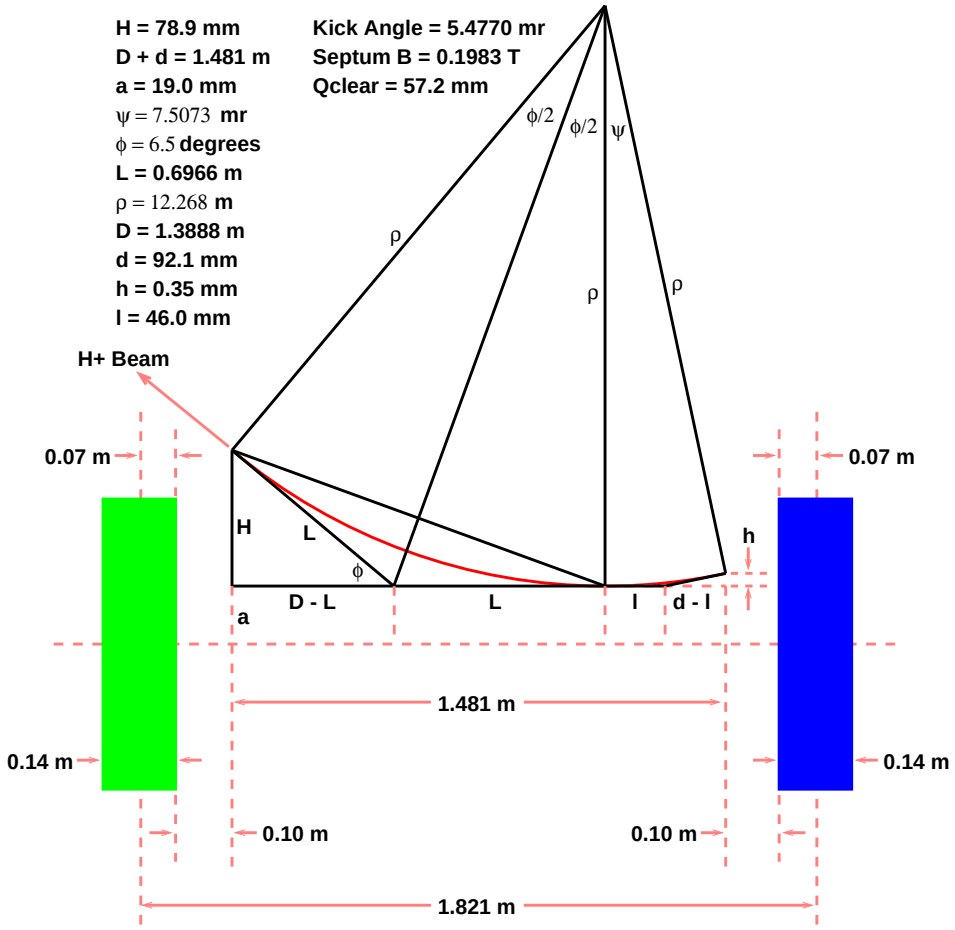

Figure 23: Nominal extraction trajectory of the beam leaving the synchrotron.

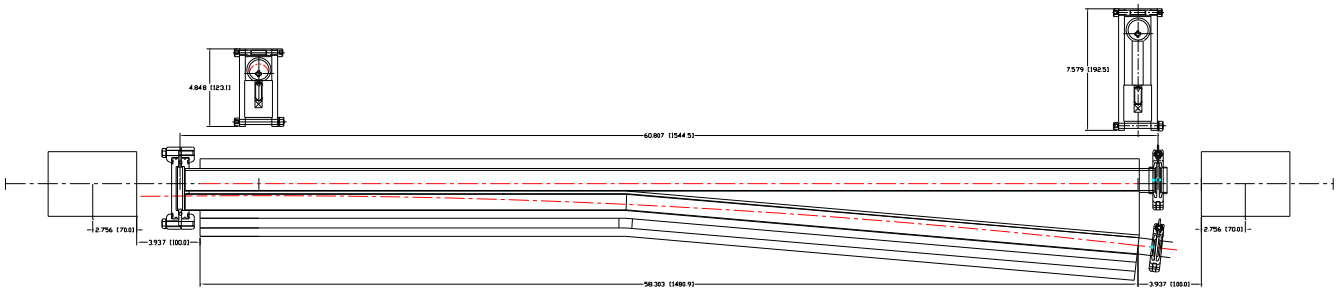

Figure 24: Extraction Septum Magnet

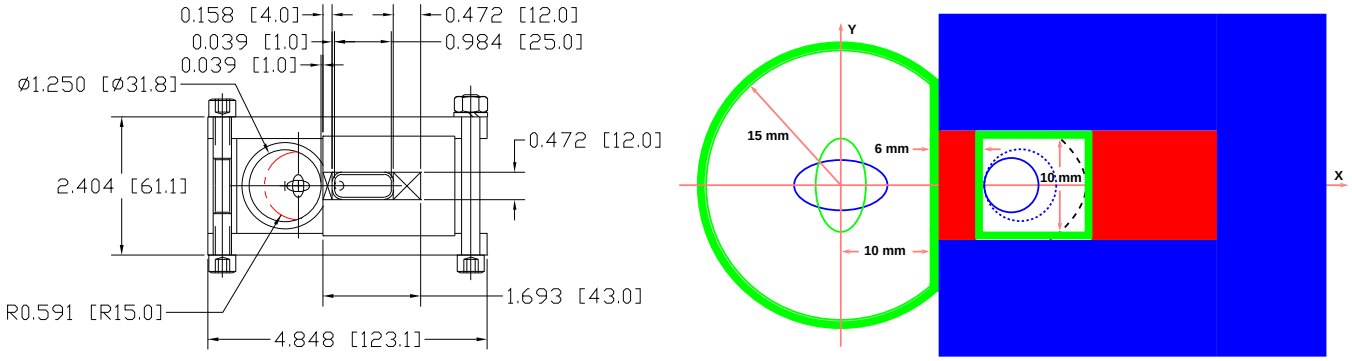

Figure 25: Upstream end of septum magnet, and septum magnet apertures.

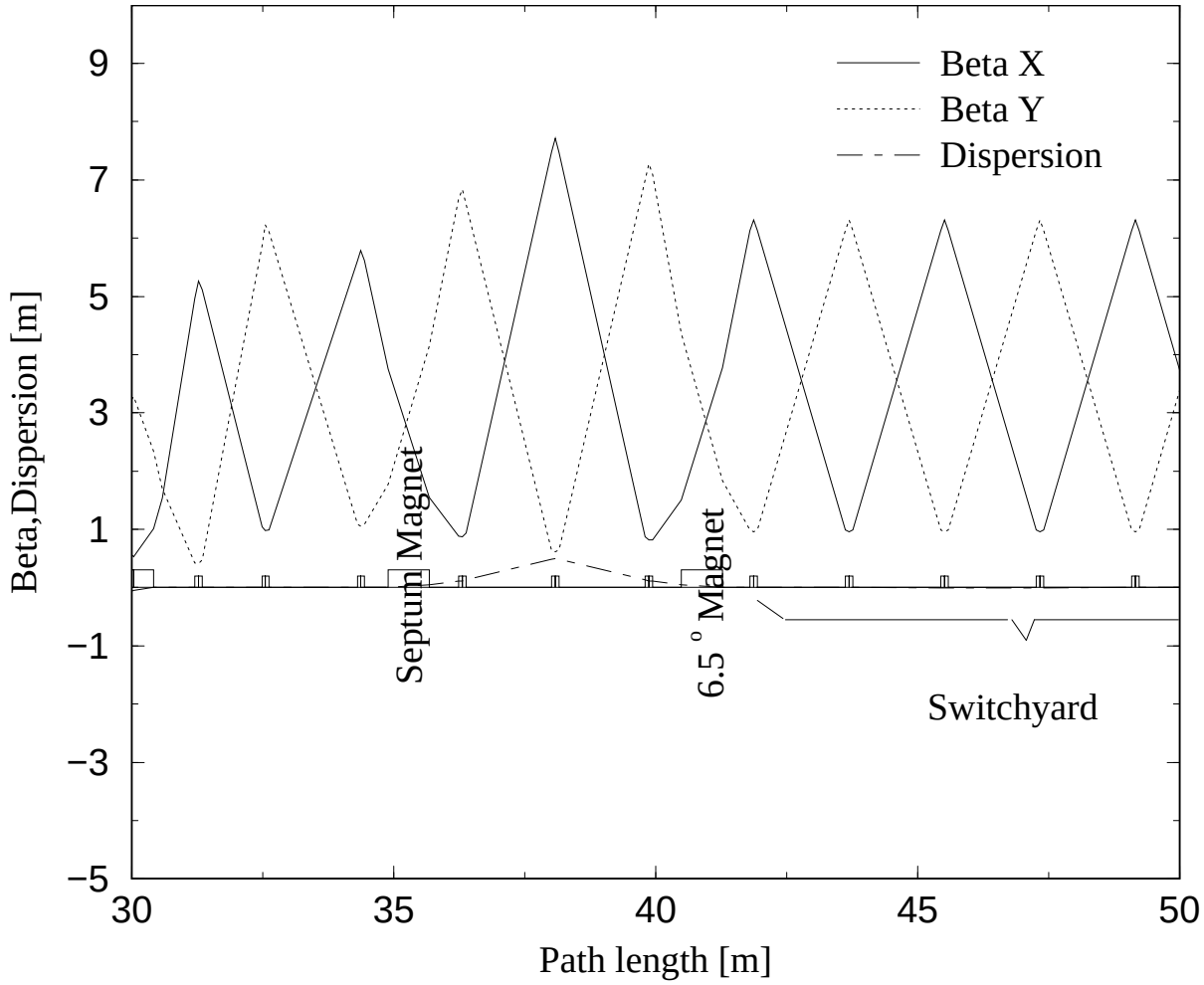

Figure 26: The *extraction line* interface between the extraction septum magnet and the *switchyard* simultaneously suppresses the dispersion initiated by the septum magnet, and smoothly matches the beta functions to the FODO cell structure of the *switchyard.*

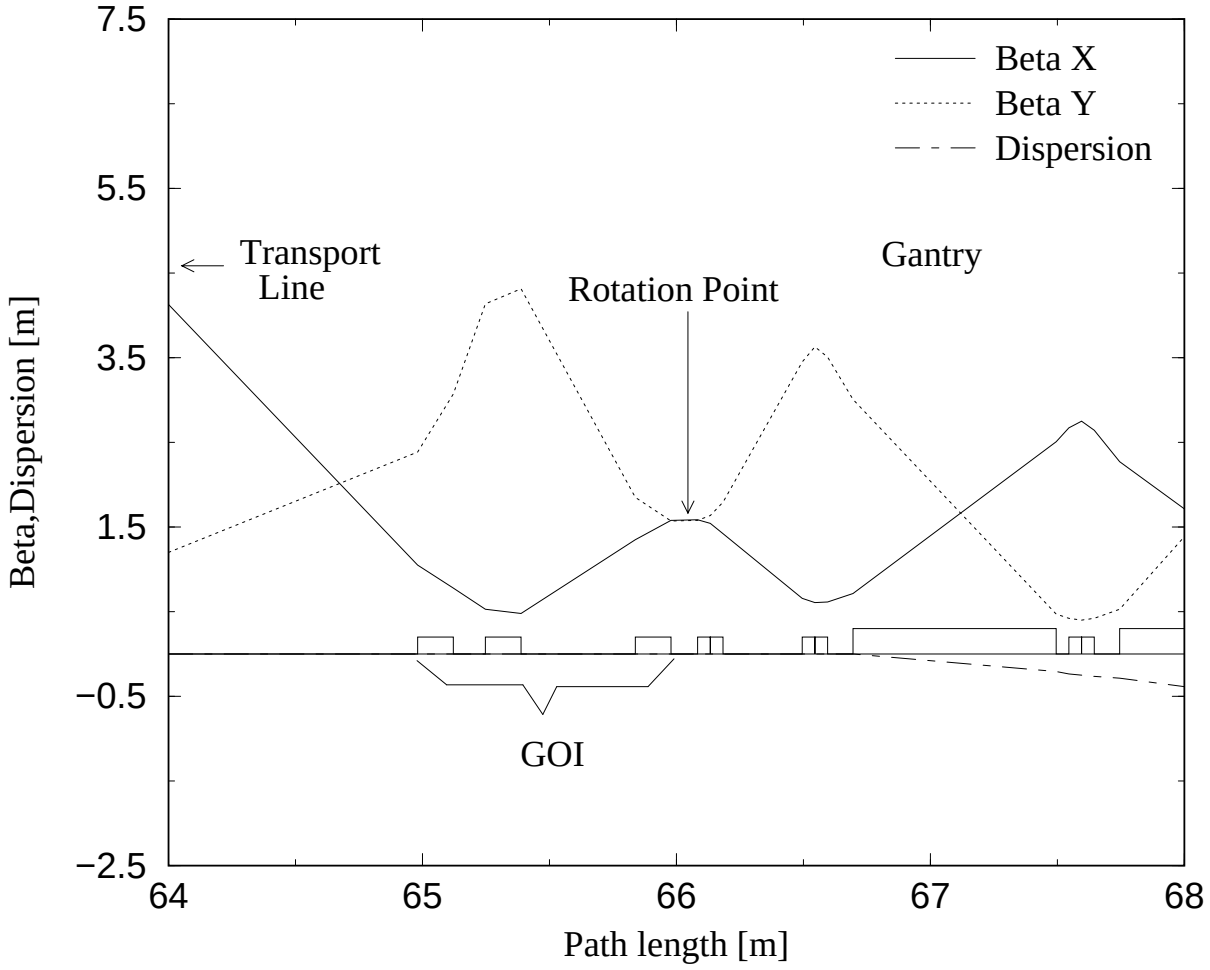

Figure 27: The *gantry optical interface*. The locations and strengths of the three "GOI" quadrupoles are set such that the alpha functions are zero, and the horizontal and vertical beta functions are equal, at the rotation point.

4 Injector

Based upon the beam delivery requirements for the injector as specified in the RCMS system specification, summarized in **Table 7**, an electrostatic tandem configuration was chosen for the injector accelerator. The injector is required to provide proton beam pulses at 30 Hz with a pulse width varying between 25 and 100 nanoseconds at a delivered energy of 7 MeV. The maximum beam current will be 2.71 mA resulting in a maximum charge per pulse of 1.7×10^9 protons. This requirement can be met with a tandem accelerator using currently available technology. The cost of this type of accelerator is approximately one third of the cost of an equivalent RF driven accelerator. The beam emittance requirements for the injector have been compared to test data on the tandem and found to be achievable. A side elevation view of the injector is shown in **Figure 28** (dimensions in inches) and a plan view showing the general arrangement of support equipment is shown in **Figure 29**.

Repetition Rate, f_{rep}	[Hz]	30
Synchrotron injection energy	[MeV]	7.0
Normalized rms emittance, ϵ	[μm]	0.15
Momentum width at injection (rms) σ_p/p		0.001
Total momentum width, $\Delta p/p$		$\pm$0.0023
Total kinetic energy width, ΔK	[keV]	$\pm$32
Injected pulse length Δt	[ns]	25–100
Injected protons per pulse, min		1.0×10^7
Injected protons per pulse, max		1.7×10^9
Maximum pulse to pulse intensity variation		6
Overall length	[m]	$\sim$ 8.0
Source current	[mA]	0.064–2.72

Table 7: Beam delivery requirements and specifications for the RCMS injector.

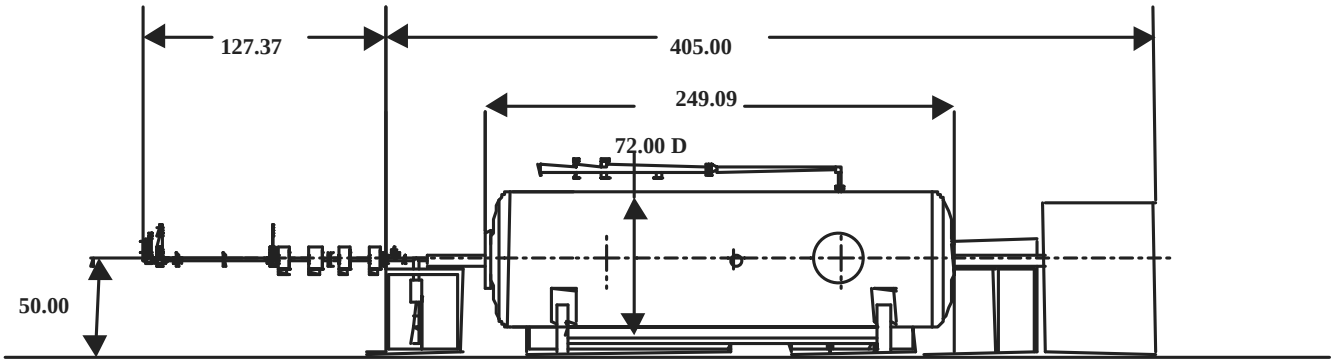

Figure 28: Side elevation view of the RCMS proton injector. (HEBT structural supports are not shown.)

The height of the proton beam centerline is 50 inches above the facility floor. This exactly matches the height for injection into the synchrotron. The total length of the machine is 532.37 inches as shown, using a straight High Energy Beam Transport (HEBT) section. The HEBT section employs four quadrupole magnets to match the circular output beam from the tandem accelerator to the phase space requirements of the synchrotron. If facility requirements necessitate repositioning of the injector, a bend can be accommodated in the HEBT section. The bend would include the addition of one or more dipole magnets between the second and third quadrupole magnets in the HEBT.

A beam diagnostics section is located in the HEBT downstream of the quadrupoles. The diagnostics include a beam pulse charge integrator, a beam position monitor, two beam profile monitors, and a retractable Faraday cup. The arrangement and function of these diagnostics are described in more detail later.

The support equipment required for injector operation is shown in **Figure 29**. It is important to note that the

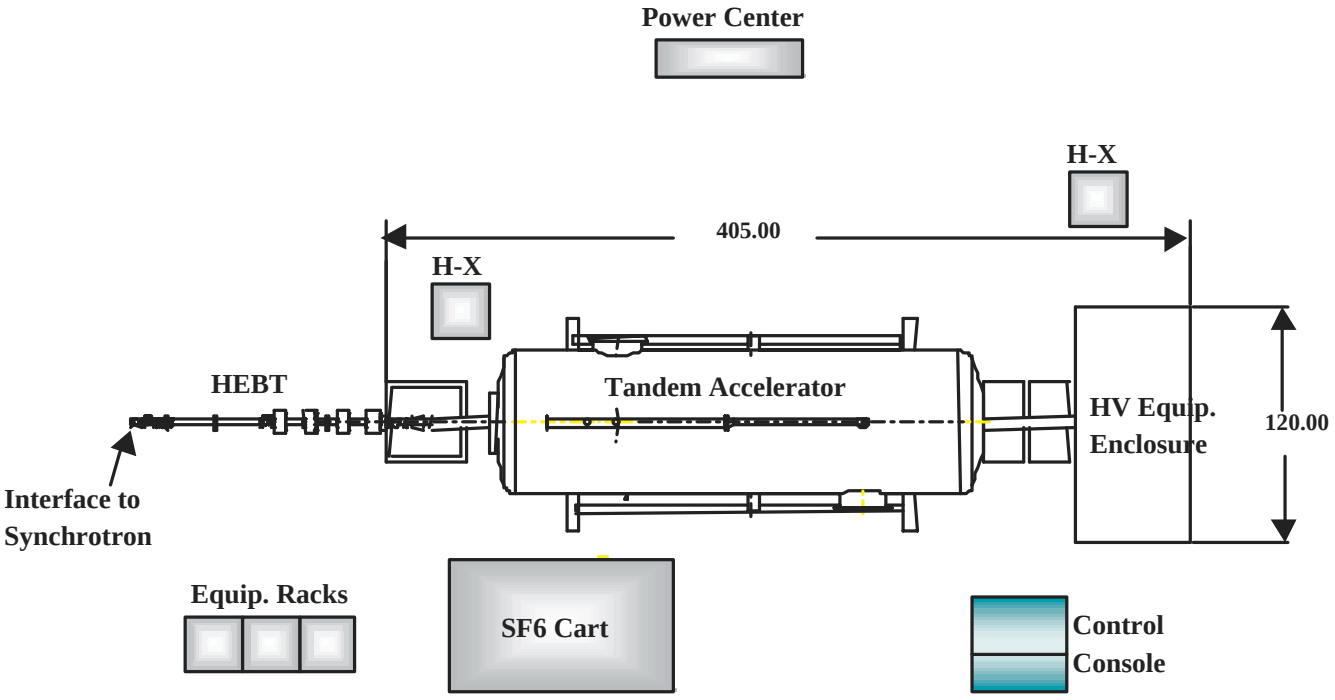

Figure 29: Plan view of RCMS injector equipment. Dimensions are in inches.

control console, the equipment racks, the SF_6 cart, and the two heat exchange carts (facility water to coolant) should be close to the injector. The power center that houses all of the circuit breakers can be located against a wall and away from the injector.

4.1 Ion source and Low Energy Beam Transport

The protons are provided by an ion source located within the high voltage safety enclosure. The ion source is a toroidal-discharge volume-production type as developed by BNL. To provide intense pulses, the plasma arc power supply is a fast pulse driver. Its pulse width and drive current are adjustable to allow optimization of the injector efficiency at a given beam current level. Typically the arc driver pulse width will be set to a value somewhat larger than 100 microseconds to allow the beam current to reach a steady value before a second pulse driver connected to a set of electrostatic deflector plates allows the beam to pass to the accelerator section. This second driver will set the precise width between 25 and 100 nsec needed for operation. A preset delay between the two pulse drivers will prevent transient effects in the source pulsing from reaching the accelerator.

The extractor electrode is positioned about 5 mm from the anode aperture of the ion source. The relatively small opening in the extractor allows the assembly to be designed for differential vacuum pumping, thereby minimizing ion source gas streaming into the accelerator. Unwanted electrons are swept out of the extracted negative ion beam by means of a small dipole magnet located in this region. The beam is further accelerated to 20 keV by means of another downstream electrode.

An Einzel lens beyond the acceleration gap serves to focus the beam prior to pre-acceleration. A general-purpose electrostatic acceleration tube is provided between the Einzel lens and the main accelerator. In this region the beam energy is increased to 75 keV. Differential vacuum pumping is provided before and after the acceleration tube to further reduce any unwanted gas streaming into the accelerator.

A high voltage safety enclosure is provided around all of the ion source power supplies. The door of the enclosure is interlocked to the power supplies by means of a mechanical system of high reliability that shorts the ion source equipment to ground if the door is opened.

De-ionized water is used in the coolant loop for the equipment located in the high voltage safety enclosure. This is temperature controlled by means of a water to water heat exchanger located near the HV enclosure.

4.2 Accelerator

The tandem accelerator is enclosed within a pressure vessel containing SF_6 insulating gas at a pressure of 80 psig. The tank is made of carbon steel and conforms to the standards of the ASME. Ports are provided for two windows, electrical feedthroughs, generating voltmeter, corona triode needle assembly, capacitive pick off, and SF_6 gas fill. The window ports are large enough for personnel access to the inside of the tank for installation and servicing.

Inside the tank is the central charging system, the HV terminal containing the beam stripper and beam focusing magnets, and a pair of electrostatic acceleration columns. The negative ion beam from the source is accelerated to terminal voltage of 3.5 MV and stripped of electrons. The resulting positive ion beam is further accelerated to 7 MeV at the point that it leaves the tank. The HV terminal charging system utilizes two Pelletron^{TM} chains. Voltage stability of the terminal is approximately 1 kV, which is considerably better than the requirement of 32 kV for RCMS. The HV terminal houses two foil stripper changers, each containing 25 foils. It is anticipated that foil stripper changer replacement would be after several years at the planned rate of operation. The acceleration tubes are of an organic free design capable of withstanding high electrical gradients. They are designed to magnetically suppress unwanted electrons that are generated from stray proton bombardment of the acceleration tubes or from premature stripping from particle collisions. Estimated radiation at a distance of 1 meter from the accelerator during operation is 2.5 mrad per hour, thus facilitating local control and operation for commissioning and routine checkout functions.

4.3 High Energy Beam Transport

The HEBT section is a simple straight section from the output of the accelerator to the input of the synchrotron inflector. The HEBT contains four quadrupole magnets for transitioning the proton beam from a circular configuration as it leaves the tandem accelerator to the acceptance criteria of the synchrotron. A series of three X-Y steering magnets are also provided to correct beam transmission.

A retractable Faraday Cup is provided near the accelerator output along with a vacuum pumping station that reduces unwanted gas streaming into the synchrotron. Since the HEBT is rather short (approx. 3.5 meters) there is no other vacuum pumping between the accelerator and the synchrotron inflector. A vacuum isolation valve with roughing port is located just upstream of the mechanical interface with the synchrotron inflector.

A second retractable Faraday cup/beam stop is provided prior to injection into the synchrotron inflector. This unit serves as a commissioning diagnostic as well as for daily checkout prior to normal operation. The general arrangement of the beam diagnostics section is shown in **Figure 30**. The pulse charge integrator serves as direct feedback to the control system to enable delivery of the prescribed patient treatment doses per voxel. The BPM provides fine beam steering feedback while the two beam profile monitors permit a determination of the beam convergence/divergence at entrance to the inflector as well as beam size.

Because of the physical clearance requirements with the synchrotron, all quadrupoles are located at least 2.2 meters upstream from the beam properties match point as shown in **Figure 30**. The geometric match point (physical interface) is approximately 0.4 meters upstream of the beam interface. It is expected that this match point is the inlet flange to the synchrotron inflector.

4.4 Control system

The Injector Control System is configured so that complete stand-alone local control and operation of the injector can be accomplished. This capability facilitates commissioning and maintenance.

The local processor is a commercial PC class computer with hard disk capacity of at least 10 GB, a color monitor, a mouse and a printer. Injector parameters are interfaced to localized controllers through optically isolated A/D, D/A and digital I/O modules. Each localized controller is connected to the next unit in line or to the PC by fiber optic link. The local processor is connected to the Treatment Control System (TCS) by means of an Ethernet link and hardwire as necessary.

The Injector local processor receives beam pulse requirements (intensity, pulse number) from the Treatment Control System. During a treatment cycle, the measured key beam pulse characteristics will be stored in the local processor for later interrogation by the TCS.

The beam diagnostic section provided in the last 2 meters of the HEBT is an integral part of the control system. This section provides the delivered beam characteristics that are fed back to the injector local control to maintain

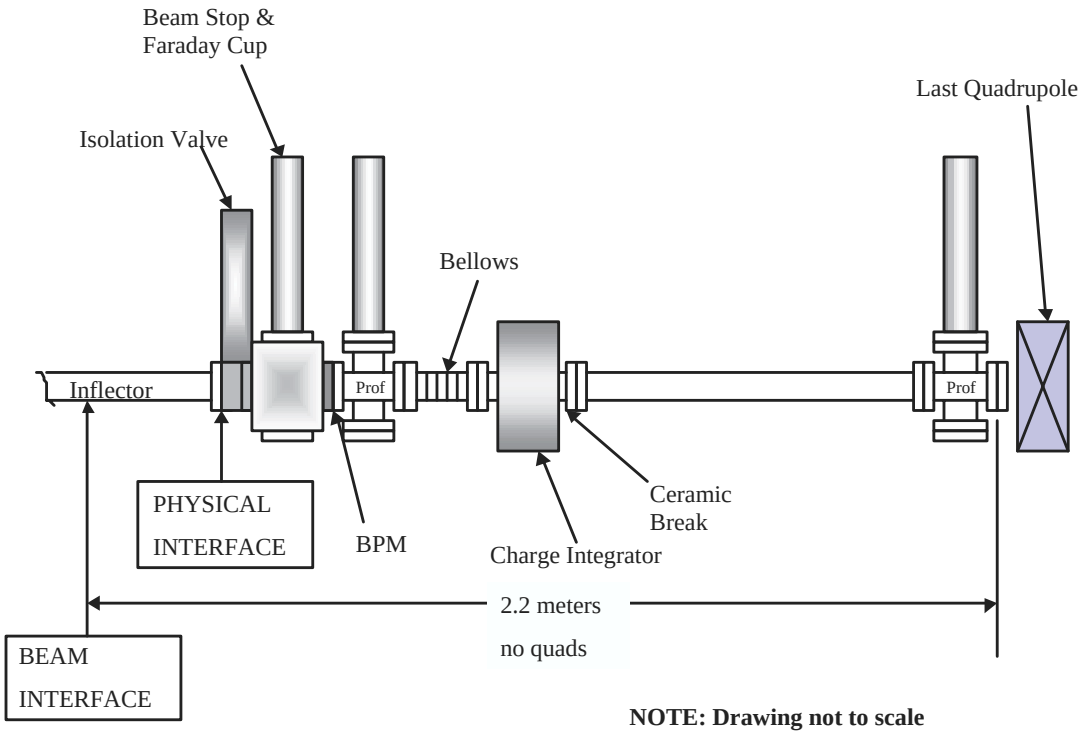

Figure 30: Arrangement of the beam diagnostics section.

proper operation for patient treatment. A beam pulse charge integrator is provided for pulse to pulse intensity control.

4.5 Insulating gas (SF_6) system

The tandem accelerator tank requires an operating pressure of 80 psig of sulfur hexaflouride (SF_6) gas to minimize the probability of electric breakdown from the high voltage terminal operating at 3.5 MV. SF_6 is quite expensive (approximately $2000 per cylinder) as well as being heavier than air, and so can cause asphyxiation. The total charge of gas for the accelerator is 1674 pounds, or 15.2 cylinders at 110 lbs each per standard cylinder.

When periodic maintenance is required, approximately every 6 months, the gas must be pumped out and saved for refill. To accomplish this, a high-speed processing cart is provided. The cart can pump the entire volume to a vacuum level of 50 torr in about five hours, which represents about 1% of the total charge remaining. This amount of gas would be sacrificed upon venting and opening the pressure vessel. If an overnight pumpout is permitted, the amount of wasted gas can be reduced further. Recharging the accelerator tank will take about 1 hour, after which high voltage conditioning can take place. Reconditioning of the acceleration columns after an up to air opening will take on the order of 1 hour.

The SF_6 cart is approximately 4500 pounds, dry. This combined with its size (109" long, 61" wide, 78" high) suggest that the unit be placed close to the accelerator in a permanent location.

4.6 Operation and maintenance

Normal operation of the injector during patient treatment is controlled by the Treatment Control System (TCS). The TCS will direct the beam pulse train intensity in accordance with the patient treatment plan. During startup for each day, it is anticipated that the injector will run through an automatic series of calibration runs where beam is delivered to the Faraday cup/beam stop located in the HEBT section. Once all is well, this would be followed by synchrotron injection trials. During the automatic calibration, the local processor will control injector operation. Once this operation is completed, the local processor will tell the TCS that the injector is READY.

It is expected that normal maintenance of the injector will be very infrequent. The estimates in **Table 8** are based upon actual operating experience with similar tandem accelerators and with all of the other injector components.

MAINTENANCE FUNCTION	DURATION (hours)	FREQUENCY
Accelerator HV terminal/stripper (with pressure vessel pumpout & refill)	20	Annually
Ion source filament change	8	Monthly
Ion source electrode change	16	Annually
Check lube vacuum pumps	2	Every 2 weeks
Drain/change backing pump oil	6	Every 3 months
Drain/change turbopump oil	6	Every 6 months
Check/top off water HX loops	0.5	Every week
Replace rack air filters	2	Annually

Table 8: Estimated frequency and duration for routine maintenance of the RCMS injector.

5 Gantries

5.1 Layout and mechanics

The RCMS gantry shown in **Figure 31** is approximately 8 meters long, from the rotation point to the iso-center, with a height of ±6 meters. Accurate beam delivery places high demands on the gantry with regard to rigidity, precision, control system, and project realization. In particular, the mechanical structure has to be optimized for minimum deformation within a reasonable total weight of the total structure. The light magnets used in the RCMS gantry are a significant advantage, in this regard. A first conceptual design has been developed in a feasibility study by ACCEL Instruments GmbH and MAN Technology. MAN Technology has had many years of experience in the design, calculation, planning and construction of large high precision mobile structures, for example for Radio-Telescopes. Further, MAN Technology has already developed concepts and calculation tools, as well as a design, for a gantry to be used for the purposes of radiation tumor therapy.

Number of gantries	2 + 2 additional
Rigidity	
Deformation of the optical axis	± 0.5 mm envelope to ideal optical beam path
Deviation of the angle of rotation	± 0.1°
Weight	
Dipole	320 kg
Number of dipoles	2+5
Quadrupole	52 kg
Number of quadrupoles	2+1+4+5
Shielding block behind beam inlet	Ø 400 mm × 1000 mm (= 1000 kg)
Kinematics	
Range of gantry rotation movement	±180° (plus 20° overshoot)
Rotational speed	$\leq 6°/s$
Rotational acceleration	$\leq 2°/s^2$
Movement of patient table	x, y, z directions, rotation around vertical axis ±95°
Lifetime	20 years
Load cycles	Approx. 530,000 (6 start-stops/h, 12 h/day, 365 days/year, slewing angle 360°)
Dimensions	
Gantry room length, width, height	$12,000 \times 11,000 \times 12,000$ mm
Altitude of gantry rotation axis	5,000 mm (1,300 mm above the treatment room floor)
Entrance for assembly	7,000 × 7,000 mm
Treatment room diameter, length	Ø $4,900 \times 3,300$ mm
Entrance area diameter, length	Ø $4,800 \times 800$ mm
Air conditioning	
Range of operating temperature	+20°C ± 5°C
Temperature gradient in the operations room	$\leq 3°C$
Temperature change in the operations room	$\leq 1°C/h$
Humidity of air	< 70%, without condensation

Table 9: Principal specifications for the RCMS gantries.

Table 9 lists the rigidity parameters, and other principal parameters, for the gantry. The **deformation of the optical axis** is *the linear displacement of each individual beam optic element from its adjusted position under*

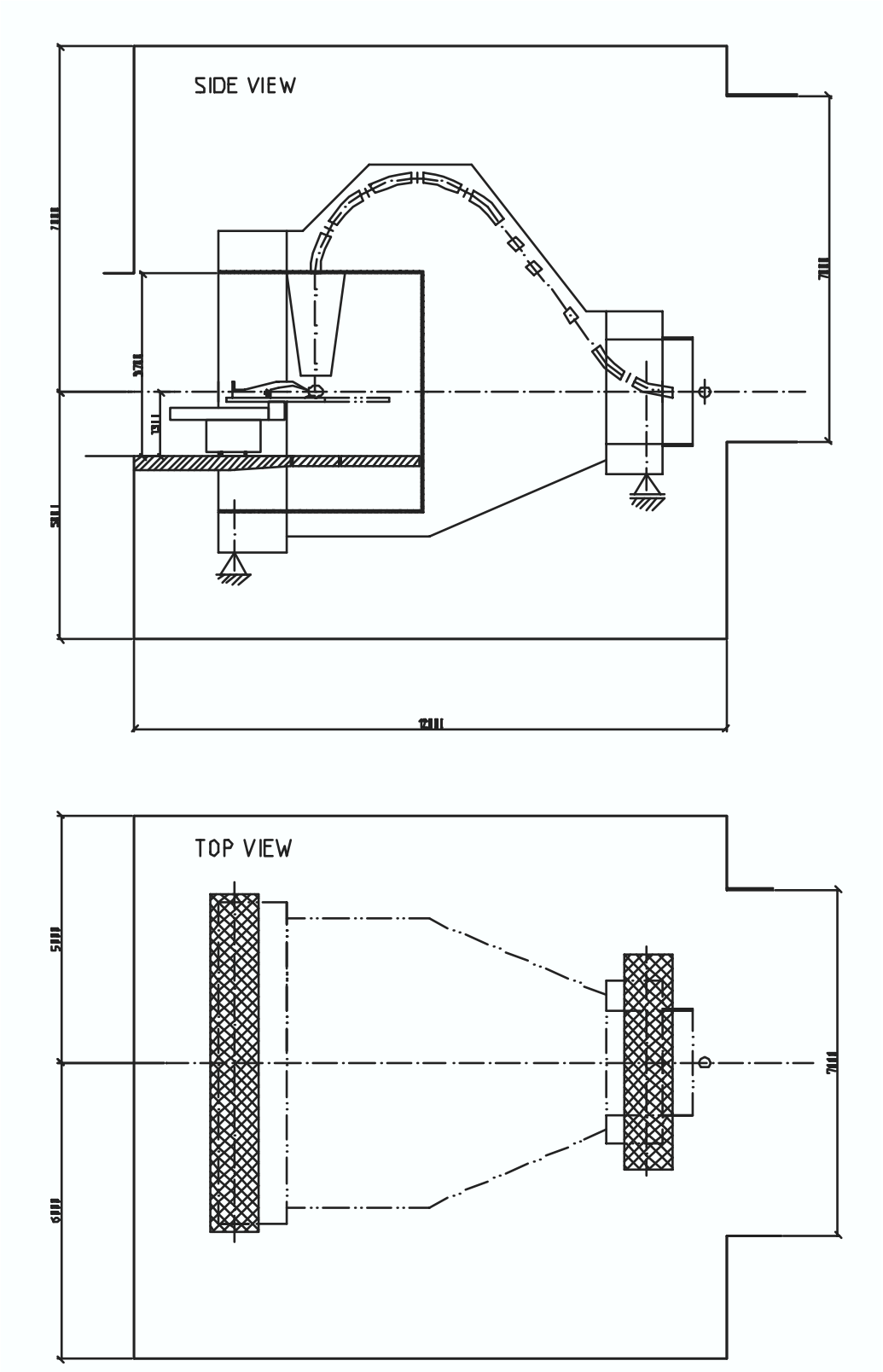

Figure 31: Gantry overview, showing side and top views of the arrangement of the gantry, magnets, nozzle, and couch, in a treatment room.

different operating conditions (rotation position, thermal dilatation). Transient displacements, for example those that occur for example during angular acceleration, are not taken into account. Thus, the deformation of the optical axis corresponds to the highest individual value. The **deviation of the angle of rotation** is *the angular deviation between the demanded position of the last beam guide element (dipole) referred to the gantry's axis of rotation and the position actually taken.*

The gantry is constructed as a three-dimensional structure. On the treatment room side, the gantry is supported by a fixed bearing which supports axial and radial loads. On the beam inlet side, the structure is supported by a bearing allowing axial displacement (movable bearing). Thus, the gantry is fixed in the axial direction at the treatment room bearing, with thermal expansion compensated by the bearing near the beam inlet. The gantry is balanced around its rotation axis. The cables and wires necessary for the operation of the beam guide elements will be guided by means of a cable twister. Gantry movement is realized by a gear motor/gear ring drive that allows high precision positioning. Each gantry is controlled by means of an individual independent computer unit that ensures mutual braking of the main drive units, soft start and soft deceleration functions, control of the auxiliary drive units for the treatment room, and supervision of the limit switches. The nominal position of the gantry is defined via an interface to Treatment Control System for that room.

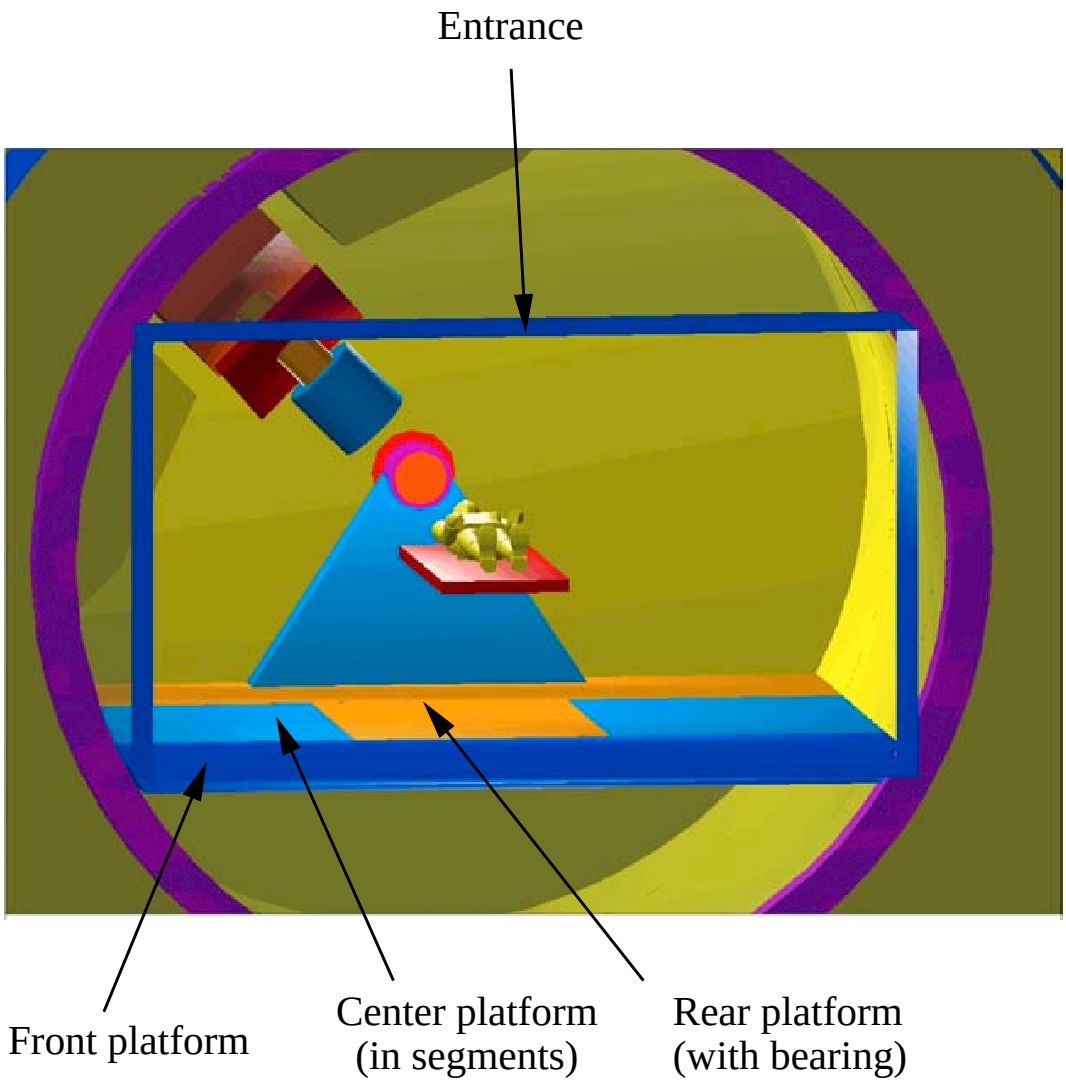

Figure 32: The treatment room enclosure at the end of the gantry.

5.2 Treatment room

The treatment room shown in **Figure 32** is conceptually divided into three regions:

- Entrance to the treatment room with front platform
- Central area with the beam outlet and central platform
- Rear area with treatment room rear platform and its bearing

The entrance to the treatment room has a cross section in the form of a segment of a circle with the dimensions Ø 4,800 mm × 3,700 mm height of the entrance. The treatment room itself has a cylindrical shape, with a diameter of approximately 4,900 mm and a length of approximately 3,300 mm. Access to the treatment room is via a three-piece platform designed for a load capacity of 250 kg/m^2. The front part of the platform is fixed to the supporting structure, onto which is also mounted the patient couch. The central part of the platform has a length of approximately 1,000 mm, depending on the nozzle dimensions. It is constructed from open-able segments in an arrangement that is governed by the nozzle position. The cover in the central part of the platform might be implemented as a rolling floor, depending on customer preference, and safety issues. The rear part of the treatment room platform counter rotates relative to the gantry, so that it is always flat and stable.

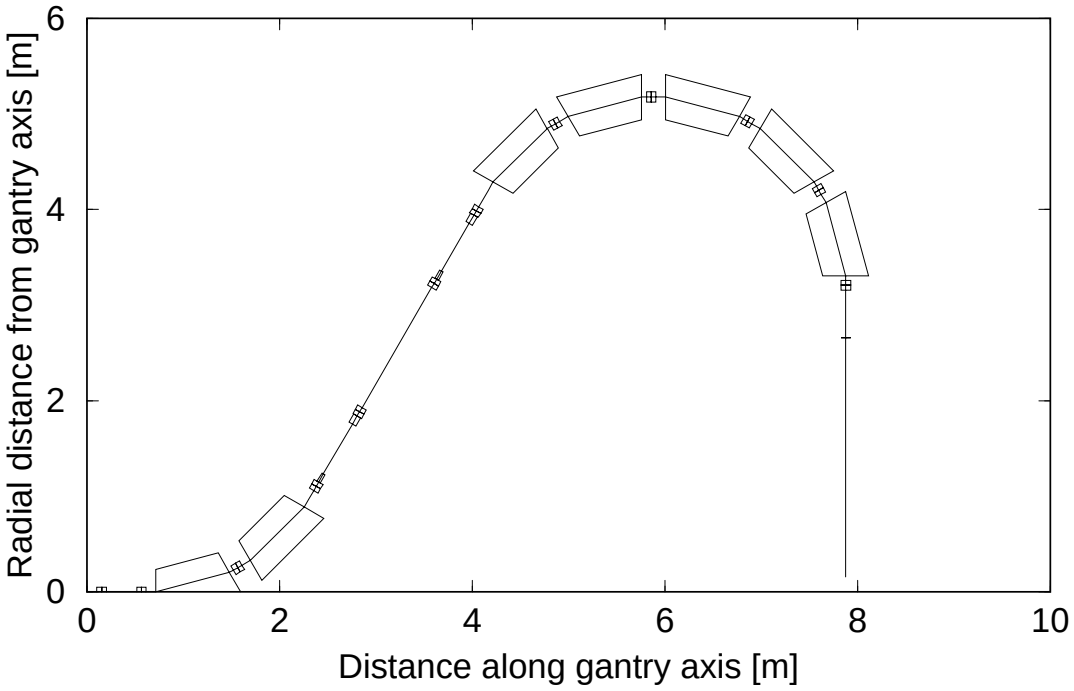

Figure 33: Magnet layout in the RCMS gantry, with a total of seven 30° dipoles and 12 quadrupoles. The total weight of magnets on the gantry is only about 2.9 tonnes.

5.3 Gantry and nozzle optics

Figure 33 shows that each gantry dipole deflects the beam by 30 degrees, maximizing the "packing factor" (the ratio of integrated dipole length to the total length) in the arc. The gantry has a free space of more than 3 meters from the last magnet to the isocenter – a distance that can be increased, if necessary.

Figure 34 (LEFT) shows the beam optics functions for the gantry. In order to make the beam transport through the gantry independent of the gantry rotation angle the horizontal and vertical beta functions are made identical at the input rotation point, and the slopes of the beta functions are made zero. The dispersion function and its slope

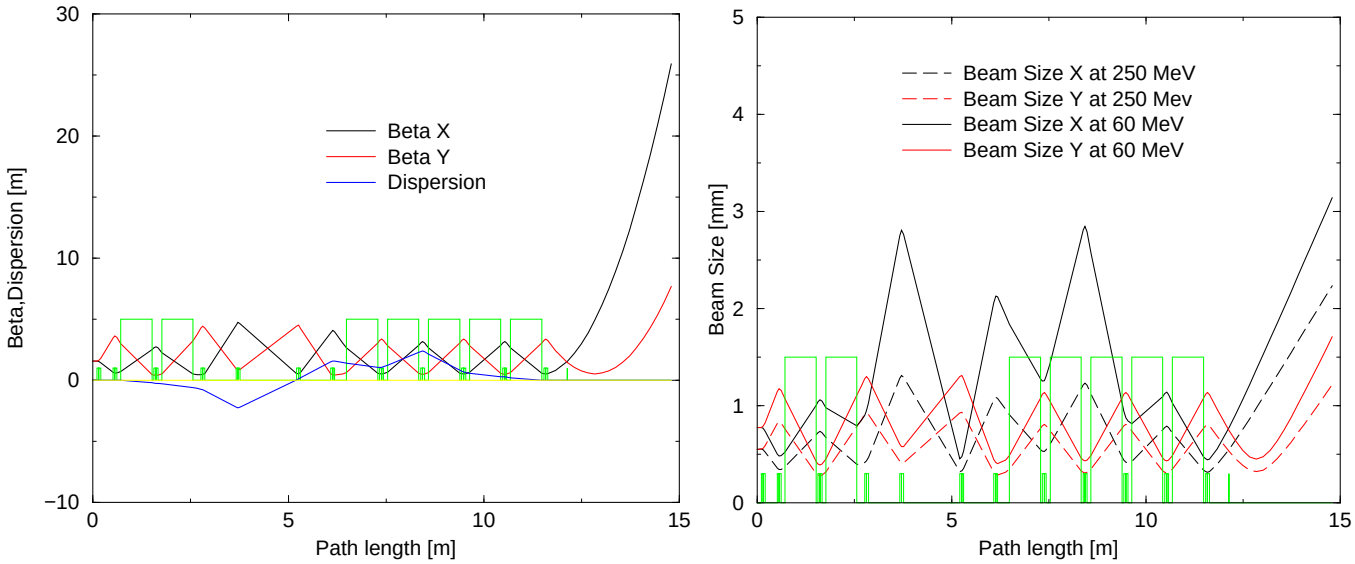

Figure 34: Gantry optics and beam sizes. The tall green boxes represent dipoles, and the small ones quadrupoles. LEFT: beta and dispersion functions. RIGHT: beam sizes in the gantry, assuming an unnormalized transverse emittance of $\epsilon = 0.381\mu m$ and a momentum spread of $\pm\Delta p/p = 0.0011$ at low energy extraction, and $\epsilon = 0.193\mu m$, $\Delta p/p = 0.0004$ at top energy. The radius of the aperture in the gantry is 10 mm.

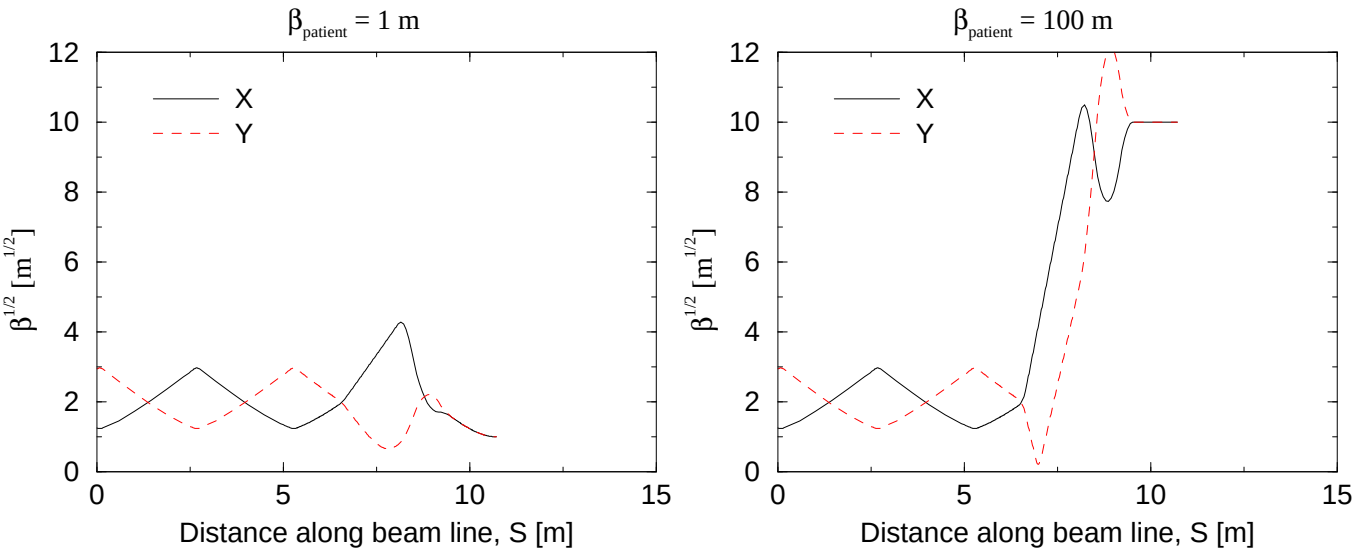

Figure 35: Variable focusing optics with a spot scanning nozzle, with more than a factor of 10 range in spot size.

must also be zero at the rotation point. Two quadrupoles between the rotation point and the first gantry dipole adjust the beta functions to be nearly periodic, thus providing the minimum beam size throughout the magnet region. The "bridge" between the first set of dipoles (bending the beam up) and the second set of dipoles (bending the beam back to the iso-center) contains four quadrupoles, keeping the beta functions small while providing the right phase advance to match the dispersion to zero at the end of the gantry. **Figure 34** (RIGHT) shows the beam sizes in the gantry. The incoming beam emittance and momentum spread vary with the beam energy. The solid lines show the beam size at 60 MeV. The horizontal beam size is dominated by the momentum spread and is large where the dispersion is large. At top energy (dashed lines) the transverse beam emittance dominates the total beam sizes.

The gantry design can accommodate either a passive scattering or a spot scanning nozzle. Two scanning magnets with a magnetic length of 30 cm and a field of 0.8 T provide a scanning field of $\pm$20 cm. The positioning of the scanning magnets downstream of the arc dipoles allows for small aperture magnets upstream, keeping the total weight of magnets on the gantry down to less than 3 tonnes. While the optics shown in **Figure 34** is optimized to produce a round beam at the first scattering target of a scattering nozzle, the strength of the last quadrupole can be varied to provide a smaller horizontal beam size at the iso-center. **Figure 35** shows that variable focusing optics can readily be added as part of a spot scanning nozzle upgrade, allowing the spot size to vary by more than an order of magnitude. It is also possible to add advanced imaging facilities, such as a PET camera or a proton radiography system, to the nozzle [10].

6 Radio frequency system

The voltage for bunch stability and acceleration is provided by one ferrite loaded RF cavity with two gaps, driven by commercially available solid state amplifiers. During the 16.7 ms acceleration cycle the radio frequency increases from 1.2 MHz to 6.0 MHz, a rapid change that drives the design of the RF system. Basic RF parameters are shown in **Table 10**.

Repetition rate, f_{rep}	[Hz]	30
Harmonic number, h		1
Frequency range, F_{RF}	[MHz]	1.188 – 6.002
Number of cavities		1
Number of gaps		2
Maximum total gap voltage, V_{RF}	[kV]	7.5
Number of solid state amplifiers		4
Power per amplifier	[kW]	5

Table 10: Basic RF parameters.

The RF frequency follows the increasing speed of the protons as they are accelerated. The synchronous phase ϕ_S is given by the ramp rate and stays below 52 degrees throughout the acceleration cycle. The RF voltage at injection is tuned to match the longitudinal profile of the injected bunch. Along the energy ramp, the voltage is increased to provide a bucket area sufficiently larger than the bunch area to minimize beam losses. This is accomplished through the sinusoidal voltage function

$$V_{acc}\,[\mathrm{kV}] \;=\; 7.5\,\sin\left(2\pi\left(\frac{t\,[\mathrm{ms}]}{37.3}\right)+0.201\right) \qquad \text{for } 0<t<16.7\ [\mathrm{ms}] \tag{11}$$

where the maximum accelerating voltage of $V_{RF} = 7.5$ kV is reached after approximately 8 ms. **Figure 36** shows the RF voltage, frequency and synchronous phase during acceleration.

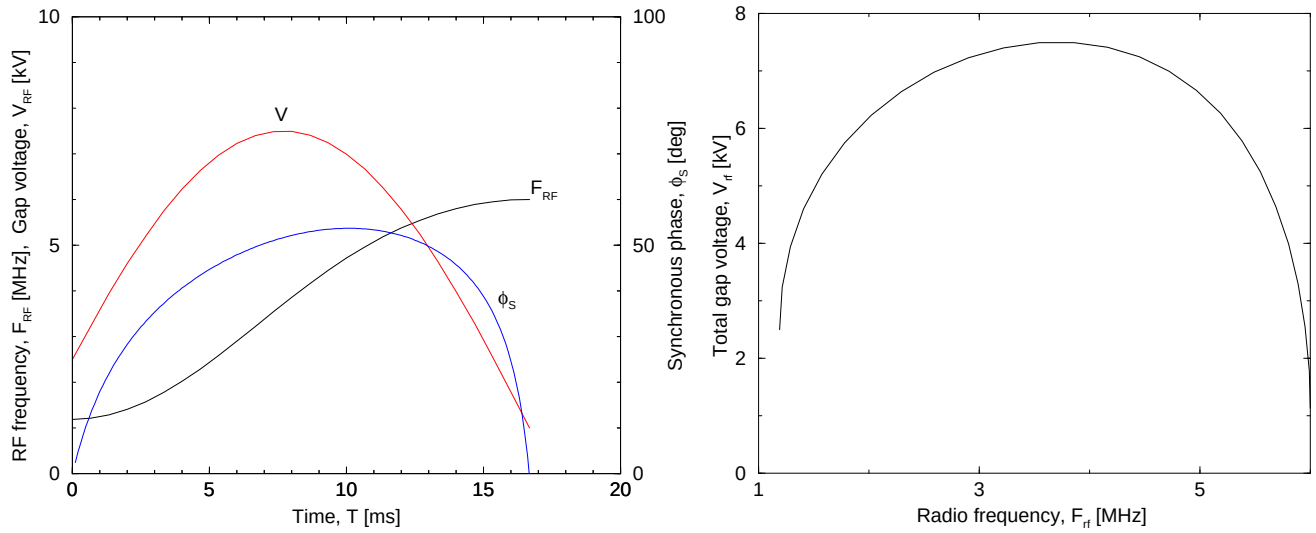

Figure 36: LEFT: RF frequency F_{RF}, RF gap voltage V_{RF}, and synchronous RF phase ϕ_s during acceleration. RIGHT: Total gap voltage V_{RF} as a function of RF frequency F_{RF}.

In **Figures 37** and **38** the bucket and bunch dimensions during acceleration are shown. The bucket length, momentum acceptance and area are computed analytically. The bunch length, momentum width and area are obtained from a 10,000-particle simulation including space charge [11]. The RF parameters are tuned to always provide bucket area sufficiently larger than the bunch to minimize beam losses.

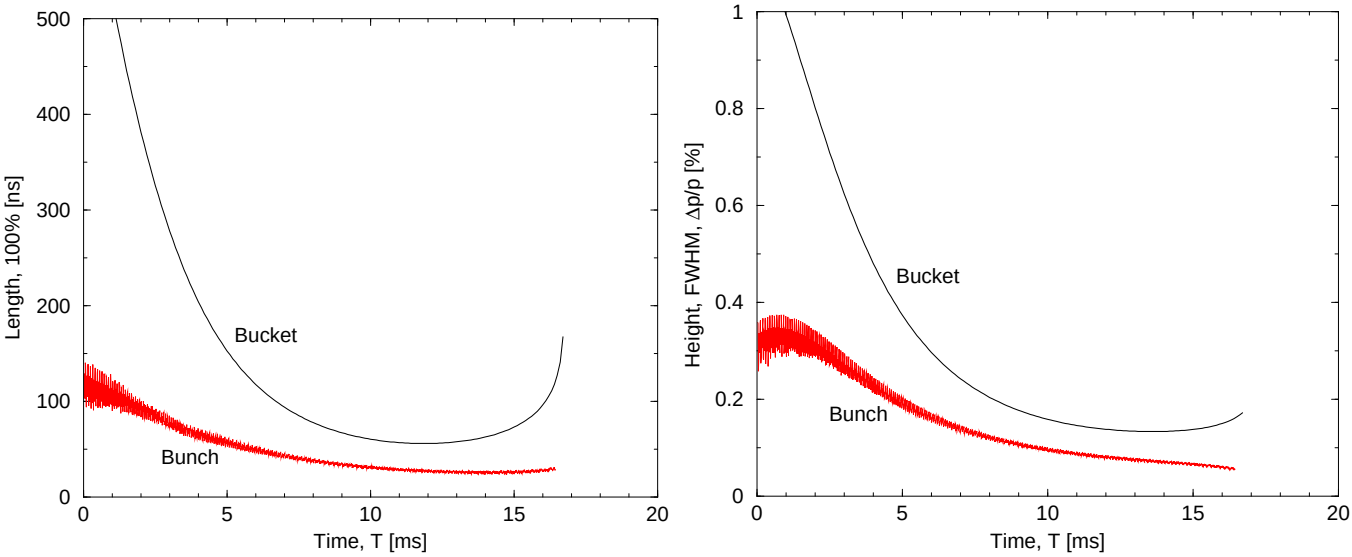

Figure 37: LEFT: Full bucket and bunch length during acceleration. RIGHT: FWHM momentum acceptance and momentum spread.

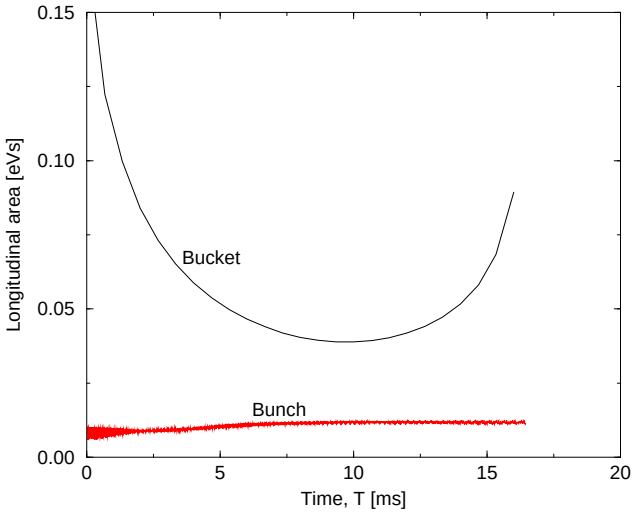

Figure 38: Bucket and bunch area during acceleration.

A ferrite loaded cavity with two gaps provides the RF voltage. The cavity is loaded with 14 rings of 4L2 ferrite per gap. The rings have an inner diameter of 18 cm, an outer diameter of 50 cm, and are 2.5 cm thick. Each ring has an inductance of $L_0 = 1.175$ μH at zero frequency, and $L = 0.063$ μH at 6 MHz. The magnetic field in the ferrite does not exceed 15 mT. The capacitance of a gap is approximately $C = 100$ pF. The cavity is tuned dynamically in a push-pull configuration, at the 30 Hz repetition rate, and operated on resonance at all times. In this way, the drive power is minimized. The tuning current is DC coupled and ranges from zero to 1500 A. Two 5 kW solid state amplifiers per gap provide the necessary RF power. The cavity and the configuration of the tuning current are shown in **Figures 39** and **40**.

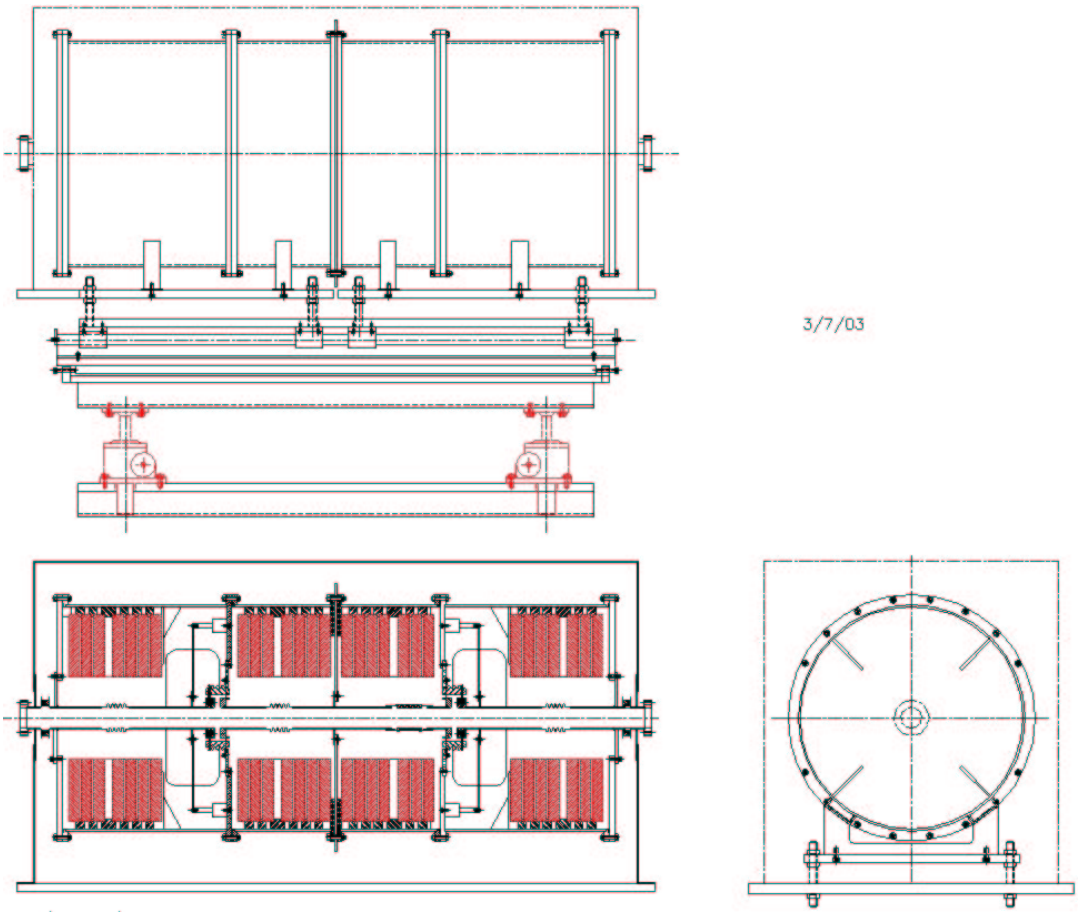

Figure 39: Ferrite loaded RF cavity with two gaps.

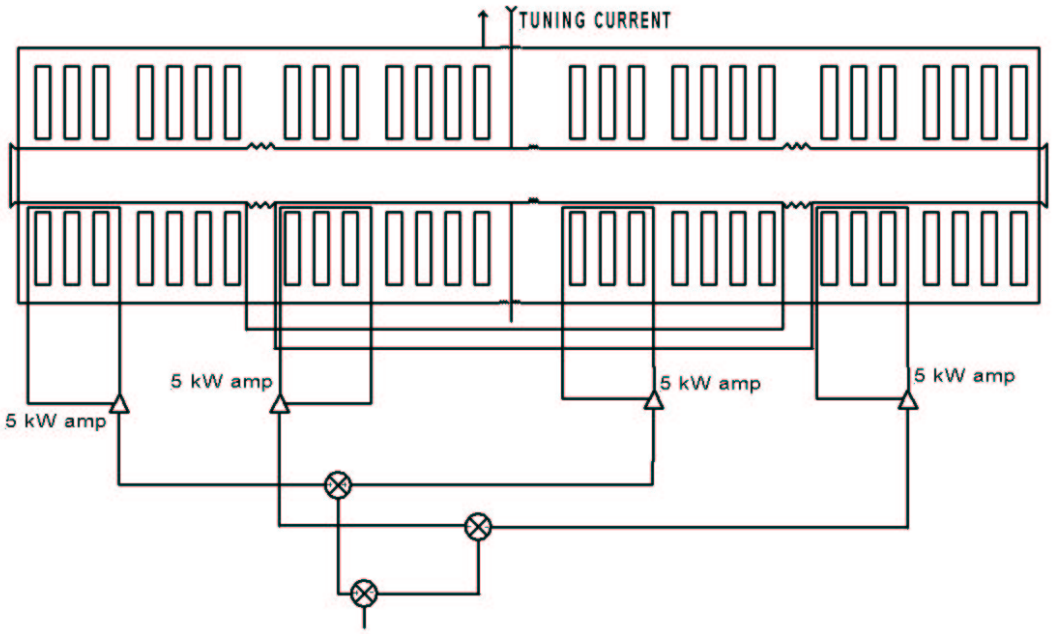

Figure 40: Schematic of electrical tuning loops and amplifiers.

The low level RF system is a state-of-art digital system, based on experience gained at Brookhaven's Relativistic Heavy Ion Collider and Oak Ridge's Spallation Neutron Source. Drive frequencies are generated in Direct Digital Synthesizers (DDS), with a time resolution equivalent to frequencies of up to 32 MHz. RF voltages and frequencies are set in open loops. Corrections are made in a feed-forward manner, from cycle to cycle. For example, a fraction of the the measured phase error can be applied in the next cycle so as to eliminate the phase error over time.

The RF can be switched off within 10 μs of the receipt of a beam-inhibit signal, dumping any beam that is currently in the synchrotron, and disabling the acceptance of beam on following acceleration cycles.

7 Magnets

Three different types of magnet are used in the RCMS synchrotron, beam delivery lines, and treatment rooms: dipoles, quadrupoles, and dipole correctors. The main dipoles are responsible for bending the beam through a large angle (for example, 30° in the gantries), while the quadrupoles keep the beam focused, and the relatively weak dipole correctors are used to keep the beam going down the middle of the beampipe. Sextupole magnets are not required in the RCMS. **Table 11** lists the distribution of the 3 different kinds of dipole, two kinds of quadrupoles, and three kinds of dipole correctors that are used

	DS dipole synch	DT dipole transport	DG dipole gantry	QS quad synch	QG quad gantry	DCH dip corr synch H	DCV dip corr synch V	DCG dip corr gantry
Synchrotron	14			10		4	4	
Extraction		1			3			
Research Room		2			4			2
Fixed vertical		2	7		21			6
Fixed horz. 1		4			7			2
Fixed horz. 2		4			8			4
Gantry 1		2	7		21			6
Gantry 2		2	7		25			8
Gantry 3		2	7		25			8
Gantry 4		2	7		25			8
TOTAL	14	21	35	10	139	4	4	44

Table 11: The total count, and the distribution, of dipoles, quadrupoles, and dipole correctors in the RCMS facility.

Table 12 lists major parameters for the DS, DT, and DG dipoles that are used in the synchrotron, transport lines, and gantry, respectively. The synchrotron dipole shown in **Figure 41** has a saddle coil fabricated from commercially available water-cooled bus, with a magnet core in a laminated "chevron" geometry. The beam transport dipole is similar in design to synchrotron dipole. The gantry dipole shown in **Figure 42** uses a water-cooled coil with a tube/plate method of heat transfer. This dipole has a solid core design.

Table 13 lists major parameters for the two kinds of quadrupole, QS and QG, used primarily in the synchrotron and in the gantry. The synchrotron quadrupole shown in **Figure 43** contains a water-cooled coil which uses the tube/plate method cooling method, and also uses a laminated core design. The gantry quadrupole shown in **Figure 44** maintains its temperature via a water-cooled bus, fabricated from commercially available copper bus. This quad has a solid core design and is mounted in tandem with the neighboring DG dipole, as shown in **Figure 44**.

Dipole corrector parameters are listed in **Table 14.** All dipole corrector are air-cooled. The synchrotron dipole corrector cores are laminated. Two types of correctors – vertical and horizontal – are necessary in the synchrotron, in order to accommodate the oval beam tube. The gantry design contains a single corrector type allowed by the gantry's round beam tube.

		Synch (DS)	Transp (DT)	Gantry (DG)
Magnet type		H-type	H-type	H-type
Magnet shape		chevron	chevron	sector
Dipole bend angle	[deg]	25.714	22.5	30
Dipole bend radius	[m]	1.693	1.693	1.5278
Dipole sagitta	[mm]	10.6	8.2	0
Magnetic length	[m]	0.760	0.665	0.80
Physical length incl coils	[m]	0.845	0.750	0.82
Max. field (top)	[T]	1.44	1.44	1.59
Max. dB/dt	[T/s]	228	0.053	0.032
Inductance	[mH]	0.766	0.67	3.9
Resistance (DC)	[mΩ]	1.0	0.9	1.1
Resistance (AC)	[mΩ]	1.0	N/A	N/A
Max. current	[A]	2569	2569	871
Gap width	[mm]	60	60	40
Gap height	[mm]	30	30	20
Magnet weight	[kg]	410	360	320

Table 12: Dipole parameters corresponding to RCMS optics version 2.1.

		Synch (QS)	Gantry (QG)
Magnetic length	[m]	0.14	0.06
Physical length incl coils	[m]	0.26	0.166
Inner radius	[m]	0.020	0.01
Max. pole tip field (top)	[T]	0.5	0.8
Max. gradient	[T/m]	23.8	35
Gap radius	[mm]	15	10
Max. current	[A]	500	100
Number of turns per pole		8	8
Inductance	[mH]	0.065	0.25
Resistance (DC)	[Ω]	0.9	0.5
Resistance (AC)	[Ω]	1.0	N/A
Magnet weight	[kg]	52	25

Table 13: Quadrupole parameters corresponding to RCMS optics version 2.1.

		DCG Gantry	DCH Synch Horz	DCV Synch Vert
Gap Height (iron to iron)	[mm]	22	32	52
Width	[mm]	60	90	70
Iron length	[mm]	100	100	100
Physical length incl coils	[m]	0.15	0.15	0.15
Integrated Field	[Tm]	0.0073	0.0073	0.0073
Inductance	[mH]	1.60	3.5	4.3
Resistance (DC)	[mΩ]	0.1	0.16	0.26
Max. current	[A]	15	15	15
Power	[W]	22.5	36	58.5

Table 14: Correction dipole parameters, corresponding to RCMS optics version 2.1.

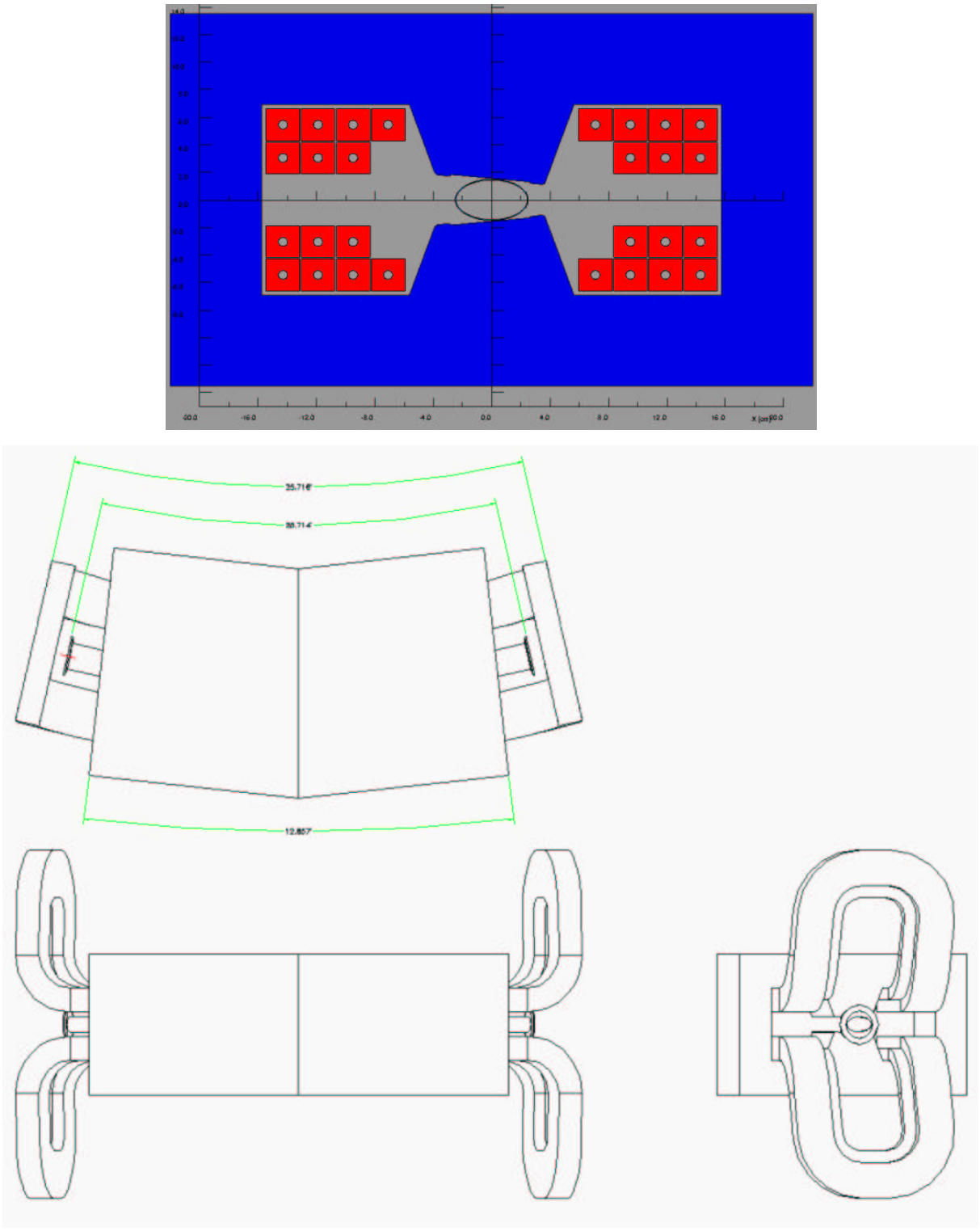

Figure 41: Perspective, cross section, and plan drawings of the DS synchrotron combined function arc magnet, with 7 turn coils, a 30 mm vertical gap, and an elliptical beam pipe.

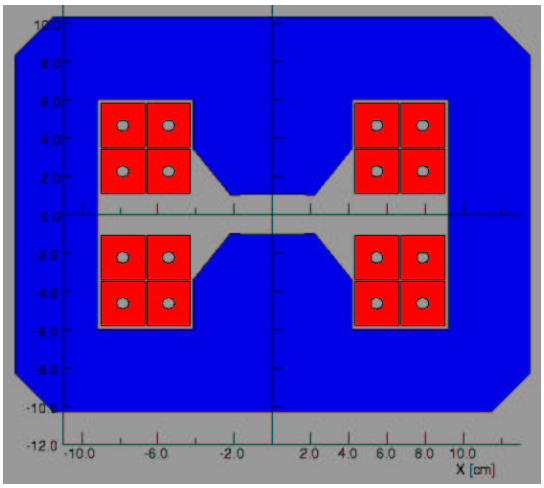

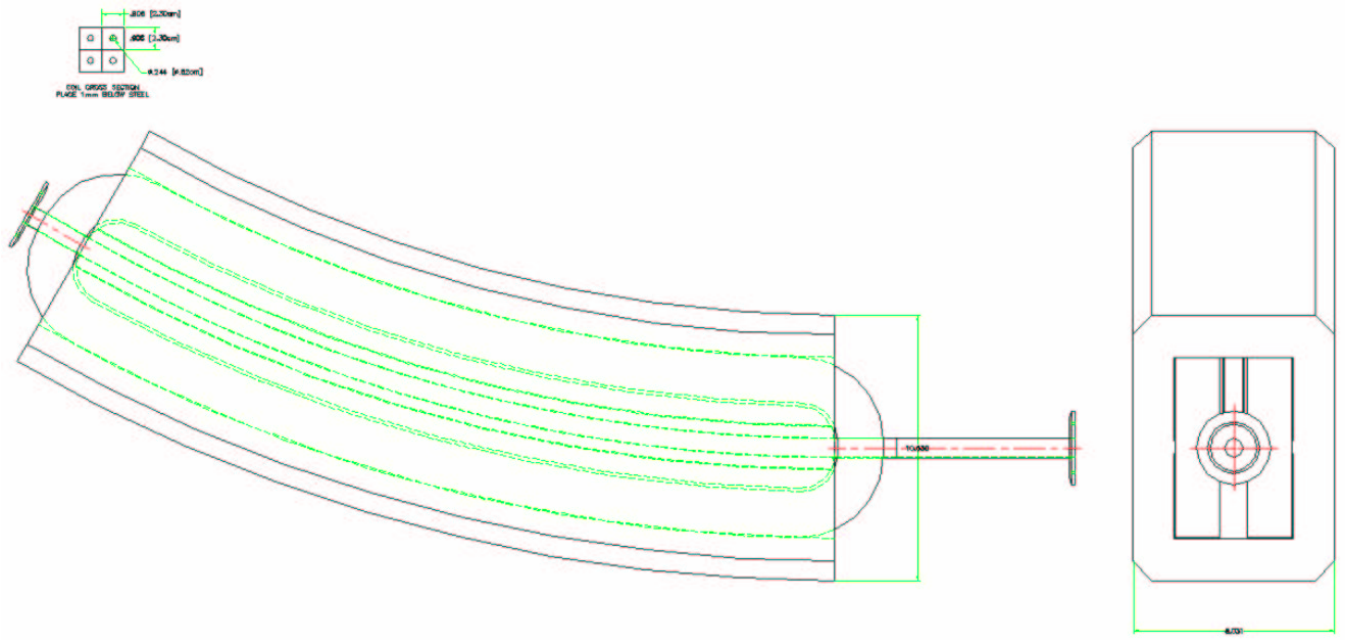

Figure 42: Cross section, plan, and end drawings of a DG gantry dipole.

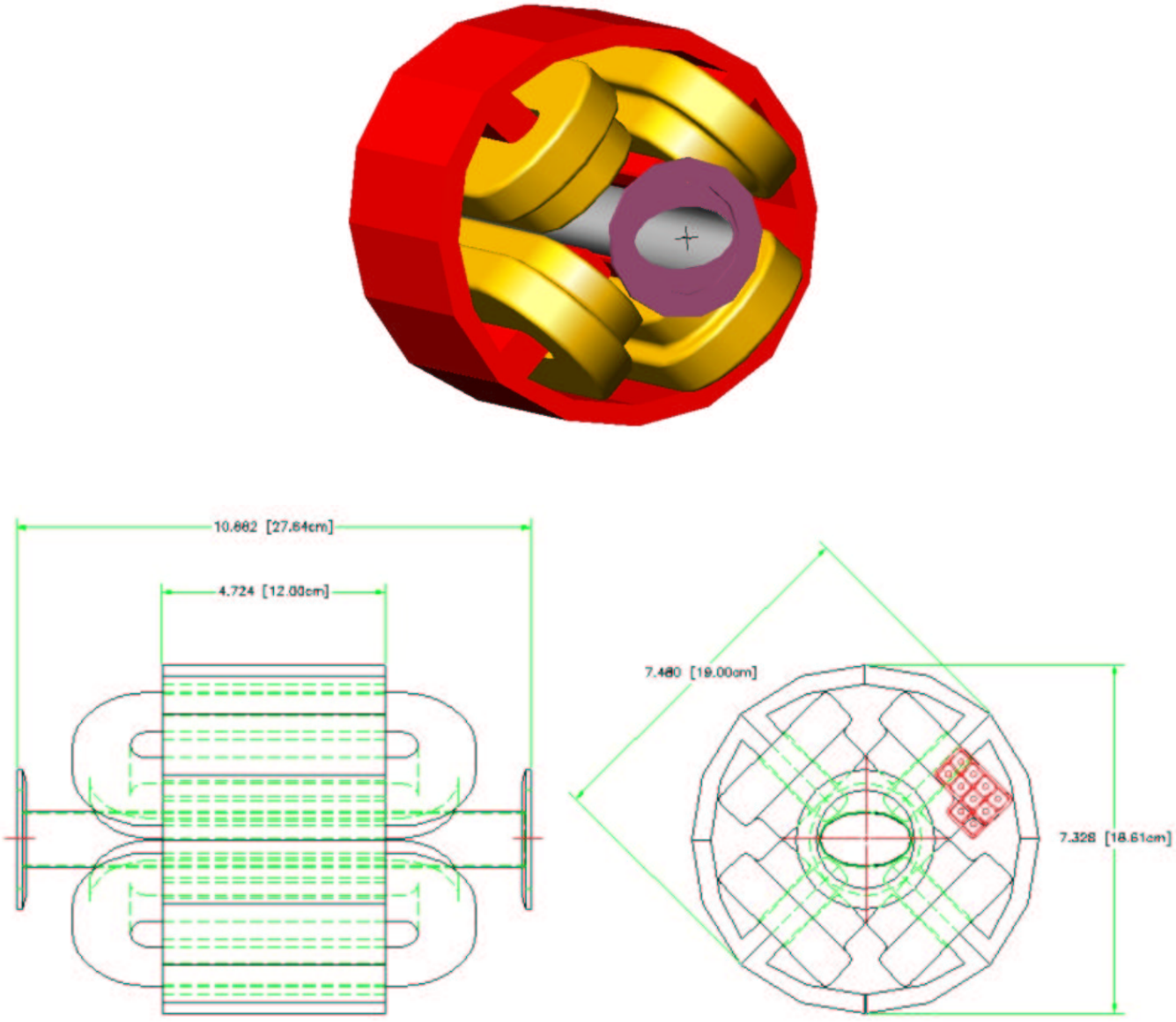

Figure 43: Plan and perspective views of a QS synchrotron quadrupole, with a 20 mm pole tip radius.

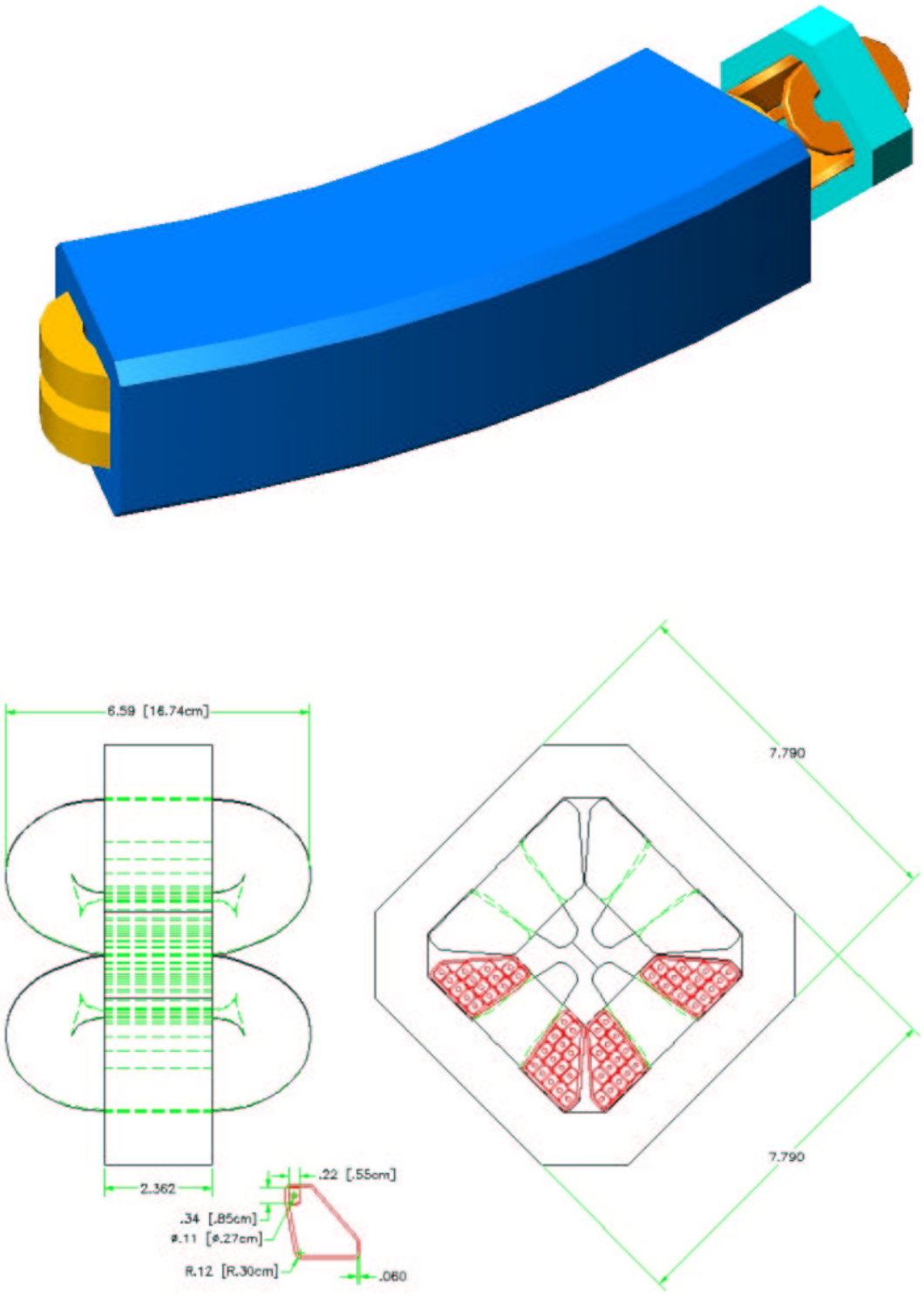

Figure 44: Perspective view of a gantry half cell, and plan view of a QG gantry quadrupole.

8 Power supplies

8.1 Synchrotron main magnet power supply

The main magnet power supply of the RCMS is a single 30 Hz series resonant power supply that drives all 14 dipole magnets in series. Similar resonant power supplies have been used successfully for more than two decades in rapid cycling combined function synchrotrons, such as the Cornell electron synchrotron (60Hz) and the Fermilab proton booster (15 Hz). Such systems are extremely reliable because of their simplicity. Besides their simplicity, resonant power supplies have the major advantage of continuously exchanging stored energy between the magnets and capacitors, with the power supply providing only the losses. This makes them very economical to operate. It also greatly reduces the power line swing, when compared to a rapid cycling programmable power supply; this is a third advantage in choosing a resonant system. The large variations in reactive power flow that otherwise occur cause voltage flicker problems, which can be very costly to solve.

The power supply generates a current of the form

$$I_m(t) \;=\; I_{dc} \,-\, I_{ac}\,\cos(2\pi f t) \tag{12}$$

where a direct current bias of $I_{dc} = 1480$ Amps is added to the sinusoidal alternating current ($I_{ac} = 1090$ Amps) to ensure that the minimum current matches the required field at injection. Beam is injected into the ring at $t = 0$ when $I = 390$ Amps; beam is extracted sometime before $t = 16.66$ ms when $I_m(t) = 2570$ Amps. Except for iron saturation effects the beam momentum is directly proportional to the dipole current.

Figure 45 shows a schematic of the power supply system. Two capacitor banks with DC bypass chokes are used in series with the magnets of the synchrotron. The resonant circuit is driven by one programmable excitation power supply. In a series resonant topology the excitation power supply delivers the full magnet current, but at a significantly reduced voltage when compared to a non-resonant system. The chokes are designed with secondary windings which are connected to provide coupling between the individual resonant circuits. The current and output voltage waveforms are illustrated in the bottom portion of **Figure 45**. **Table 15** shows the main parameters of the synchrotron main magnet power supply system.

8.2 Synchrotron quadrupole power supplies

The three synchrotron quadrupole power supplies are much less demanding in power and performance than the main magnet power supply. Two of the power supplies, "QS1-PS" and "QS2-PS", each drive 4 quads in series, as shown in **Figure 46**. The third, "QS3-PS", drives two quadrupoles in series. All three are independently programmable, in order to be able tune the acceleration cycle, for example, to compensate for field saturation effects in the dipoles.

The quadrupole power supplies are standard switch mode type units, readily available commercially, with proven high reliability. High power programmable power supplies are in routine operation, for example, at the BNL AGS Booster. Switch mode supplies have the advantage of operating at a high frequency, typically 40 kHz, allowing very good regulation and economical filtering. Each supply has a thyristor controlled pre-regulator, which reduces the amount of reactive power the supply draws from the line. **Table 16** shows the main parameters of the synchrotron quad power supplies. **Figure 46** also shows the 4 quadrupole power supply operating current and voltage. The output of the 2 quadrupole power supply is approximately half of this.

8.3 Dipole correctors

There are 8 dipole correctors in the synchrotron, and 46 others in the beam transport and delivery beam lines (2 in the R1 line; 6 in the FG line; 4 in the F1; 4 in the F2 line; 6 in the G1 line; 6 in the G2 line; 6 in the G3 line; 8 in the G4 line; 2 in the T3 line; and 2 in the T4 line). Their power supplies are linear output stage power supplies with a switch mode pre-regulator to maintain 6 volts between collector and emitter under all load and current requirements. These power supplies are bipolar current programmable current regulated at ± 20 Amps and ± 35 Volts. Their design is identical to that used for Spallation Neutron Source (SNS) correctors. All corrector power supplies will be installed in standard 19 inch racks with 6 supplies per rack.

Repetition Rate, f_{rep}	[Hz]	30
Topology		Series Resonant
Number of excitation power supplies		1
Excitation power supply voltage	[V]	$\pm$ 250
Maximum power supply current	[A]	3000
Nominal peak current		2700
Injection current	[A]	390
Direct current, I_{DC}	[A]	1480
Alternating current, I_{AC}	[A]	1090
Number of capacitance banks		2
Number of bypass chokes		2
Number of dipoles		14
Capacitance per bank	[mF]	10.58
Inductance of choke	[mH]	5.32
Inductance of dipole	[mH]	0.76
Resistance of choke	[mΩ]	10
DC resistance per dipole	[mΩ]	1
Quality factor		28
Magnet stored energy	[kJ]	39.0
Capacitor stored energy	[kJ]	12.8
Choke stored energy	[kJ]	26.2
Maximum reactive power	[MW]	4.5
Capacitor losses	[kW]	7.4
Choke losses	[kW]	98
Magnet losses (total)	[kW]	53
TOTAL losses	[kW]	163

Table 15: Synchrotron main magnet power supply specifications.

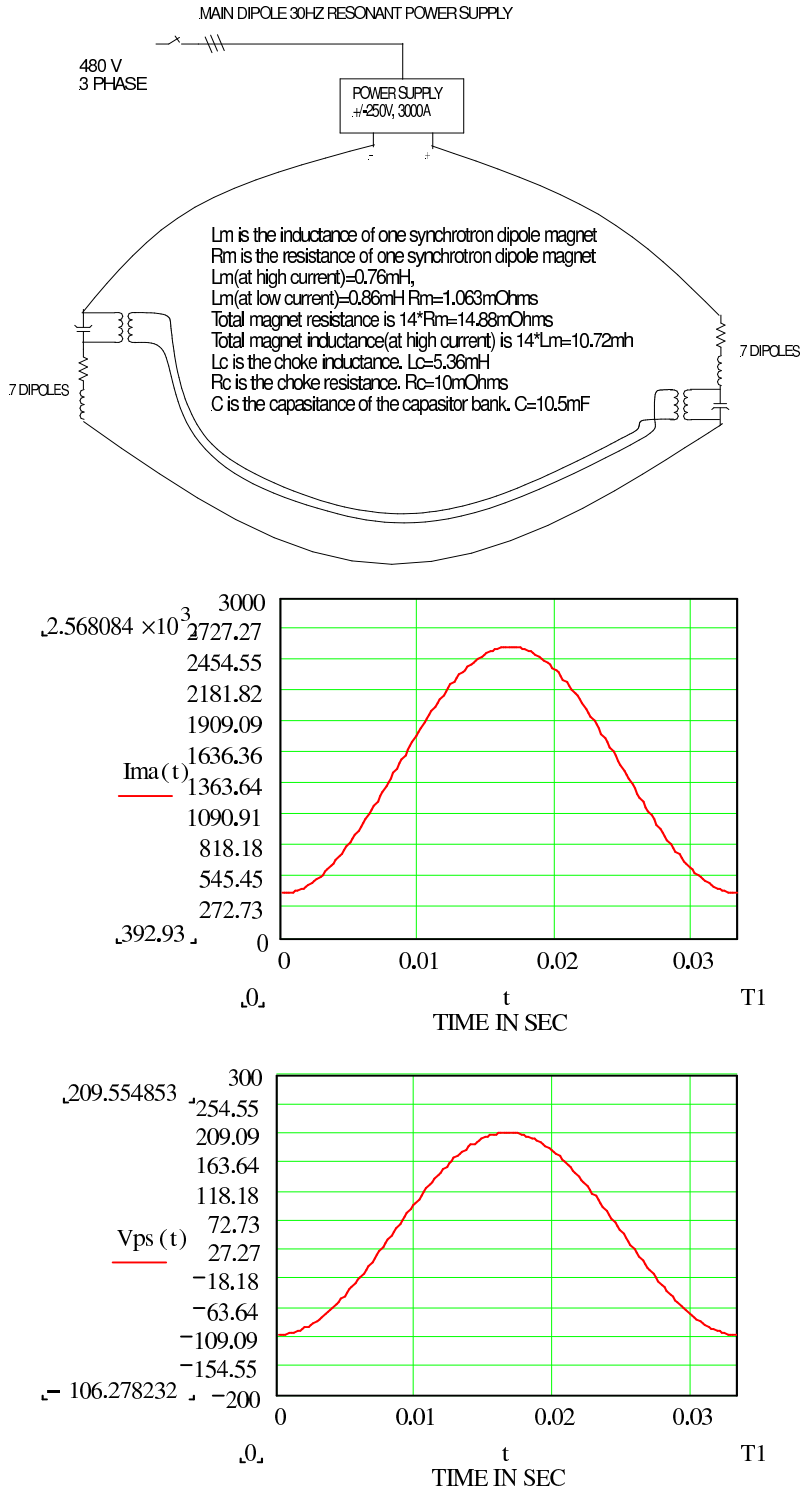

Figure 45: The resonant synchrotron main magnet power supply, which provides up to 3000 Amps at ±250 Volts. Current and output voltage waveforms are shown in the bottom 2 plots.

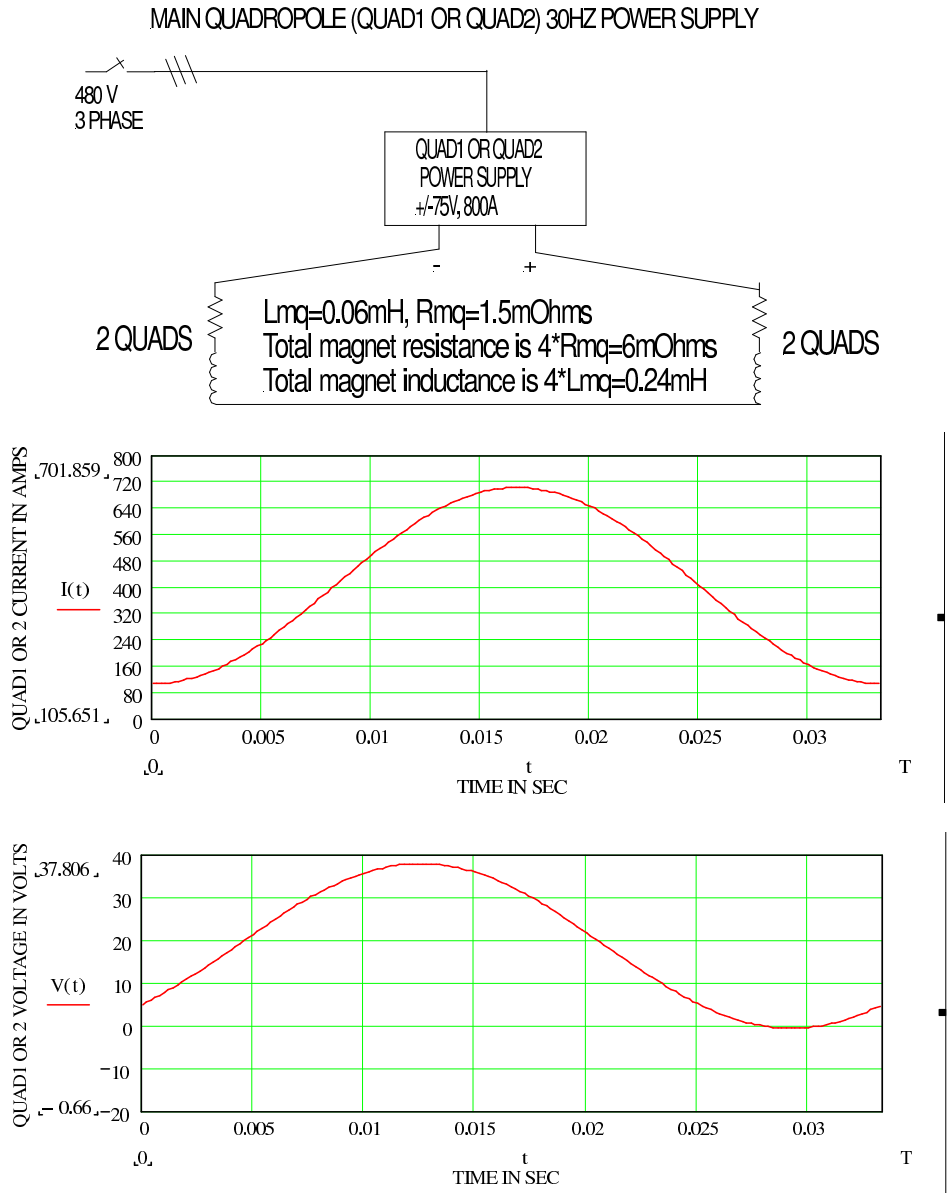

Figure 46: Synchrotron quadrupole power supply, type QS1-PS including current and voltage waveforms.

	Units	**QS1,2-PS**	**QS3-PS**
Repetition Rate, f_{rep}	[Hz]	30	30
Topology		Switch Mode	Switch Mode
Number of power supplies		2	1
Power supply voltage	[V]	± 75	± 75
Maximum power supply current	[A]	800	800
Nominal peak Current	[A]	700	700
Number of magnets		4	2
Inductance per magnet	[μH]	60	60
DC resistance per magnet	[mΩ]	1.5	1.5
Total magnet power loss	[kW]	1.3	0.62

Table 16: Synchrotron quadrupole power supply specifications.

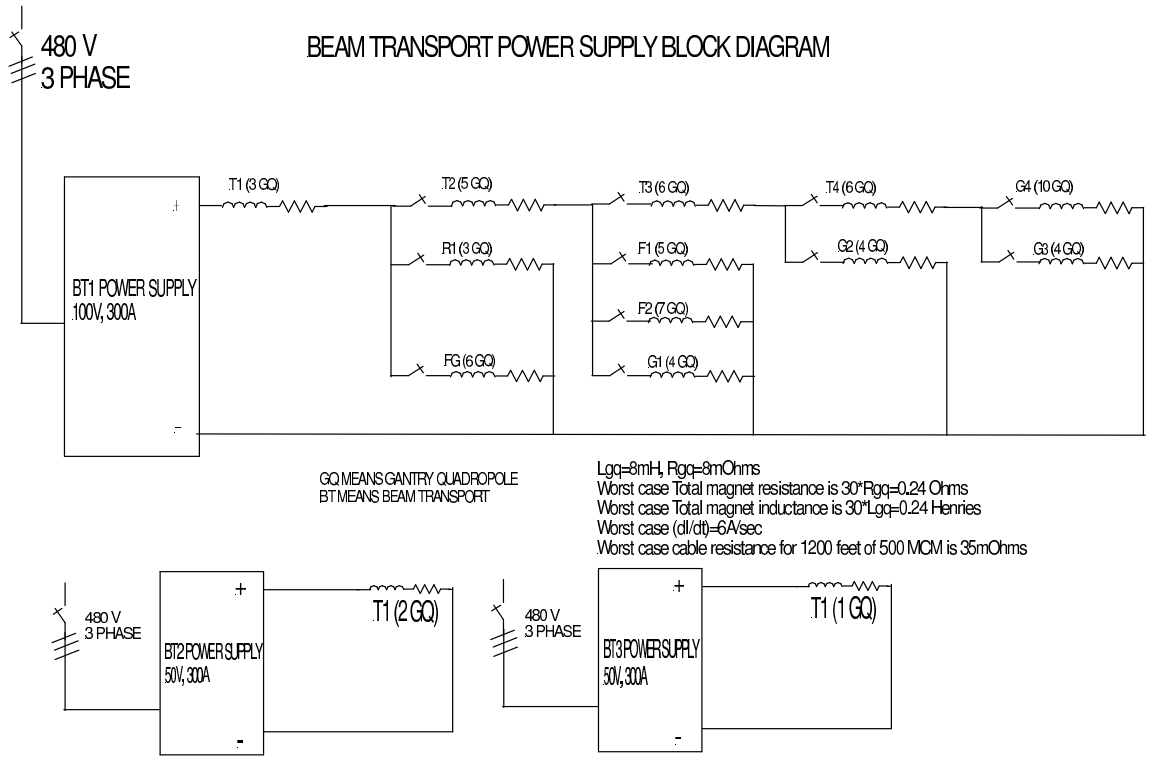

Figure 47: Beam transport power supply connections.

8.4 Beam transport and gantry power supplies

The beam lines will operate one at a time. Thus, costs are reduced by arranging for all of the main beam transport and gantry power supplies to switch from one extraction load to another, through DC switches. These switches are rated to operate about 100,000 times under zero current conditions, once every 10 minutes. They are controlled by Programmable Logic Controllers (PLCs), that set a switch pattern corresponding to the selected beam line.

All of the DC main power supplies have a 12 pulse rectifier topology that uses phase control thyristors. There is one transport supply; one gantry dipole supply; six gantry quadrupole supplies; one DT dipole supply; and one DX (6.5° bend) dipole supply. **Figure 47** shows the beam transport power supply connections. Here power supply BT1 is is rated at 100 VDC, 300 ADC; BT2 and BT3 are rated at 50 VDC, 300 ADC. The label T1 includes all the quad magnets between the ring and the fixed gantry. T2 includes all the quad magnets between the fixed gantry and gantry 1. T3 includes all the quad magnets between gantry 1 and gantry 2. T4 includes all the quad magnets between gantry 2 and gantry 3. G4 includes all the quad magnets between gantry 3 and gantry 4.

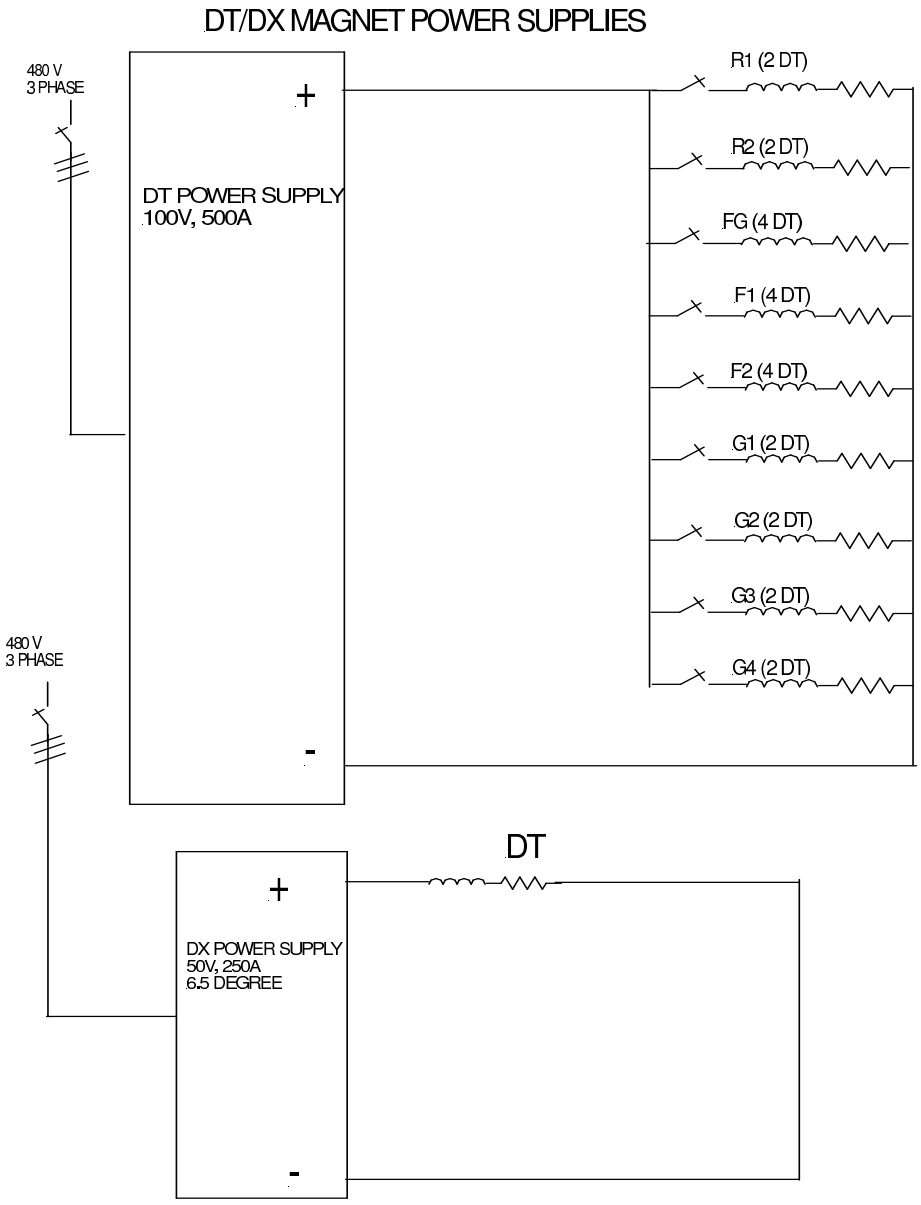

Figure 48: DT and DX power supply connections.

Figure 48 shows the DT and DX (6.5° bend) power supply connections. The DT supply is rated at 100 VDC, 500 ADC; the DX supply is rated at 50 VDC, 200 ADC. **Figures 49** and **50** show the gantry dipole and quadrupole power supply connections. The dipole power supply is rated at 150 VDC, 1000 ADC; the quad supplies are rated at 50 VDC, 300 ADC.

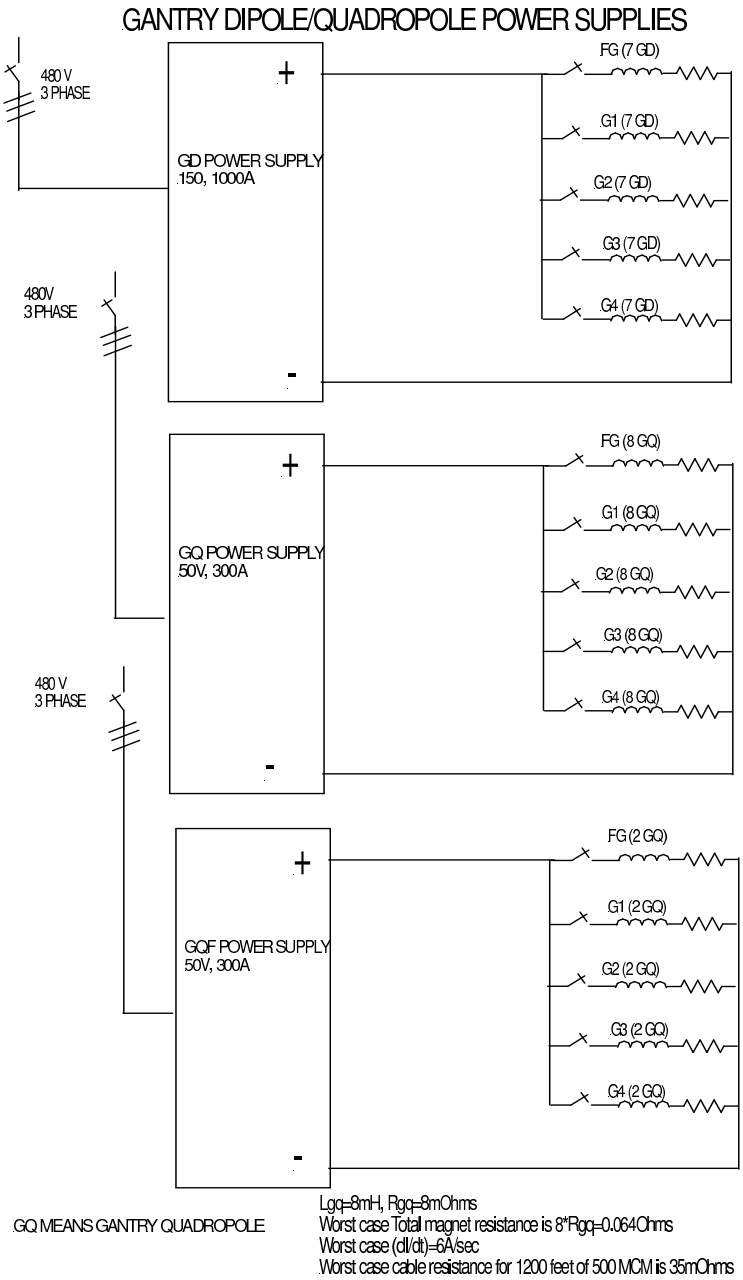

Figure 49: Gantry dipole and quadrupole power supply connections

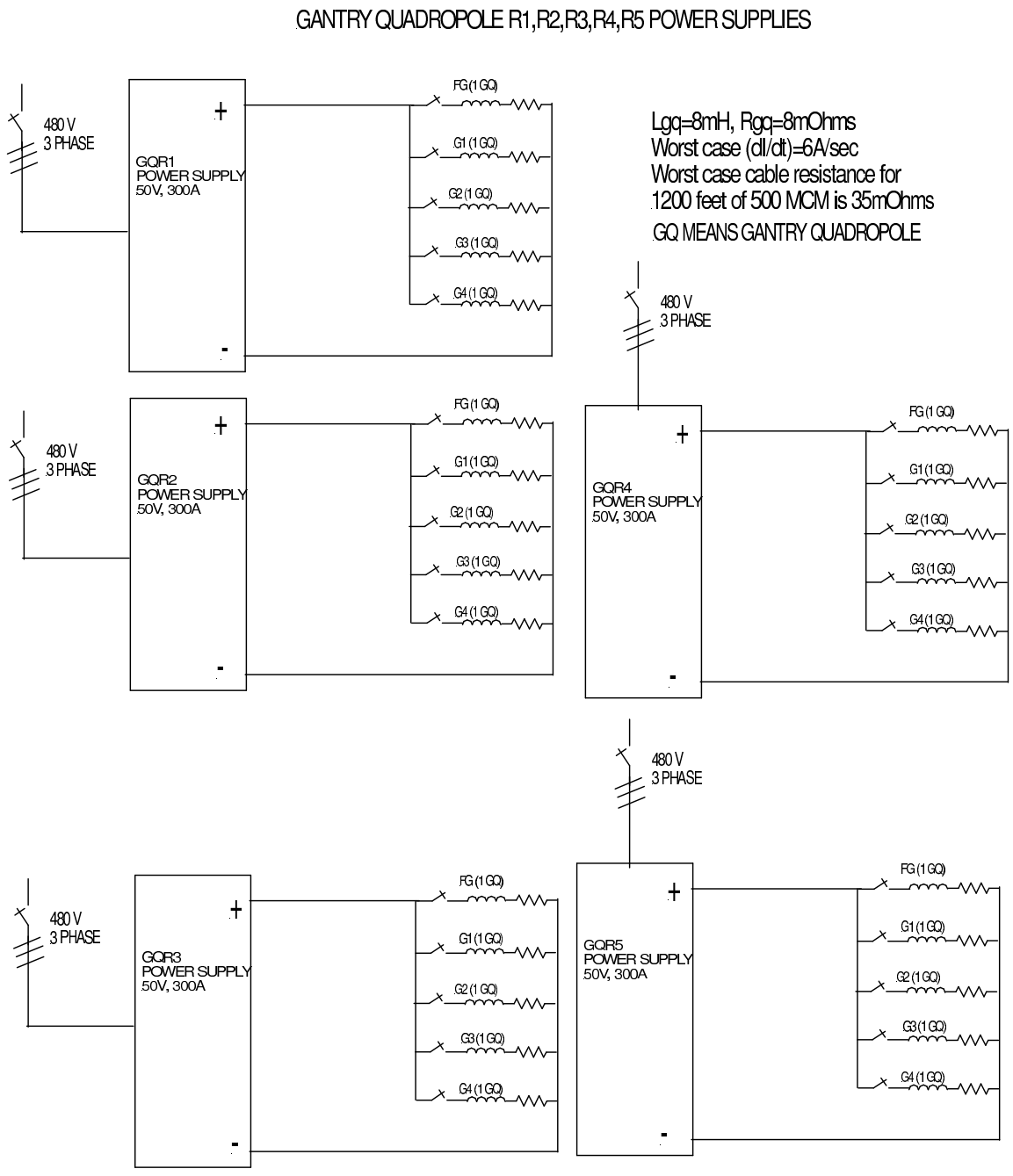

Figure 50: Additional gantry quadrupole power supply connections. The R1, R2, R3, R4, and R5 supplies are used for beta function matching at the gantry rotation point.

8.5 Power supply count and input requirements

Current and voltage specifications for the magnets, and power supply counts, are listed in **Table 17**, for lattice version 2.2. **Tables 18** and **19** list the input power requirements and other parameters for all the RCMS power supplies.

Power Supply	**Max Current**	**Max Voltage**	**Magnet Type**	**Magnet Count**	**Switch Count**
DS	3000	± 250	DS	14	0
QS1,2,3-PS	800	± 75	QS	$4+4+2$	0
BT-PS1	300	100	QG	63	11
BT-PS2	300	100	QG	2	0
BT-PS3	300	100	QG	1	0
GD-PS	1000	100	DG	5×7	5
GQ-PS	300	50	QG	5×8	5
QGF-PS	300	50	QG	5×2	5
QR1-PS	300	50	QG	5×1	5
QR2-PS	300	50	QG	5×1	5
QR3-PS	300	50	QG	5×1	5
QR4-PS	300	50	QG	5×1	5
QR5-PS	300	50	QG	5×1	5
DT-PS	500	100	DT	6×2, 4×3	9
DX-PS	250	50	DX	4	0
54 Corrector	20	35		54	0

Table 17: Power supply performance summary, and count.

Power supply	Max Voltage (V)	Max Current (A)	Input RMS (kVA)	Peak power (kW)	Heat in air (kW)	Heat in water (kW)	Mag. losses (kW)	**TOTAL** (kW)
Main dipole	250	3000	312	750	20	20	53	198
Main quad 1	75	800	9.4	60	2	2	2	6
Main quad 2	75	800	9.4	60	2	2	2	6
Main quad 3	75	800	7.9	60	2	2	1	5
Beam transport 1	100	300	44	30	1.5	1.5	25	28
Beam transport 2	100	300	13	30	1.5	1.5	5	8
Beam transport 3	50	300	11	15	1.5	1.5	4	7
Gantry dipole	50	1000	50	50	10	10	12	32
Gantry quad	50	300	22	15	1	1	12	14
GQF	50	300	22	15	1	1	12	14
GQR1	50	300	10	15	1	1	4.5	6.5
GQR2	50	300	10	15	1	1	4.5	6.5
GQR3	50	300	10	15	1	1	4.5	6.5
GQR4	50	300	10	15	1	1	4.5	6.5
GQR5	50	300	10	15	1	1	4.5	6.5
DX	100	500	74	50	3.5	3.5	40	47
DT	50	250	19	12.5	1	1	10	12
54 Correctors	35	20	87	0.7	0.32	0	0.7	55
TOTAL			**731**					**465**

Table 18: Input power requirements. Corrector supplies are air cooled with 208 V input. All others are water cooled and have 3-phase 480 V input. The main dipole total power includes 105 kW due to choke and capacitor losses.

Power supply	Magnet plus Cable Resistance (mΩ)	Magnet Inductance (mH)	Peak Voltage (V)	Peak Magnet Current (A)	Peak PS Input Current (A)	RMS Op. PS Input Current (A)
Main dipole	15	11	250	2700	1289	375
Main quad 1	9	0.24	75	700	103	11
Main quad 2	9	0.24	75	700	103	11
Main quad 3	6	0.12	40	700	103	9.5
Beam transport 1	275	240	83	300	52	53
Beam transport 2	51	16	16	300	52	15
Beam transport 3	43	8	13	300	26	13
Gantry dipole	120	225	120	1000	86	60
Gantry quad	100	64	30	300	26	26
GQF	80	16	24	300	26	26
GQR1	45	8	13.5	300	26	12
GQR2	45	8	13.5	300	26	12
GQR3	45	8	13.5	300	26	12
GQR4	45	8	13.5	300	26	12
GQR5	45	8	13.5	300	26	12
DX					86	89
DT					21	23
54 Correctors	1500	5	30	20	218	240

Table 19: Parameters of the RCMS power supply system.

9 Instrumentation

The Instrumentation System will provide measurements of beam intensity, losses, position, transverse and longitudinal beam size, as well as inputs to the Safety and Monitoring System (SMS). The medical application of this facility demands the necessary system calibrations, and performance reliability. The scope of the design will not adhere to the patient treatment standards that are required for the nozzle diagnostics. The Treatment Control System is responsible for verifying successful delivery of each pulse via the on-nozzle chamber diagnostics which are separate from this system.

The Rapid Cycling Medical Synchrotron (RCMS) will produce 1×10^7 to 1.7×10^9 protons per bunch, 30 times per second. The injection energy will be 7 MeV, extraction energy ranges from 60 to 250 MeV. The medical application of this facility demands reliable instrumentation for commissioning and operation. Features of the instrumentation include relatively low intensity and low energy beams, fast repetition rate, and rapidly sweeping RF. This proposal focuses on established techniques and commercially available instruments with a proven reputation. We take advantage of the operational instrumentation experience gained at the BNL Collider-Accelerator Department. The proposed instrumentation is summarized in **Table 20**.

Beam Line	**WCM**	**CBM**	**CTX**	**BLM**	**Flag**	**BPM**
Synchrotron	1	2		8	1	6
Beam Transport			1		1	1
Research Room						2
Fixed Beam 1			1		1	2
Fixed Beam 2					1	2
Fixed Beam 3						2
Gantry 1				4	2	3
Gantry 2				4	2	2
Gantry 3				4	2	2
Gantry 4			1	4	2	3
Total	1	2	3	24	12	25

Table 20: RCMS instrumentation distribution. WCM: Wall Current Monitor, CBM: Circulating Beam Monitor, CTX: Transport Current Transformer, BLM: Beam Loss Monitor, Flag: Beam Profile Monitor, BPM: Beam Position Monitor.

9.1 Circulating Beam Monitor

To measure the beam intensity through the acceleration cycle, a custom DC responding current transformer system will be designed. The transformer will be located in the synchrotron straight section upstream of the extraction kicker, mounted around a ceramic break, and enclosed in a shield. A beam transformer front-end amplifier, along with a normalizer, baseline restore, calibration pulse generator, and computer interface electronics also will be designed. There will be an additional redundant system installed in the synchrotron to increase the reliability of the measurement. A processed signal from this system will serve as a beam inhibit input to the *Safety and Monitoring System* (SMS), which will have the capability of interlocking the machine in the event that the measured intensity does not conform to the desired cycle parameters. (See Chapter 10). The current transformer system will be calibrated using a standardized current source.

The RCMS revolution frequencies at injection (7 MeV), and minimum extraction (60 MeV) energies are 1.188 and 3.34 MHz respectively. At 10^7 protons/bunch, this yields circulating beam currents of 2 μA and 6.1 μA.

9.2 Transport Current Transformer

The transducer and analog signal processing electronics for this system are commercially available. The Bergoz Integrating Current Transformer (ICT) in conjunction with Beam Charge Monitor (BCM) electronics will be used to measure bunch intensity at three locations in the extraction transfer lines. The Integrate-Hold-Reset version of the BCM electronics will be triggered as a bunch passes every 33 ms. The highest BCM gain setting is 18 mV/pC of beam charge (noise $<$ 10 mV rms or about 3×10^6). Employing a 12-bit ADC yields a resolution of 2.4 mV/LSB. For extraction intensities of $1 \times 10^7 = 1.6$ pC, and $1 \times 10^9 = 160$ pC, this yields respective digitizer outputs of 12, and 1200 counts. The beam line device includes a ceramic break, transformer mount and enclosure similar to the Circulating Beam Monitor design. A typical current transformer installed in a beam line is shown in **Figure 51**.

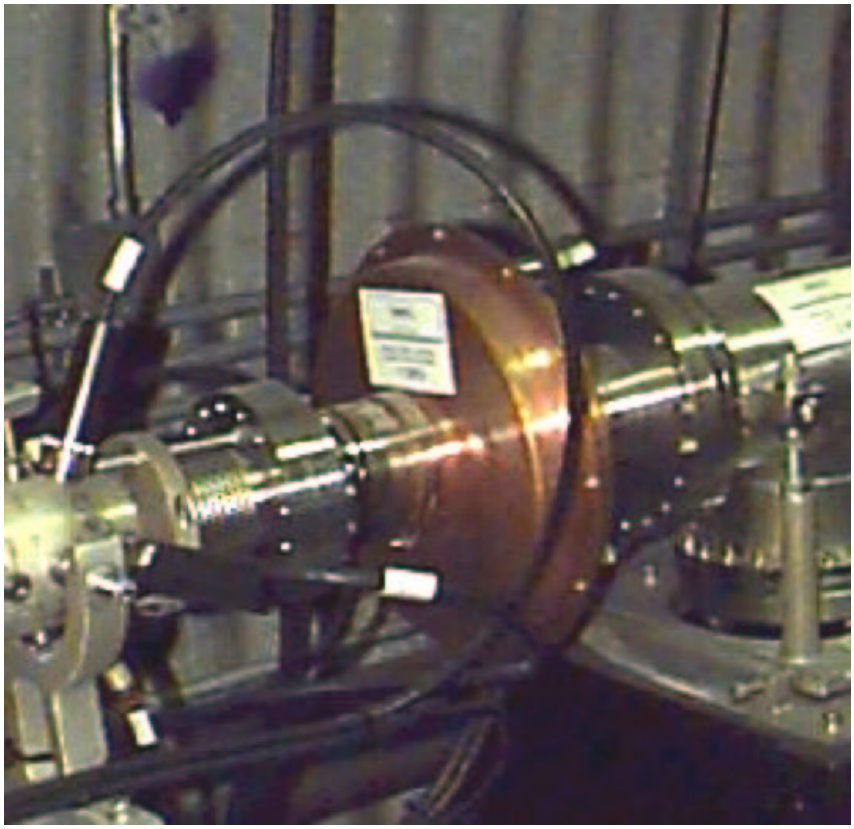

Figure 51: Current transformer installed in beam line.

9.3 Wall Current Monitor

To observe the evolution of the bunch phase and longitudinal profile during the acceleration cycle, a wide-band resistive Wall Current Monitor (WCM) will be designed and installed. The low frequency limit is on the order of a few kHz and is determined by the permeability and size of the core and the gap impedance. The gap impedance will be well controlled to a few GHz, with a frequency response within 3dB over this range. The elliptical shape of the beam pipe will cause tails on the WCM signal; a smooth transition from elliptical pipe to the round WCM is recommended. The detector will be installed with material to absorb energy propagating down the beam pipe above the cutoff frequency. Signals will travel on a good quality $7/8''$ heliax cable which should be kept as short as possible to minimize dispersion. The signal will be amplified, buffered, and sent to a high-speed digitizer which will provide data for analysis. The WCM signal also will be available to the low level rf system for beam phase control.

9.4 Beam Loss Monitor

The Beam Loss Monitor system shows where beam is being lost and how much is being lost at a given location. This information is used to tune machine parameters so that the loss is eliminated or minimized, thereby keeping activation of machine components to a minimum. The system also provides a beam inhibit input to the SMS which has the capability of interlocking the machine if losses exceed prescribed levels. Typical uncontrolled loss criteria of 1 W/m will keep the residual levels below 100 mRem/hour to allow hands-on maintenance work after a short cool down period.

The distributed loss monitor system will utilize proportional chambers and/or scintillator/PMT detectors. These detectors will be more sensitive to neutrons and low energy beam losses at injection than the traditional ion chamber detectors. Beam loss detectors will be located at 8 significant loss points around the ring. Significant loss points include the quadrupoles, injection and extraction devices, the RF cavity and collimators. The BLMs in the ring will have the capability of manual relocation to help diagnose particular beam loss problems. Loss signals will be transmitted through coaxial cables to the equipment gallery, processed by front-end electronics, and digitized for display and analysis.

9.5 Beam Profile Monitor

Princeton Scientific offers a luminescent target beam profile monitor, model No. DF120. It has a target holder, solenoid actuator, and viewing port all mounted on a 6″ O.D. conflat flange. This semi-destructive diagnostic will be inserted during commissioning, tuning, maintenance, or troubleshooting. The phosphor material is similar to Chromox 6 (chromium doped aluminum oxide). A CCD camera with lens will be mounted near the device; the video signal will be transported to a PC based video digitizer for image processing. There will be one such device in the synchrotron straight section downstream of the injection kicker, several in the extraction transport lines, and two in each Gantry. Profile measurement resolution will be on the order of 1mm or better. The flag assembly is shown in **Figure 52**.

Figure 52: Flag assembly.

9.6 Beam Position Monitor

The synchrotron will be instrumented with dual plane capacitive pick-up style beam position monitors (BPM) at the beginning, middle and end of each 180-degree arc. BPMs also will be installed in several places along each of the extraction transfer lines. Each BPM will be mechanically indexed to nearby quadrupoles.

A high impedance amplifier will be mounted near each pick-up. It will drive the signal on 3/8″ heliax, low loss, 50 Ω, phase matched cables. In the electronics service room there will be 19″ racks housing front-end electronics modules with adjustable gain (system dynamic range required > 86 dB) and BPM signal processing.

Preliminary estimates show that the BPM system could provide average closed orbit position in the synchrotron through-out the design intensity range. Since beam can be transported to only one extraction beam line (2 BPMs/line) at a time, a Keithley high frequency multiplexer can be used to route the signals to dedicated transfer line BPM electronics modules. One of the ring horizontal BPM position signals will be used for real time radial feedback for the low level rf system.

Figure 53 shows simulated output voltage waveforms from a single capacitive pick-up with electrode length $L = 4.5''$, azimuthal width $\phi = 57°$, and electrode capacitance $C = 65$ pF. A bunch width of 180 ns, a cosine squared distribution, and the minimum and maximum intensities shortly after injection are assumed. The voltage is given by [12]

$$V_c(t) = \frac{\phi L}{2\pi C} \frac{I_b(t)}{\beta_b c} \tag{13}$$

where I_b is the beam current, c is the velocity of light and $\beta_b = 0.122$.

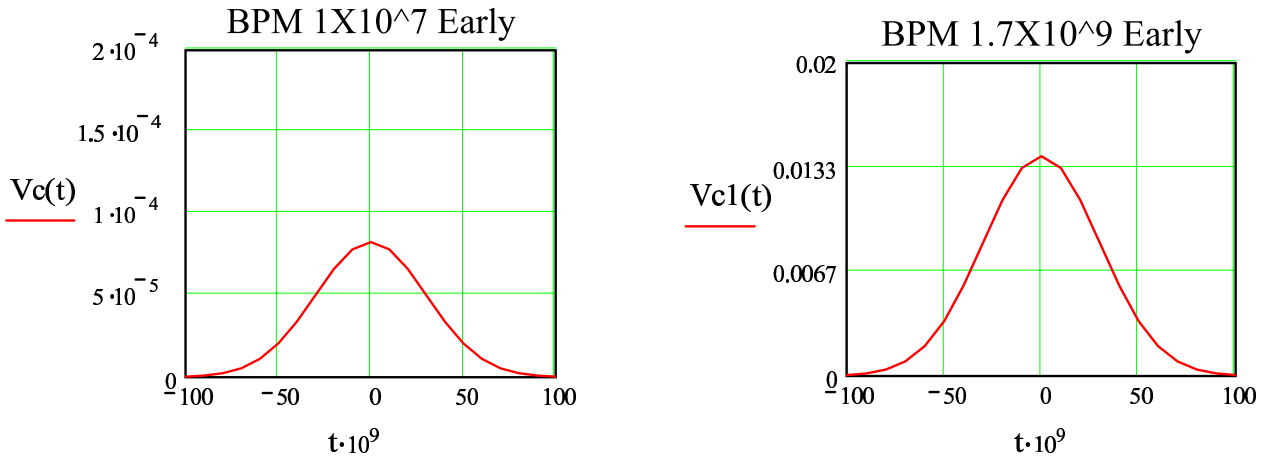

Figure 53: Simulated pick-up voltage for 1×10^7 and 1.7×10^9 protons.

10 Control systems

The RCMS controls are designed as dedicated, self contained, sub-systems with provision for all of the interfaces required to integrate easily and effectively with the clinical (Treatment Planning System – TPS) and the oversight (Record and Verify – RaV) systems of the proton therapy facility. The partitioning is designed to optimize functionality and simplify the design as well as to streamline the code and hardware verification process. This partitioning also allows independent and simultaneous development of the systems while adhering to a rigorously defined interface specification.

The RCMS specific control systems are:

- The Treatment Control System – TCS
- The Dispatcher – DS
- The Safety and Monitoring System – SMS
- The Accelerator Control System – ACS

All four of these systems are based as much as possible on standard commercial products and all required custom hardware and software implementations will be based on verified and verifiable tools and products so that commissioning and approval(s) may proceed as expeditiously as possible.

The underlying design philosophy for the RCMS controls is taken from LBL report #33749, *Performance Specifications for Proton Medical Facility* [7], but advantage is taken of the 30 Hz repetition rate of the RCMS machine to avoid custom control and measurement hardware. The control algorithms and calculations are made in standard high quality commercial processors. A separate and independent hardware based safety system monitors all critical parameters and provides redundant fail safe backup.

The formal specification of the full RCMS controls system is made in a high level simulation language with modules corresponding to the various individual elements and sub-elements and all interfaces conforming to the Interface Control Document. This specification is then a model of the operation of the full system, and can be used to compare and test the functionality of each element against the specification during design, construction, and commissioning. The software model can then be converted directly into a simulator "black box" by providing the appropriate physical interfaces. This simulation "black box" then serves as a test bench during commissioning, and later as an ongoing maintenance and verification aid, since the operation of each independent element can be tested against the known valid model.

The TCS, DS, SMS, and ACS are discussed separately in the following sections. Required interface signals and transactions are shown in **Table 21**. The reader should note that while there is *one* ACS, *one* Dispatcher, and *one* SMS for the entire facility, there is a separate TCS for each treatment room or area. It is probable, but not mandatory, that there would also be one TPS per proton therapy room (plus other identical systems for other non-proton therapy treatment or planning rooms) but only one RaV system would be required for the facility.

10.1 Treatment Control System

The TCS operates, monitors, and adjusts the entire proton delivery system to meet the treatment plan developed in the Treatment Planning System. The TCS is designed to be fail safe and uses redundancy in both measurements and critical hardware coupled with documented and validated software design to ensure this end. As indicated in **Figure 54**, the TCS for each treatment room is logically and physically independent of the other rooms and is connected to the shared resource of accelerator and beam line systems via a single switching matrix (the *Dispatcher*) that allows no more than one TCS to control the accelerator at any given time.

In **Figure 54**, the Beam Monitoring function is broken out explicitly, since the redundant ionization and proportional wire intensity and position monitoring chambers located in the nozzle are custom hardware. Similarly, at least some of the mechanical positioning functions for the couch, nozzle, and gantry are likely to be custom hardware. The remainder of the TCS is constructed of standard commercial hardware.

First, a treatment plan is entered, checked, and approved in the Treatment Planning System. Then, the full set of treatment plan parameters (position, intensity, energy, etc.) are passed to the TCS, which controls mechanical positioning of the various elements, initiates any calibration or imaging tasks, verifies custom bolus or scatterer identities, collimator and nozzle settings and, in general, prepares the system for receiving beam. Once all checks are

	To TCS	**To DS**	**To ACS**	**To SMS**
From TCS		Patient/Treatment ID* Connection Request* Accel. Simul. Request* Gantry Angle Request* Energy Request* Intensity Request* Spot Size Request* Spot Position Request* Beam Request* Beam Prohibit Treatment Room Ready Measured Intensity Measured Spot-size		Patient/Treatment ID* Connection Request* Connection Status* Simulation Status* Fault Interlocks Watchdog Replies
From DS	Connection Active Accel. Simul. Active Accel. Busy Accel. Ready Injection Pulse Extract Request Pulse		Patient/Treatment ID* Connection Request* Connection Active Treat. Simulation Active Gantry Angle Request* Energy Request* Intensity Request* Spot Size Request* Spot Position Request* Beam Request* Beam Prohibit Measured Intensity Measured Spot-size	Connection Requests* Connection Status* Simulation Requests* Simulation Status* Intensity Request* Energy Request* Spot-size Request* Beam Request* Beam Prohibit Fault Interlocks Watchdog Replies
From ACS	Standard Clock Pulse Cycle Start Pulse	Standard Clock Pulse Cycle Start Pulse Injection Pulse Extraction Request Pulse Accel. Ready Treat. Simul. Request*		Standard Clock Pulse Cycle Start Pulse Extract Request Pulse Connection Status* Simulation Status* Fault Interlocks Watchdog Replies
From SMS	Interlock Signals Watchdog Signal(s) Shutdown Signal*	Interlock Signals Watchdog Signal(s) Shutdown Signal*	Interlock Signals Watchdog Signal(s) Shutdown Signal*	

Table 21: Required interface signals between the Treatment Control System, Dispatcher System, Accelerator Control System, and the Safety and Monitoring System. An asterisk * indicates that a full handshake is required.

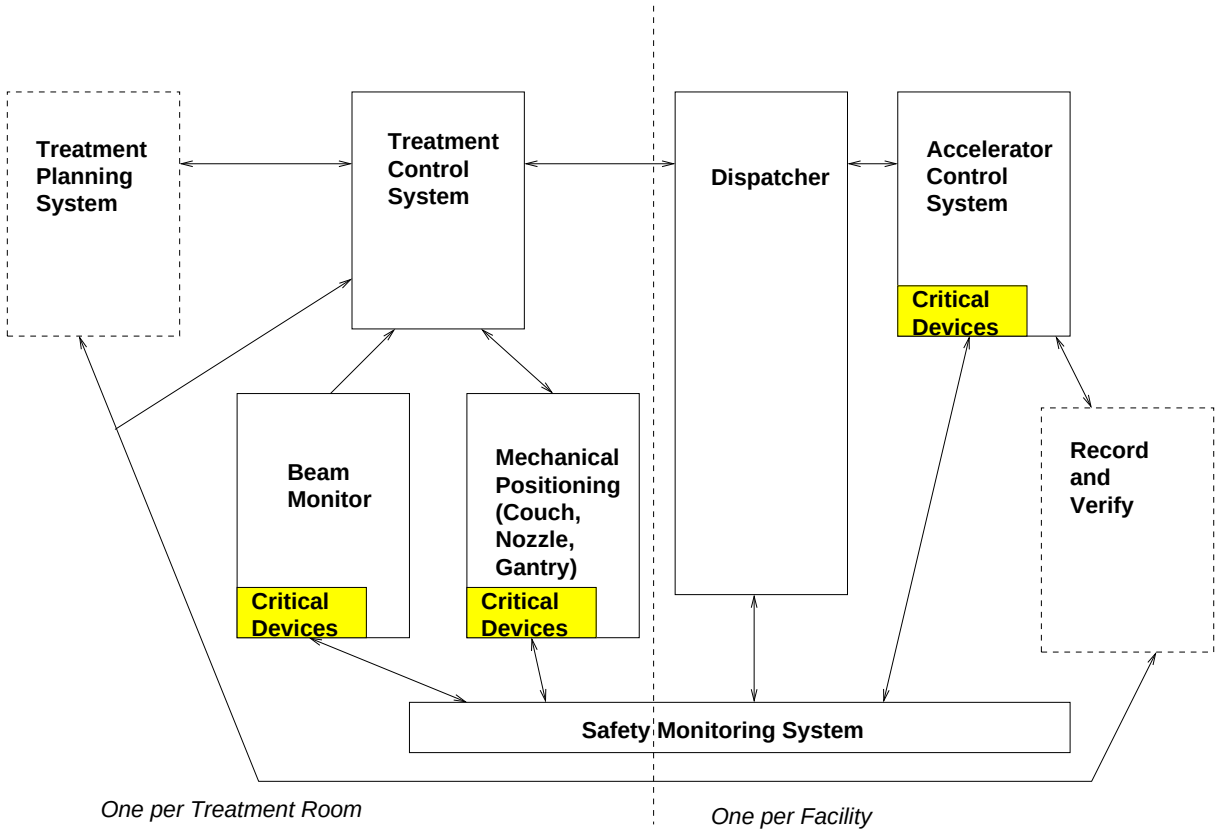

Figure 54: RCMS control system block diagram. Note that the Treatment Planning System and the Record and Verify system are shown dashed to indicate that only the interfaces to those systems are covered in this document.

complete, the TCS then requests beam from the accelerator via the Dispatcher. The Dispatcher's task is to allow only one treatment room to control the accelerator at any one time and so the TCS request from a given room may be queued for a period while waiting for control. Since the intensity and energy is re-set in the synchrotron for every pulse (once every 33 ms), the TCS is responsible for delivering intensity and energy settings for each *next* pulse. It then verifies successful delivery of each pulse by measurements from the nozzle ion chamber systems and other instrumentation. Small deviations from requested intensity levels can be accepted or even compensated on the next pulse, but large deviations will result in a safety trip.

The pulsed nature of the RCMS is a major advantage for the control system since the system can operate in a *request* mode which is more naturally fail safe. In order for a *next* pulse of protons to appear at the nozzle there must be an active request for such a pulse at a particular intensity and energy. While the RCMS is "rapid" in synchrotron terms, the 33 ms between pulses is a very generous time in which to make control decisions and adjustments.

For a passive scattering nozzle, little pulse to pulse adjustment is required. For a scanning nozzle, the TCS would control not only the beam energy and intensity, but also the steering magnets in the gantry. In both the scanning and scattering cases, the TCS would also compare the pulse to pulse beam profiles against the treatment plan and either correct (where applicable) in the next pulse or fault on a deviation.

The physical implementation of the TCS is shown in **Figure 55**. It is likely to be a VME or PXI crate (to maximize the availability of commercial interface modules) controlled by a single board computer running a stable multitasking commercial operating system. As indicated in **Figure 55**, the colored boxes (Accelerator Interface and Gated Integrator) are almost certainly custom hardware, but the control lines to the Couch, Nozzle, and Gantry can be implemented using standard commercial interface boards. The Operator Interface is a standard display/keyboard/mouse, and the communication to the Treatment Planning system is via a private TCP/IP connection. Not shown are connections to the backup safety system, to auxiliary instruments (CT, PET, or other imaging), or to the Record and Verify System – the single, central, record keeping system for the complex.

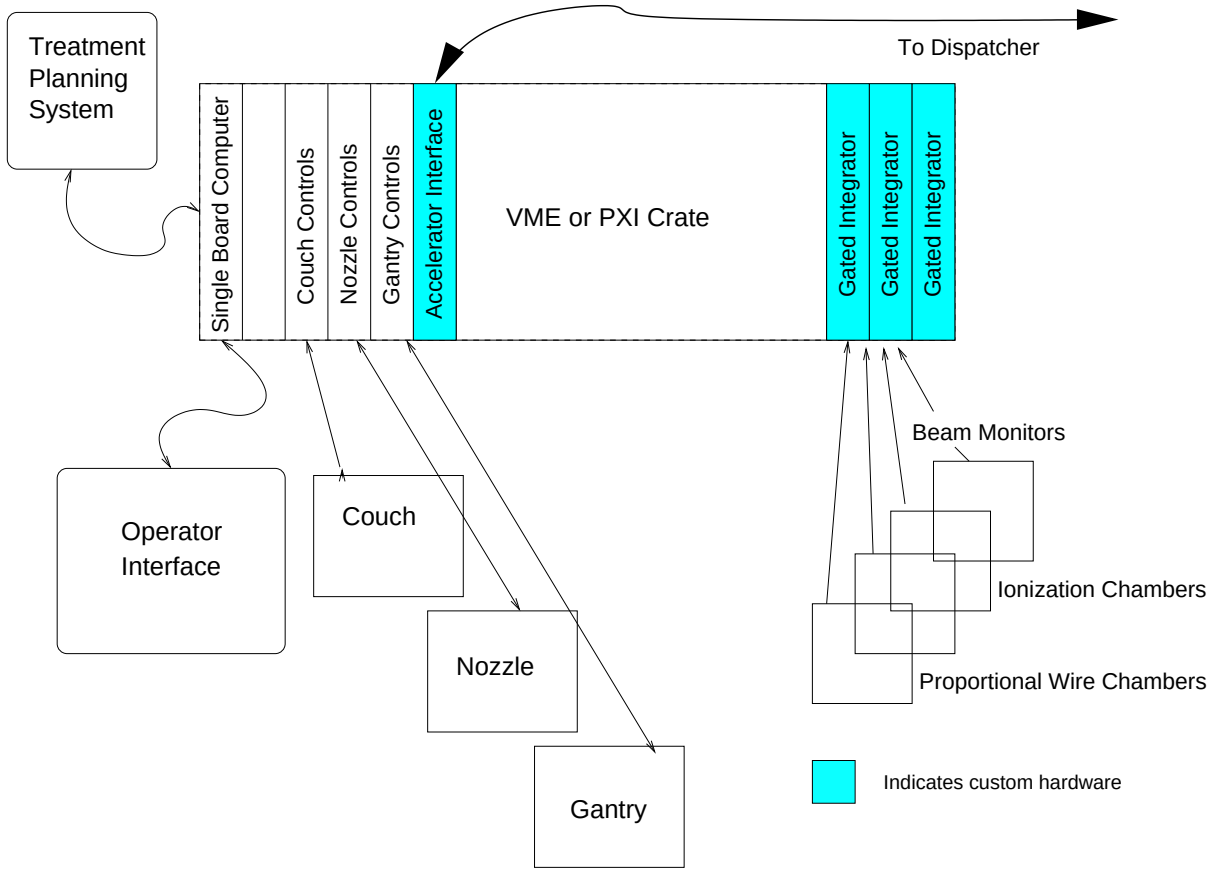

Figure 55: Treatment Control System implementation diagram

The connections to the accelerator all run through the Dispatcher so that only one treatment room (TCS) can be *live* at once. The connections to the Accelerator Control System are either implemented as request-handshake pairs or as set point values (e.g. pulse energy or intensity). The entire control system is synchronous and is driven by the central accelerator clock – a super-multiple of the basic 30 Hz repetition frequency – all intensity and position measurements are gated off phase delayed versions of this central clock. The clock is the only Accelerator signal that is not interrupted by the Dispatcher – all TCS systems are, at all times, running in synchronism with the accelerator but no more than one room is in actual control of the accelerator at any given time.

The TCS has two main modes of operation – *maintenance* and *treatment*. Normal turn on in the mornings will be via the *maintenance mode* which will check the operational integrity of the controls and all of the operating subsystems (couch, gantry, and other auxiliary items). Once the startup checks are satisfactorily completed, the system is ready to be placed into *treatment mode* and proceed. The system *mode* is communicated to the DCS and SMS in a pro-active fashion in order to ensure that no accelerator control can be exercised by a TCS in *maintenance mode.*

10.2 Dispatcher System

The Dispatcher is a many to one switching system allowing multiple TCS systems and the TCS simulator to control the single accelerator. Except for the basic timing signals that are continually available to the TCS systems, all other communications with the accelerator run through the DS. This separation allows simpler design and commissioning of the ACS and TCS systems and separates out the necessary interlock functions that allow a multiple treatment room facility to operate smoothly. The DS is implemented as a standard commercial controller with no custom hardware required. The signals being switched are noted in **Table 21**.

10.3 Accelerator Control System

The Accelerator Control System operates the synchrotron and beam transport systems in a manner that safely and reliably satisfies the requirements of the TCS. The design makes maximal use of commercial components and the design and validation of custom hardware and software will follow industry and FDA standards. The system will operate in two distinct modes that will be appropriately interlocked.

In *treatment mode* the ACS is entirely slave to the TCS, responding to pulse-to-pulse requests for beam, synchronous with the 30 Hz cycle rate of the synchrotron. For treatment with a passive scattering nozzle, there will be little pulse-to-pulse adjustment. A series of beam requests at fixed values of intensity and spot size will be typical, with energy changes at longer intervals. For treatment with a scanning nozzle, pulse-to-pulse changes in intensity and/or spot size will occur along with the transverse position scan at the nozzle. At longer intervals the energy will be changed in small steps to accomplish the scan in depth. Additional steps will be executed for each treatment scenario when changing between treatment rooms. Power will be removed from the prior transport line and switched to the new line in accordance with its gantry angle and initial energy. **Table 22** indicates the principal accelerator output parameters and equipment settings that will be changed in response to TCS requests.

Change in TCS Request	**ACS Changes Required**
Intensity	Gains in low level RF instrumentation and feedback controls Gains and/or integrator gate widths in beam instrumentation Gantry quadrupole currents (if emittance changes with intensity)
Spot Size	Gantry quadrupole current(s)
Scanned Beam Spot Position	Nozzle scanning magnet currents
Energy	"Extraction Request" pulse timing RF frequency at extraction Extraction kicker voltage Septum magnet current Beam transport magnet currents
Gantry Orientation	Gantry steering magnet currents
Treatment Room	Beam transport magnet currents Transport magnet power routing switch Transport instrumentation signal switch

Table 22: Accelerator Control System responses to Treatment Control System requests.

The configuration of the software will minimize processing activity during *treatment mode* operation, with no access allowed for tuning settings or transfer functions applied thereto. Output parameter requests will be implemented by robust handshake with the TCS via the Dispatcher System and settings will be verified at the lowest possible level. Critical software tasks will be required to respond in a deterministic manner to watchdog signals sent by the independent Safety and Monitoring System. **Table 21** lists the signals that are included in the ACS interface to other RCMS control systems.

The ACS will be put in *treatment mode* upon successful completion of the morning turn on sequence with full verification of facility performance over its full dynamic range. During turn on and during shutdown and maintenance periods, the ACS will be in *maintenance mode*. Routine turn on will be fully automated, with progressive activation of the injector, synchrotron, and then each beam line in turn with command and measurement by the corresponding TCS. It will be possible to put an individual beam line off line for gantry or TCS maintenance. That line would need to be re-verified in order to be put into *treatment mode*. While in *maintenance mode*, the ACS will make available automated turn on and turn off processes along with applications for tuning and diagnosing particular subsystems.

The prohibition on changing settings and conversion values will be removed in *maintenance mode*.

A history of selected synchrotron and beam transport settings and measurements will be locally recorded by the ACS during each treatment. This record will be delivered to the Record and Verify System during the time between treatments. Accelerator performance records will also be stored in the ACS file system as needed to support RCMS maintenance. These logs will be taken off line as part of routine maintenance procedures.

The basic physical architecture of the ACS is shown in **Figure 56**. A master clock signal will be derived from the synchrotron dipole magnet controller and will be distributed throughout the facility. A local area network (LAN) will be used for sharing data within the RCMS control systems. There will be no routing to public networks.

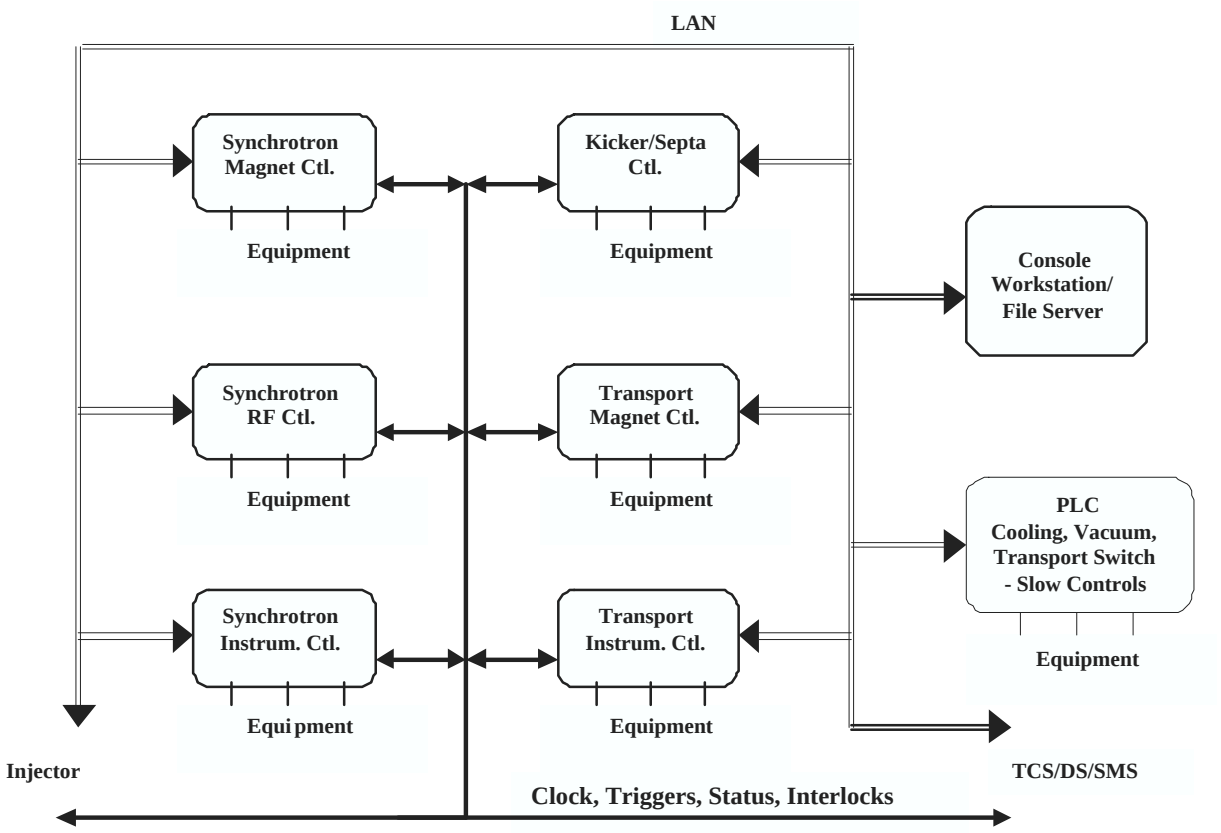

Figure 56: Physical architecture of the Accelerator Control System.

Separate interface assemblies consisting of a single board computer (SBC) and I/O bus modules will control the major synchrotron subsystems and the individual beam lines. The SBCs will run a commercial, real-time operating system. The majority of controller I/O will be provided by the use of commercial boards. Custom boards will be required for some subsystems. Where appropriate, PLC systems will be used to implement slow state control and monitoring. For the principal subsystem equipment items, **Table 23** lists the character of the I/O required and whether custom modules are likely to be required. In addition, some custom modules may be required for signal fan-out and distribution.

A workstation computer running a Linux or UNIX operating system will serve as the ACS operations console. While in *treatment mode*, the workstation will provide a standard passive display of accelerator status information. An alarm display will be included, with some level of automated assistance in fault diagnosis and recovery.

While in *maintenance mode*, the operations console will be used to supervise automated turn on and turn off procedures or to run applications for tuning or diagnostics. Due to the small size and relative simplicity of the RCMS, generic user interface applications for equipment control, live parameter display, data logging, and data viewing will be adequate for most *maintenance mode* needs. Custom applications developed for RCMS commissioning will be available as aids for tuning and diagnostics. Commercial applications may be used for specialized instrumentation displays. **Table 24** lists the anticipated set of applications for the ACS console computer. While in *maintenance*

Item	**Digital I/O**	**Custom?**	**Analog I/O**	**Custom?**
Synchrotron magnets (fast ramped)	Y	N	Y	N
Transport magnets (quasi-dc)	Y	N	Y	N
Injection/Extraction Kickers/Septa	Y	N	Y	N
RF high level system	Y	N	Y	N
RF low level system	Y	**Y**	Y	**Y**
Clock system	Y	**Y**	N	
Circulating beam monitors	Y	N	Y	N
Beam loss monitors	Y	**Y**	Y	**Y**
Transport current transformers	Y	N	Y	N
Wall current monitors	Y	N	Y	N
Beam position monitors	Y	N	Y	N
Beam flags/video	Y	N	N	
Vacuum pumps	Y	N	Y	N
Vacuum valves	Y	N	N	
Vacuum instrumentation	Y	N	Y	N
Water system	Y	N	N	
Transport power switch	Y	N	N	
Injector interface	Y	N	N	
DS interface	Y	**Y**	N	
SMS interface	Y	**Y**	N	

Table 23: I/O interfaces to ACS equipment.

mode, the ACS will have the ability to connect to a simulated TCS interface in order to exercise ACS systems independently of the TCS.

10.4 Safety and Monitoring System

In order to assure safe operation, an independent Safety and Monitoring System will monitor the operation of both the ACS and the TCS. The SMS will interlock operation of the RCMS if the checks of the ACS and TCS are not fully satisfied. The SMS must be designed and implemented independently and must not share any custom hardware or software components with ACS or TCS controls. The SMS itself must operate in a failsafe manner.

Watchdog or heartbeat connections will be implemented to ensure the health of various critical software tasks running in the ACS and TCS. The preferred stimulus for the watchdog function will be a periodic hardware signal generated by the SMS. Local heartbeats could be acceptable as long as they do not depend on the local system clock shared by the controls functions.

Safety-critical devices and beam parameters will be independently monitored by the SMS. To the extent possible, contacts, sensors and data paths that are separate from those used for control will be used for SMS inputs. Key shut-off devices (e.g. RF and extraction power supplies, beam plugs, etc.) will be directly interlocked by failsafe signals from the SMS.

Applications for RCMS Operations

1. Summary Status Display (for treatment mode)
2. Automated Turn On
3. Automated Turn Off

Diagnostic and Commissioning Tools

1. Generic Parameter Control & Display
2. Logged Data Display & Analysis
3. Ramp and Acceleration Tuning
4. Injection Tuning
5. Extraction Tuning
6. Transport Control & Analysis
7. Beam Profile Monitor (Flag/Video) Display
8. Fault Diagnosis and Recovery

Table 24: Accelerator Control System console applications.

11 Vacuum system

The vacuum systems of RCMS can be divided conveniently into the synchrotron vacuum system and the transport line vacuum systems. The operating pressure of the synchrotron is to be $< 10^{-7}$ Torr. This is required not only to minimize beam scattering by residual gases, but also for the reliable operation of injection and extraction devices and the accelerating cavity. The vacuum requirement in the transport lines is less stringent. Here the vacuum level is to be 10^{-6} Torr for the operation of the beam diagnostic equipment and for the lifetime of the vacuum pumps. The small beam pipe aperture in both synchrotron and the transport lines has a rather limited conductance, making it necessary to have vacuum pumps positioned at relatively short spacing.

11.1 Synchrotron vacuum requirements

A pressure of 10^{-7} Torr or lower is needed in the synchrotron. The beam-residual gas interactions to be considered in assessing the required vacuum level are nuclear scattering and multi Coulomb scattering. Due to the low beam intensity of less than 10^9 protons per cycle, no beam induced pressure increase is anticipated.

The nuclear scattering cross sections σ_n are proportional to the geometrical cross section of the residual gas nucleus and are approximately 7, 5 and 1×10^{-25} cm^2 for CO, H_2O and H_2, respectively, the common residual gases in a clean high vacuum system. The beam loss due to nuclear scattering is given by

$$\Delta I/I = \int c\beta\sigma_n N dt, \tag{14}$$

with N being the residual gas density in the vacuum system. At the design pressure of 10^{-7} Torr, N will be approximately 7×10^9 atoms/cm^3. Assuming a residual gas composition of 40% H_2, 40% H_2O and 20% CO, the resultant $\Delta I/I$ will be approximately 3×10^{-7} over the 16 ms acceleration cycles. This is insignificant compared to other losses such as those at injection and extraction.

Multi-Coulomb scattering causes growth of the RMS beam size. The fractional increase in beam size can be calculated by [13]

$$\Delta\sigma_y/\sigma_y = k\beta_y N/(p^2\epsilon)dt, \tag{15}$$

with σ_y the transverse beam dimension, $k = 1.085 \times 10^{-23}$ (GeV/c)^2 m^3 sec^{-1}, β_y the betatron amplitude (< 20 m), p the momentum (in GeV/c) and ϵ the transverse emittance. The fraction of beam growth will be approximately 0.01 over 16 ms at a vacuum of 10^{-7} Torr and is relatively small compared with the beam size growth when beam transverses any windows.

Although these effects are small, devices such as the injection and extraction kickers which operate at high voltages need a vacuum of 10^{-7} Torr or better for their reliable operation. The low operating pressure will also extend the lifetime of the high vacuum pumps beyond the machine lifetime.

11.2 Synchrotron vacuum systems

The layout of the synchrotron vacuum system is shown in **Figure 57**. The two 180 degree arc sections will have 14 vacuum chambers. They are grouped into three types. Type A will have a dipole chamber, a BPM housing and a bellows welded together into one chamber. Type B will be the same as type A except that it will have a pump port instead of a BPM. Type C will have a quadrupole pipe, one pump port, one BPM and two bellows. Most of the chambers will be made of inconel 625 for its mechanical strength, its non-magnetic properties as well as its high resistivity which reduces eddy current and heating [14]. The dipole chambers will have an elliptical cross section of 3 cm x 5 cm with a 0.64 mm wall and a bending angle of 25.7 degrees as shown in **Figure 58**. The quadrupole pipes will have a diameter of 3cm with a 0.64 mm wall. There will also be 8 quadrupole pipes in the two straight sections interfacing with beam components. KF type quick-disconnect flanges with more radiation resistant elastomer seals such as Propyl or Buna-N will be used to join various chambers together. There will not be any gate valves in the synchrotron. However, gate valves will be positioned at injection and extraction lines thus isolating the synchrotron vacuum from the injector and the transport lines in the event of fault.

The strength and the deflection of the elliptical-shaped dipole chambers under the atmospheric load with Eddy current heating have been extensively analyzed using ANSYS code. The results are shown in **Figures 59** and **60**. For a 0.64 mm wall inconel 625, the maximum Von Mises stress is less than 22 kpsi as compared to the yield strength

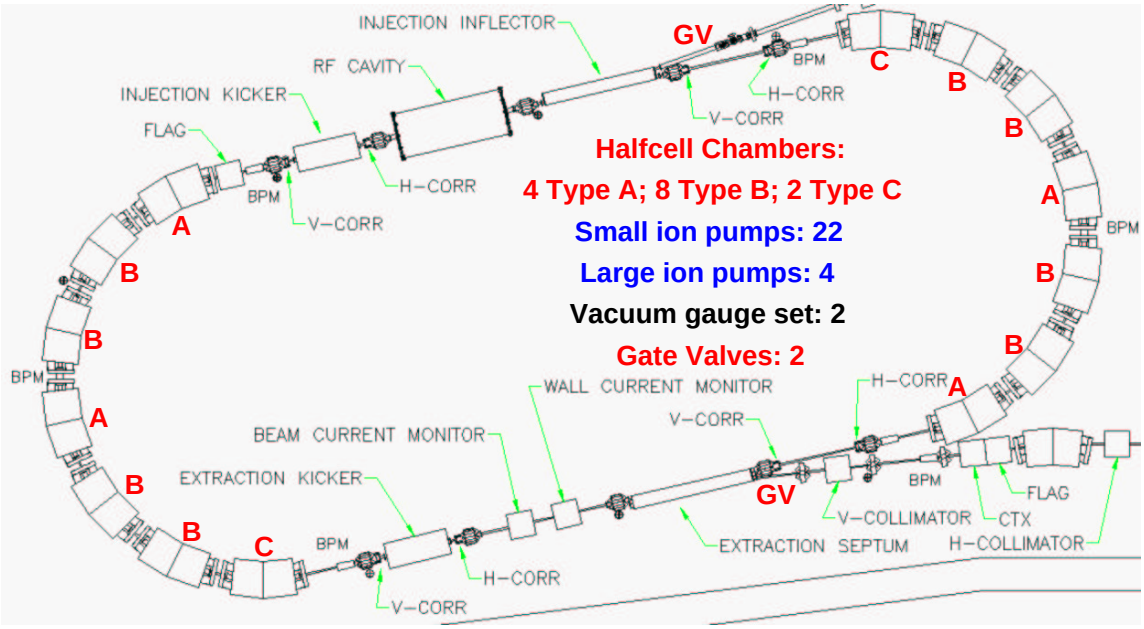

Figure 57: Layout of the synchrotron vacuum chambers and other vacuum components.

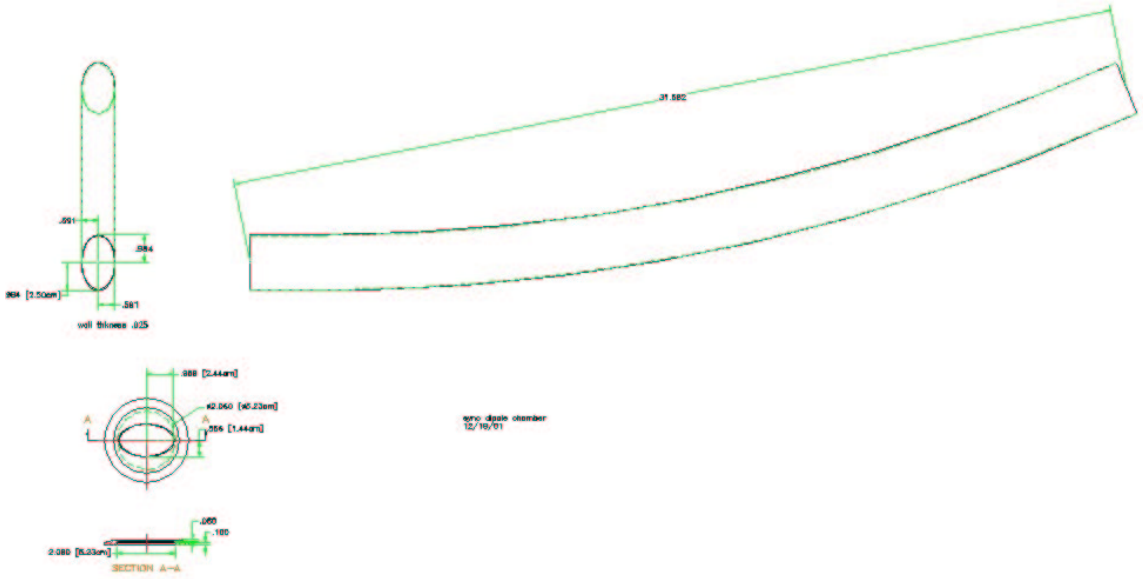

Figure 58: Schematic of synchrotron dipole chamber.

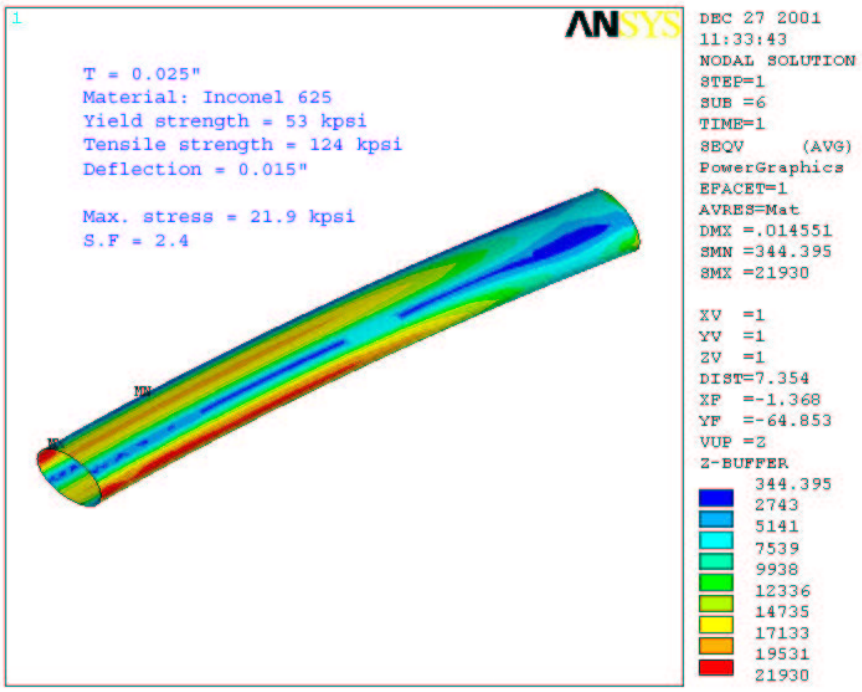

Figure 59: Von Mises stress in the 50 x 30 mm elliptical dipole chamber, made of 0.64mm thick inconel 625.

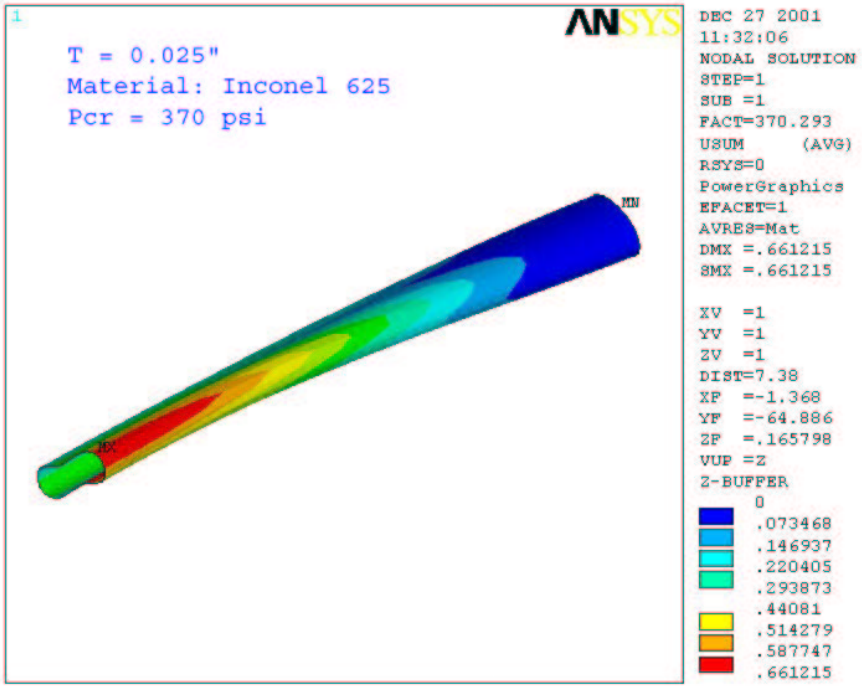

Figure 60: Buckling load and mode shape of synchrotron dipole chamber.

of 53 kpsi, a safety factor of 2.4. The maximum deflection is less than 0.4 mm. The buckling load for the dipole chamber is over 300 psi, providing a significant safety margin.

With inconel which has 60% higher resistivity than stainless steel, the eddy current heating from 30Hz pulsing magnets is still significant. The eddy current heat load is estimated to be 112 watts per meter in the dipole chambers for the 250 MeV mode of operation. The temperature and outgassing of a prototype vacuum chamber with this heat load have been measured to be $< 100°$ C and 10^{-9} Torr l/(s cm^2), respectively. The pressure profile in the two arcs has been calculated using the above outgassing rate for various pumping schemes and is shown in **Figure 61**. Due to the small cross section and the corresponding small pumping conductance ($\propto$ R^3) of the synchrotron vacuum chambers and pipes, large pumps positioned at large spacing are not effective. Instead, small pumps at shorter intervals will provide a lower average pressure. The design vacuum is achieved with one 20 l/s ion pump per chamber.

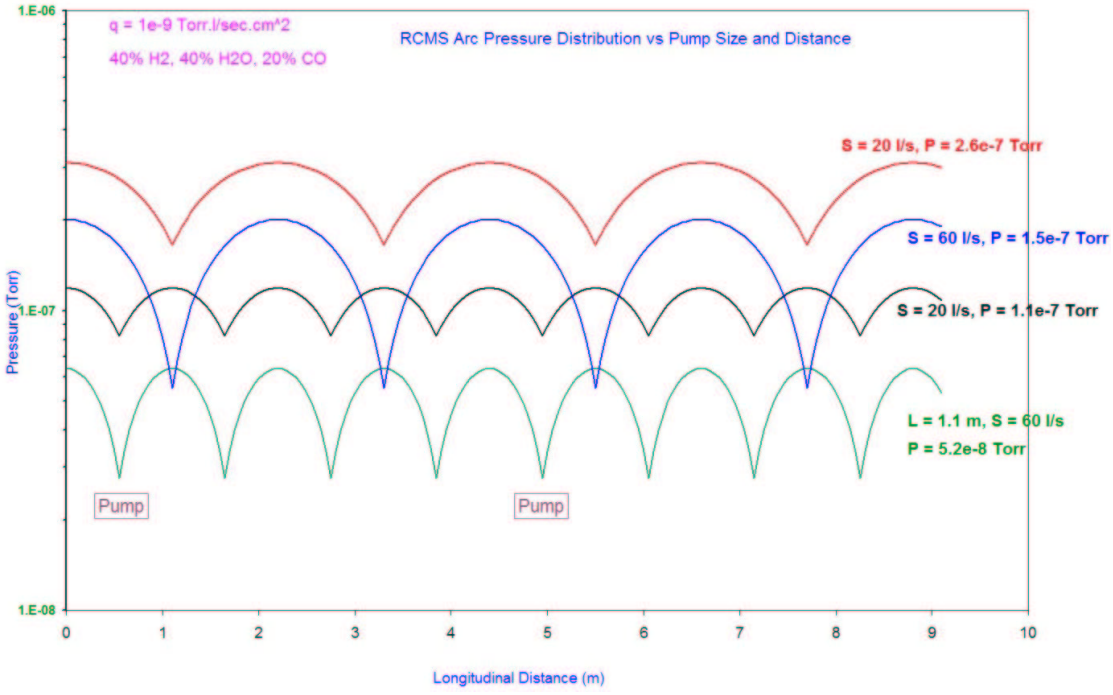

Figure 61: Pressure profiles in synchrotron arc sections with various pumping schemes.

11.3 Transport line and gantry vacuum systems

The transport line vacuum system includes the extraction line from the synchrotron and the transfer lines which go to the research room, the fixed targets, and the multiple gantries. A vacuum of 10^{-6} Torr is sufficient in the beam transport lines and is mainly for the operation of the beam diagnostic equipment and for the lifetime of the vacuum pumps. The beam pipes for the transport lines will be made of either stainless steel or aluminum tubes of 2 cm in diameter. The pressure profile in the transport lines with various pump arrangements is shown in **Figure 62**. As in the synchrotron, due to the limited beam tube conductance, the average pressures are almost identical for 20 l/s and 60 l/s pumps positioned at 10 m intervals.

There are air gaps in the transport lines to allow the operation of the 360° rotating gantries. The impact of these air gaps and windows on the beam due to nuclear (beam loss) and multi Coulomb (growth in rms beam size) scattering is summarized in **Table 25**. Here various window materials, and thickness and length of air gaps are considered for the 60 MeV and 250 MeV operating modes. The beam loss due to nuclear scattering is insignificant for all cases. The growth in beam size is significant for aluminum windows and for air gaps between the fixed transport line and the rotating gantries. Alternatively, a Ferrofluid type rotary seal with magnetic coupling may be used between the fixed beam line and the rotating gantry vacuum pipe, eliminating the windows and the air gap. Beryllium will be used as window material at the beam exit of each gantry.

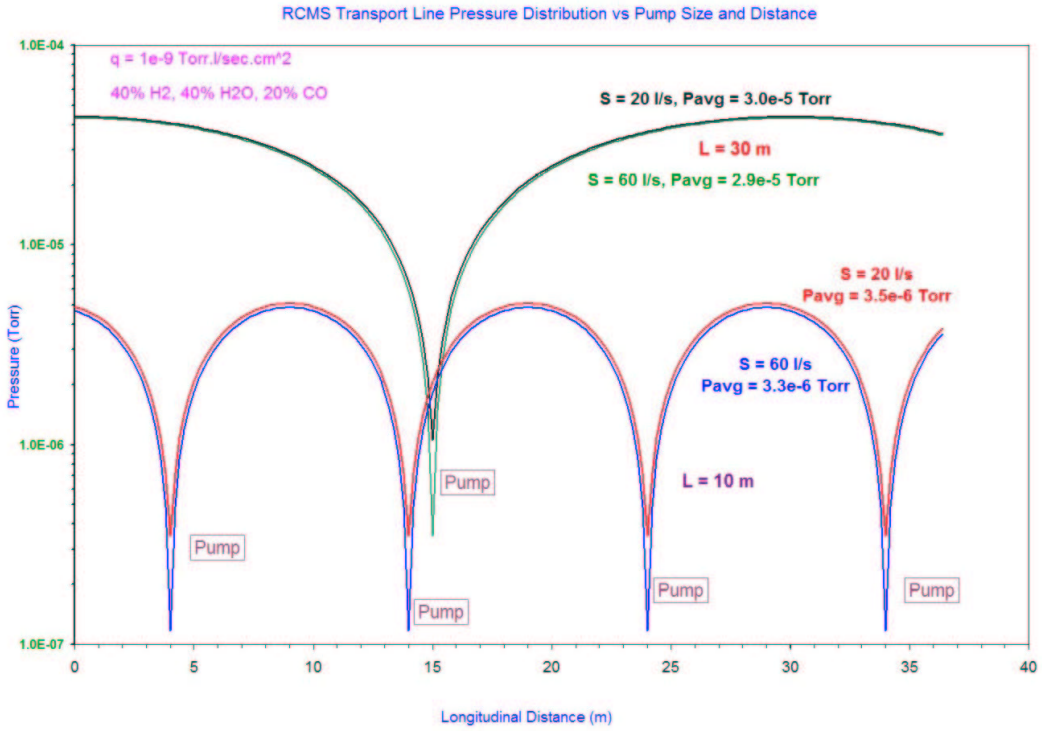

Figure 62: Pressure profiles in transport lines with various pumping schemes. Due to limited conductance of the small radius beam tubes, average pressures of 3×10^{-6} Torr are achieved with either 20 l/s or 60 l/s pumps positioned 10m apart.

	Synch 10^{-7} Torr	B.T, 30 m 10^{-4} Torr	Al window 5 mil	Be window 3 mil	Air gap 10 cm	Gantry, 12 m 1 Torr*
$-\Delta I/I$	2.7×10^{-7}	4.2×10^{-8}	4.2×10^{-4}	2.5×10^{-4}	2.0×10^{-4}	1.7×10^{-5}
$\Delta\sigma/\sigma$ (60 MeV)	0.005	1.2×10^{-4}	30	1.23	6.7	1.05
$\Delta\sigma/\sigma$ (250 MeV)	0.009	3.6×10^{-5}	9	0.37	2.0	0.32

Table 25: Comparison of beam loss and rms beam size growth due to synchrotron and transport vacuums, and air gap and windows at gantries. *The last column assumes that each gantry is at storage vacuum of one Torr without active pumping.

11.4 Vacuum pumps, instruments and control

Diode type sputter ion pumps will be used throughout the RCMS as high vacuum pumps for reliability, lifetime and cost. They will be powered by the conventional DC +5kV power supplies. The sputter ion pump current, proportional to the pressure level, provides a detailed pressure profile throughout RCMS. In addition, a few sets of Pirani and cold cathode vacuum gauges will be positioned at strategic locations to monitor the absolute pressure inside the beam pipes. One residual gas analyzer will be installed in the ring and one in the transport line to provide a quick analysis of the partial pressure composition. Portable turbomolecular pump/dry mechanical pump stations will be used to pump down each vacuum section during start up, maintenance and repair. These will supplement the sputter ion pumps in the event of leaks until the next window of opportunity for repair.

All electronic devices including gauge controllers and pump power supplies will be located in the control room, away from radiation present near the synchrotron and beam lines. These devices with local and remote capabilities can be operated through front panel switches and will communicate with the vacuum programmable logic controllers (PLCs) through RS485 or Ethernet type links for remote monitoring and control. The PLCs with their own application software will provide the interlock logic and on-line menus for the operation of all the vacuum devices. Ethernet type links will connect the PLC to the VME crate and/or the front end computer for monitoring, logging and control of the vacuum devices. Redundant hardwired interlocks will be provided for the *Safety and Monitoring System* to abort the beam during vacuum faults.

A summary of all the vacuum components in the synchrotron and in the transport lines is given in **Table 26**. Components for the extraction line are included in the "Research" column; those downstream are in the "Target" column. The components for the transfer line between Gantries 1 and 2 is listed as the "standard" for all gantries.

Description	Synch.	Research Room	Target	Gantry*
Dipole+Quad Chamber	14	2	13	8
Dipole+Quad Y-Chamber		2	3	1
Quad Pipe	8	12	18	20
Sputter Ion Pumps, 200 l/s	4			
Sputter Ion Pumps, 20 l/s	22	2	5	3
Cold Cathode and Pirani Gauge Set	2	2	3	3
Residual Gas Analyzers	1	1		
Turbopump/Dry Pump Stations, 200 l/s	1			1
Operating vacuum level (Torr)	10^{-7}	10^{-6}	10^{-5}	10^{-5}

Table 26: Numbers of vacuum components in synchrotron and transport lines. *These numbers are for Gantry 2 which is the "standard" gantry.

References

[1] *Pre-Conceptual Design of a Proton Therapy Accelerator*, C. Ankenbrandt et al, FERMILAB-Pub-92/136, 1992.

[2] *Pre-conceptual Design of a Rapid Cycling Medical Synchrotron*, S.Peggs (editor), BNL C-A/AP/6, October 1999.

[3] *RCMS - A Second Generation Medical Synchrotron*, S.Peggs et al, Particle Accelerator Conference, June 2001.

[4] *The Rapid Cycling Medical Synchrotron - RCMS*, S.Peggs et al, European Particle Accelerator Conference, May 2002.

[5] Private communication with E. Pedroni et al, PSI, 2002.

[6] *Treating Cancer with Protons*, M. Goitein, A. Lomax, E. Pedroni, p.45, Physics Today, September 2002.

[7] *Performance Specifications for a Proton Medical Facility*, W.T. Chu et al, LBL Report #33749, 1993.

[8] *Design of the RCMS Lattice Optics*, J.Cardona et al, European Particle Accelerator Conference, May 2002.

[9] *Linear and Non Linear Studies at RHIC Interaction Regions and Optic Studies in the Rapid Cycling Medical Synchrotron*, J.Cardona, Ph.D. thesis, Stony Brook University, to be published, 2003.

[10] *Feasibility of PET of Dose Distribution in Proton Therapy*, J.Beebe-Wang et al, European Particle Accelerator Conference, May 2002.

[11] *Beam Dynamics Simulation in the RCMS*, J.Beebe-Wang et al, European Particle Accelerator Conference, May 2002.

[12] *Beam Position Monitoring*, R.E. Shafer, Accelerator Instrumentation, AIP Conference Proceedings 212, New York, 1990, pp. 26–58

[13] G. Guignard, CERN 77-10, p. 33, June, 1977.

[14] *The RCMS dipole aperture and beam pipe*, S.Peggs et al, BNL C-A/AP/9, February 2000.